

國立台灣大學醫學院藥理學研究所

博士論文

Graduate Institute of Pharmacology

College of Medicine

National Taiwan University

Doctoral Dissertation

探討養分缺乏影響癌細胞代謝及 HIF-1 α 表現的
分子機制

The molecular mechanisms for nutrient
deprivation-induced energy homeostasis and
HIF-1 α induction in cancer cells

巫清安

Ching-An Wu

指導教授：林琬琬 博士

Adviser: Wan-Wan Lin, Ph.D.

中華民國 103 年 10 月

October, 2014







國立臺灣大學博士學位論文

口試委員會審定書

探討養分缺乏對癌細胞代謝的影響及 HIF-1 α 表現的分子機制

The molecular mechanisms for nutrient deprivation-induced energy homeostasis and HIF-1 α induction in cancer cells

本論文係巫清安君 (D96443001) 在國立臺灣大學藥理所完成之博士學位論文，於民國 103 年 10 月 3 日承下列考試委員審查通過及口試及格，特此證明

口試委員：

林 琮 琮 (簽名)

(指導教授)
黃 齊 華

陳 昆 鋒

陳 彥 州

許 文 達

系主任、所長

陳 青 周

(簽名)





誌謝

還依稀記得當年剛踏進這個實驗室時心中的不安，轉眼間現在的我已經要往人生另一個階段邁進。回首這段求學的日子，其中的酸、甜、苦、辣仍歷歷在目，最令我懷念的，我想就是這段日子裡陪我一起打拼的夥伴了。

首先要感謝的就是我的指導老師林琬琬教授，很感謝您這些日子的教導，不只在實驗上，在做人處世上也都讓我獲益良多。再來要感謝婷茵學姊在實驗上的指導與幫助，當我實驗有問題時，妳總是停下手邊的工作與我討論、給我建議，生活上就像好朋友般說說笑笑，互吐苦水，雖然總是吐槽妳，但就像我說的，很快就妳就會開始懷念了，至少我已經開始。感謝彰勳學長陪我吃了七年的午餐，一起吃真的比較好吃。謝謝好同學盈慶，這段時間的甘苦只有你最能體會，喝了妳這麼多年的咖啡，以後喝不到怎麼辦啊。謝謝鈴雅，雖然少了妳午餐只剩我跟學長兩個人，但和男朋友一起吃才是對的。還有已經畢業的西瓜學姊、南霖學長、文翔、明慧、思穎、何小瓜、翊翔、佑如、育誠、宜潔、振綜、欣霓、惟筑、儀芬、凱君，以及志成學長、麟晏學姊、彥呈學長、美瑩學姊、志明學長、國廷學長、Prakash、很吵很煩愛跳樓的瓊禎、妍君、吳小Q、馬達、momo、涓清、上德、德維、Aru等，謝謝你們與我一起走過這段日子。感謝華景讓我喝遍台北飲料店。也感謝口試委員符老師、陳醫師、陳老師、黃老師抽空給我指導。就像我曾說過的，當有一天離開這裡時，能帶走的只有裝在腦子裡東西，現在我要帶著與大家一起在實驗室打拼的記憶、友誼與祝福離開了，希望你們未來的日子一切順利。

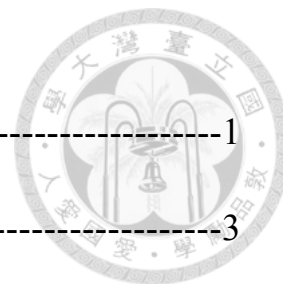
我很感謝我的家人，在我背後給我支持，讓我無後顧之憂完成學業，你們的支持與鼓勵是最能依靠的後盾，也感謝老婆伊翎在這段時間的諒解與支持，還為我生下了可愛的政穎，謝謝你們。

七年多的博士生涯在寫完這份誌謝文時終於進入最後尾聲，最後僅以此論文獻給我的家人。

巫清安 謹誌於
國立台灣大學藥理所
民國 103 年 秋

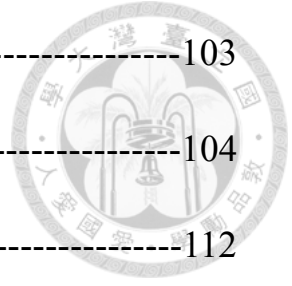


Table of contents



Abbreviations-----	1
English Abstract-----	3
中文摘要-----	5
Introduction-----	7
Specific Aims-----	25
Materials and Methods-----	26
Part I: Nutrient deprivation induces the Warburg effect through ROS/ AMPK-dependent activation of pyruvate dehydrogenase kinase	
Results-----	37
Discussion-----	46
Figures-----	54
Part II: Beclin-1-independent autophagy positively regulates internal ribosomal entry site-dependent translation of hypoxia-inducible factor 1 α under nutrient deprivation	
Results-----	69
Discussion-----	80
Figures-----	87

Conclusion	103
Appendix	104
References	112
Publications	137





Abbreviations:

3-MA: 3-Methyladenine

AMPK: AMP-activated protein kinase

ATG: Autophagy-related gene

C.C: Compound C

CAT: Chloramphenicol acetyltransferase

CHX: Cycloheximide

CMA: Chaperone-mediated autophagy

DCA: Dichloroacetate

DN: Dominant negative

G6PDH: Glucose-6-phosphate dehydrogenase

-Gal: -Galactosidase

Glc: Glucose

GLUT4: Glucose transporter 4

HBSS: Hank's buffered salt solution

HIF-1 α : Hypoxia-inducible factor 1 α

HUVEC: Human umbilical vein endothelial cells

IRES: Internal ribosome entry site



ITAF: IRES transacting factor

LDH: Lactate dehydrogenase

NAC: N-acetyl-cysteine

PDH: Pyruvate dehydrogenase

PDK: Pyruvate dehydrogenase kinase

PEP: Phosphoenolpyruvate

PFK: Phosphofructokinase

PHD: Prolyl hydroxylase

PI3K: Phosphatidylinositol 3-kinase

PKM2: Pyruvate kinase M2

PTB-1: Polypyrimidine tract-binding protein

ROS: Reactive oxygen species

TCA: Tricarboxylic acid

TNF- α : Tumor necrosis factor-alpha

WT: Wild type



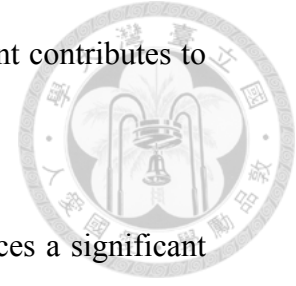


Abstract

Hypoxia and nutrient deprivation are two important phenomenon in solid cancer due to the poor blood supply. In contrast to well-studied effect of hypoxia on tumor growth, the effect of nutrient deficiencies on cancer is not well defined. In this thesis, we try to explore the effect of nutrient deprivation on tumor cell metabolism and HIF-1 α expression.

For the part I, we demonstrate that Hank's buffered salt solution (HBSS) starvation increased lactate production, cytoplasmic pyruvate content and decreased oxygen consumption, but failed to change the lactate dehydrogenase (LDH) activity or the glucose uptake. We found that HBSS starvation rapidly induced pyruvate dehydrogenase kinase (PDK) activation and pyruvate dehydrogenase (PDH) phosphorylation, both of which were reversed by inhibition of ROS and AMPK. Our data further revealed the involvement of ROS production in AMPK activation. Moreover, inhibition of PDK, ROS, and AMPK all significantly decreased HBSS starvation-induced lactate production accompanied by enhancement of HBSS starvation-induced cell apoptosis. Taken together, we for the first time demonstrated that a low-nutrient condition drives cancer cells to utilize glycolysis to produce ATP (the Warburg effect) through a novel mechanism

involving ROS/AMPK-dependent activation of PDK. Such an event contributes to protecting cells from apoptosis upon nutrient deprivation.



For the part II, Our data showed that nutrient deprivation induces a significant HIF-1 α protein expression through the internal ribosome entry site (IRES)-dependent translation. Notably inhibition of autophagy by si-ATG5, 3-methyladenine and chloroquine, but not si-Beclin-1, significantly reverses nutrient deprivation-induced HIF-1 α responses. Furthermore, it is interesting to note that different from nutrient starvation, si-Beclin 1 but not si-ATG5 can inhibit hypoxia-induced HIF-1 α IRES activation. Taken together, we for the first time highlight a link from alternative autophagy to IRES-dependent protein translation of HIF-1 α under two unique stress conditions. We demonstrate Beclin 1-independent autophagy is involved to positively regulate nutrient deprivation induced-HIF-1 α IRES activity, while ATG5-independent autophagy is involved in the HIF-1 α IRES activation caused by hypoxia.

Key words: Warburg effect; PDK; HIF-1 α ; Autophagy; IRES



中文摘要

由於血流供給不足，缺氧與養分缺乏是固態腫瘤兩個很重要的特徵。與已經被廣泛研究的缺氧相反，養分不足，這另外一個固態腫瘤的特徵對癌細胞的影響則不清楚。在這篇論文中，我們嘗試去探索養分缺乏對癌細胞代謝與缺氧可誘發性因子甲型(Hypoxia-inducible factor-1 α)的影響。

在第一部分，我們證明利用 Hank's buffered salt solution (HBSS)造成養分缺乏會增加細胞外乳糖(lactate)的產生、細胞質內丙酮酸(pyruvate)的增加，並降低細胞氧氣的消耗，但是並不會影響乳糖脫氫酵素(lactate dehydrogenase)的活性或是葡萄糖的吸收。我們發現養分缺乏會快速的誘發丙酮酸脫氫酶酵素(pyruvate dehydrogenase kinase)之活化以及丙酮酸脫氫酶(pyruvate dehydrogenase)的磷酸化，而抑制 ROS 或 AMPK 會抑制這個現象。我們也證明 ROS 的產生會促進 AMPK 的活化。更進一步來說，抑制丙酮酸脫氫酶酵素、ROS 與 AMPK 都可以顯著的減少養分缺乏所誘發的乳糖產生，同時促進養分缺乏所誘發的細胞凋亡。綜合來說，我們首次證明養分缺乏會經由 ROS/AMPK 依賴性的活化丙酮酸脫氫酶酵素這個新的機轉，來促使細胞經由糖解作用來產生 ATP，也就產生瓦氏效應，而這個作用會延緩細胞因為養分缺乏而造成的死亡。

在第二個部分，我們的證據顯示，養分缺乏會經由 cap 非依賴性的內部核糖體進入位(internal ribosome entry site)的轉譯來增加可誘發性因子甲型的蛋白表現。特別的是，藉由 si-ATG5、3-methyladenine 或 chloroquine 來抑制自噬體(autophagy)可以顯著抑制養分缺乏所誘發的缺氧可誘發性因子甲型的表現，但是 si-Beclin 1 卻沒有這效果。此外，很有趣的是，缺氧時也會經由內部核糖體進入位來轉譯缺氧可誘發性因子甲型，但是與養分缺乏不同的是，si-Beclin 1 而不是 si-ATG5 會抑制缺氧所誘發的缺氧可誘發性因子甲型內部核糖體進入位活性。綜合來說，我們首次證明養分缺乏與缺氧時替代性自噬體和缺氧可誘發性因子甲型

的 cap 非依賴性轉譯的關聯性。我們證明 Beclin 1 非依賴性的自噬體可以正向調控養分缺乏所誘發的缺氧可誘發性因子甲型的內部核糖體進入位活性，而 ATG5 非依賴性的自噬體則參與缺氧所誘發的缺氧可誘發性因子甲型的內部核糖體進入位活性。

關鍵字：瓦氏效應；丙酮酸脫氫酶酵素；缺氧可誘發性因子甲型；自噬體；內部核糖體進入位



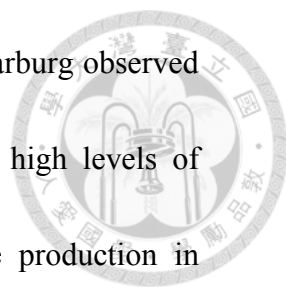
Introduction

1. Energy production in cancer cell

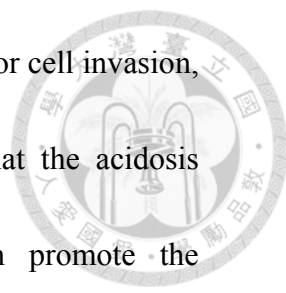
1.1 Warburg effect (aerobic glycolysis)

ATP required for normal cell proliferation and survival comes primarily from two sources. The first is glycolysis, which comprises a series of reactions that metabolizes glucose to pyruvate in the cytoplasm to produce a net of 2 ATP from each glucose. The other is the tricarboxylic acid (TCA) or Krebs cycle, which uses pyruvate formed from glycolysis to proceed a series of reactions that donate electrons via NADH and FADH₂ to the respiratory chain complexes in mitochondria. With oxygen serving as the final electron acceptor, electron transfer creates across the mitochondrial inner membrane a proton gradient, of which the dissipation through ATP synthase forms 36 ATP per glucose molecule. With limited oxygen, such as in muscles that have undergone prolonged exercise, pyruvate is not used in the TCA cycle and is converted into lactic acid by lactate dehydrogenase (LDH) in a process termed anaerobic glycolysis (Kim and Dang, 2006) (**Appendix 1**).

Many cancer cells consume glucose avidly and produce lactate rather than catabolizing glucose via the TCA cycle, which is the key process for generating



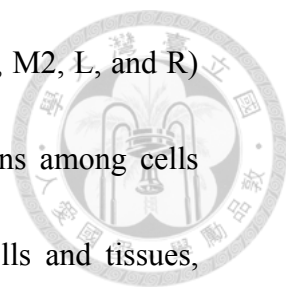
ATP in nonhypoxic normal cells. More than 80 years ago, Otto Warburg observed that thin slices of human and animal tumors *ex vivo* displayed high levels of glucose uptake and lactate production. The shift toward lactate production in cancers, even in the presence of adequate oxygen, is termed the Warburg effect or aerobic glycolysis (Warburg, 1927, 1956). Four ATP were generated from one glucose molecule in Warburg effect. To reach the energy demand, glucose uptake was enhanced in cancer cells. The avid uptake of glucose by tumors is the foundation for the detection and monitor of human cancers by fluorodeoxyglucose positron emission tomography which has been extensively used in clinical. This shift of glucose metabolism from oxidative phosphorylation to glycolysis, although inefficient in energy production, provides cancer cells with several growth advantages over the surrounding normal cells, such as the ability to survive in conditions of fluctuating oxygen levels (Pouyssegur et al., 2006), to favor tumor invasion (Swietach et al., 2007), and to suppress anticancer immune factors (Fischer et al., 2007). In the case of conditions of fluctuating oxygen levels, cancer cells don't have enough oxygen to generate ATP from oxidative phosphorylation. To survive, cancer cells reach the energy demand by reprogramming metabolic pathway to Warburg effect. In the aspect of tumor invasion and immune escape, acidosis which was induced by lactate production has been shown to involve in



these phenomenon. Low extracellular pH was shown to induce tumor cell invasion, however, the exact mechanism is unknown. It was proposed that the acidosis condition induced metalloproteinases and/or cathepsins which promote the degradation of extracellular matrix and basement membranes (Rozhin et al., 1994; Montcourrier et al., 1997). Furthermore, lactate inhibited human cytotoxic T lymphocytes proliferation and cytokinase production (Fischer et al., 2007). Most importantly, proliferating cancer cells can utilize intermediates of the glycolytic pathway as precursors for synthesis of amino acids, nucleic acids, and lipids, and thus meet the bioenergetic and biosynthetic demands of proliferation (Kroemer and Pouyssegur, 2008). Although hypoxia has been demonstrated to induce Warburg effect, how dose nutrient deprivation, another important phenomenon in solid tumor, affects cancer cells metabolism is not well defined.

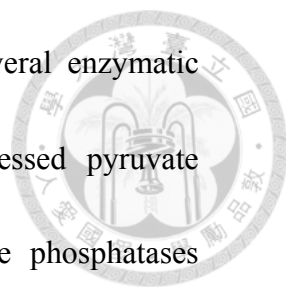
1.2 Regulation of glycolytic enzymes (pyruvate kinase, pyruvate dehydrogenase, hexokinase and phosphofructokinase) in cancer cells

In the ATP production pathway, two enzymes have been reported to control pyruvate either entering into mitochondria to conduct oxidative phosphorylation or staying in cytosol to metabolize to lactate by LDH-A (**Appendix II**). One is pyruvate kinase (PK), and the other is pyruvate dehydrogenase (PDH). Pyruvate



kinase is a tetrameric enzyme that comprises four isoenzymes (M1, M2, L, and R) with differences in their kinetic properties and distribution patterns among cells and tissues. PKM1 was found in the vast majority of normal cells and tissues, whereas PKM2, which is abundant during embryogenesis and in selected tissues such as adipose tissue and pancreatic islets, is the predominant form found in cancer cells. Unlike other pyruvate kinase isoforms, PKM2 is regulated by tyrosine phosphorylation (Christofk et al., 2008b) (**Appendix III**). Phosphotyrosine signaling downstream of a variety of cell growth signals shares the common ability to negatively regulate PKM2 activity. After receiving tyrosine phosphorylation, PKM2 is induced into a low-activity state. This regulation of enzyme activity may constitute a molecular switch that allows cells to metabolize glucose through glycolysis in a manner that is consistent with proliferating cell metabolism only when growth signals are present (Vander Heiden et al., 2009). Although counterintuitive, it is the low-activity form of PKM2 that is necessary for cell proliferation. This regulation allows PKM2 to act as a gatekeeper that dictates the flow of carbon into biosynthetic pathways versus complete catabolism for ATP production (Christofk et al., 2008a).

PDH is a component of pyruvate dehydrogenase complex (PDC). The PDC controls pyruvate entry into the TCA cycle and thus sits at the interface between



glycolysis and glucose oxidation. The PDC is composed of several enzymatic complexes and regulatory proteins. Several differentially expressed pyruvate dehydrogenase kinases (PDK 1~4) and pyruvate dehydrogenase phosphatases (PDP1, 2) tightly regulate PDC activity via reversible inhibitory phosphorylation of the pyruvate dehydrogenase E1 (PDH) subunit (Roche and Hiromasa, 2007; McFate et al., 2008). This regulation of PDC activity provides a convenient way for cells to divert pyruvate into anabolic pathways, while favoring oxidation of other fuels. PDK-1 was recently identified as an HIF-1- regulated gene, which directly ties HIF-1 activation to decreased glucose oxidation through PDH phosphorylation and PDC inhibition (Kim et al., 2006).

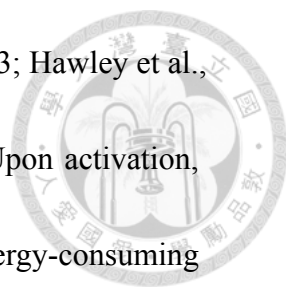
Besides PKM2 and PDH, the overexpression of some pathway enzymes and/or activities, e.g. hexokinase (HK) and phosphofructokinase isoenzymes (PFK-1), the rate-limiting enzyme and essential control point in the glycolysis, in order to support the glycolytic efficiency and/or aggressiveness in cancer cells has been demonstrated (Marín-Hernández et al., 2010; Zancan et al., 2010) (**Appendix II**).

In breast cancer cells, expression of PFK is important for the glycolytic efficiency and survival of cancer cells. In cancer cells, HIF-1 also can induce over-expression and increased activity of several glycolytic protein isoforms, including transporters (GLUT1, GLUT3) and enzymes (hexokinase, LDH-A),

which provide cancer cells with reduced sensitivity to physiological inhibitors (Marín-Hernández et al., 2009). Thus, these proteins are proposed to be the foremost therapeutic targets because their simultaneous inhibition will have greater antagonistic effects on tumor energy metabolism. Indeed, recent studies showed the abilities of acetylsalicylic acid and salicylic acid to inhibit PFK activity, implicating this action in promoting anti-tumoral effects (Spitz et al., 2009).

1.3 AMPK: intracellular energy sensor

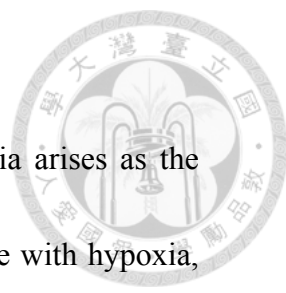
AMPK is widely expressed and exists as a heterotrimeric complex, which consists of a catalytic subunit () and two regulatory subunits (and). The mammalian genome contains seven AMPK genes encoding two (1 and 2), two (1 and 2), and three (1, 2, and 3) isoforms (Rutter et al., 2003; Carling, 2004; Hardie, 2004). The catalytic subunit is composed of three functional domains, including an N-terminal Ser/Thr protein kinase domain, a central auto-inhibitory region, and a C-terminal regulatory subunit-binding domain. AMPK acts as an intracellular energy sensor by monitoring cellular energy levels. For example, AMPK becomes activated by the tumor suppressor LKB1 complex-mediated phosphorylation at Thr-172 in response to certain energy-depleting stresses such as glucose deprivation, hypoxia, and oxidative



stress, which increase the intracellular AMP:ATP ratio (Hardie, 2003; Hawley et al., 2003; Woods et al., 2003; Xing et al., 2003; Shaw et al., 2004). Upon activation, AMPK phosphorylates and inactivates several key enzymes in energy-consuming biosynthetic pathways such as acetyl-CoA carboxylase (ACC), 3-hydroxy-3-methylglutaryl-CoA reductase (Carling et al., 1989), glycogen synthase (Young et al., 1996), thereby conserving ATP. AMPK was published to stimulate glycolysis by phosphorylation and activation of 6-phosphofructo-2-kinase (PFK-2) on Ser466 during ischaemia. However, Activation of PFK-2 is unable to stimulate glycolysis by itself (Depre et al., 1998). Overall flux can only increase if the supply of glucose 6-phosphate is also increased. Therefore, besides PFK-1/PFK-2 activation, the role of AMPK in regulating the overall flux of glycolysis is still worth to study. Since AMPK regulates energy homeostasis, how does it manipulate Warburg effect under nutrient deprivation is worth to be discovered. In addition, AMPK activation reduces protein synthesis by inhibition of mTOR signaling (Liang and Mills, 2013). Under nutrient deprivation condition, AMPK activated tuberous sclerosis proteins (TSC) and inhibited Raptor which inhibited mTOR signaling.

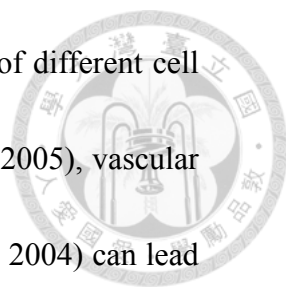
2. Hypoxia-inducible factor 1 α

2.1 Oxygen-dependent degradation



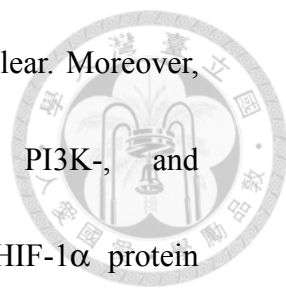
Hypoxia is a common feature in solid tumors. Chronic hypoxia arises as the tumor mass outgrows the existing stromal vascular supply. To cope with hypoxia, higher organisms have developed numerous adaptive responses to stimulate glycolysis, erythropoiesis, and angiogenesis (Semenza, 2011; Weljie and Jirik, 2011). Many of these responses are mediated by hypoxia-inducible factor 1 α (HIF-1 α). Both the stability and activity of HIF-1 α are oxygen-dependently regulated. When Pro402 and Pro564 in oxygen-dependent degradation domain are hydroxylated by HIF-1-prolyl hydroxylase (PHD), HIF-1 α is targeted by von Hippel-Lindau protein (pVHL), ubiquitinated, and degraded by 26S proteasomes (Ivan et al., 2001; Jaakkola et al., 2001). In addition, Asn803 in C-terminal transactivation domain of HIF-1 α is hydroxylated by factor inhibiting HIF-1 (FIH), which inactivates HIF-1 α by blocking its recruitment of p300/CBP coactivator (Mahon et al., 2001). Since both hydroxylation occur oxygen dependently, HIF-1 α becomes stabilized and activated under hypoxic conditions (**Appendix IV**). Although hypoxia has been well-demonstrated to induce HIF-1 α by interfering degradation, the effect of nutrient deprivation on HIF-1 α is not well-defined.

2.2 HIF-1 α mRNA Translation--Cap-dependent and -independent pathways



There is accumulating evidence demonstrating that stimulation of different cell types with growth factors (Yu et al., 2012), cytokines (Frede et al., 2005), vascular hormones (Diebold et al., 2010) and viral proteins (Wakisaka et al., 2004) can lead to the induction and activation of HIF-1 α . Contrary to hypoxia, stabilization of HIF-1 α does not seem to play a role in the non-hypoxic induction of HIF-1 α . The main mechanism implicated in this induction is an increase in HIF-1 α protein translation. The increase in protein translation alone is sufficient to shift the balance between synthesis and degradation towards an accumulation of normoxic HIF-1 α .

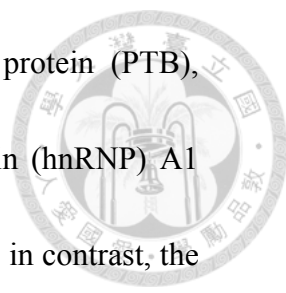
There are two basic mechanisms of initiating translation. One is cap-dependent, and the other is cap-independent (**Appendix V**). Cap-dependent translation is controlled by mTOR signaling which releases initiation factor eIF4E from 4E-BP1 to bind to the mRNA 5' cap structure. An alternative route of translation is mediated by cap-independent activation of internal ribosome entry site (IRES). In contrast to cap-dependent translation which recruits translational complex to m⁷G cap structure at the 5'UTP, IRES activation directly recruits 40S ribosomal subunit to the vicinity of the initiation codon (Komar et al., 2012). Notably, the IRES activity of some mRNAs is induced when cap-dependent translation is compromised. In the case of HIF-1 α , starvation has been shown to induce HIF-1 α



IRES activity (Lang et al., 2002), however, the mechanism is unclear. Moreover, tumor necrosis factor-alpha (TNF- α) induces NF κ B-, PI3K-, and MAPK-dependent Bcl-2 expression, which in turn stimulates HIF-1 α protein expression and IRES translation (Zhou et al., 2004). Since IRES activity can be induced on the inhibition of cap-dependent translation, we proposed that nutrient deprivation which inhibited the mTOR signaling might induce IRES activity and play an important role in protein translation under nutrient deprivation condition.

2.3 Regulation of IRES activity

IRES-mediated direct ribosome recruitment is dependent upon the presence of several proteins collected terms IRES-trans-acting factors (ITAFs) (Baird et al., 2006). ITAFs have been proposed to act as RNA chaperones (or bridges) to stabilize the functional IRES conformation and allow the mRNA to attain the correct conformation for the interaction of the 40S ribosome subunit. Besides their implication in a variety of cellular activities, ITAFs are generally believed to increase (or, in certain cases, decrease) the affinity of binding between IRES and components of the translational apparatus (Komar and Hatzoglou, 2011). One of the major challenges for researchers in this area is to determine whether there are groups of ITAFs that regulate the IRES-mediated translation of subsets of mRNAs.



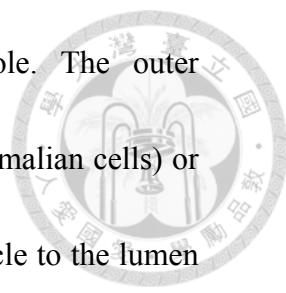
In fact, several ITAFs such as polypyrimidine tract-binding protein (PTB), upstream of N-Ras (Unr), heterogeneous nuclear ribonucleoprotein (hnRNP) A1 have been shown to enhance the IRES-mediated mRNA translation; in contrast, the ITAF HuD and HuR inhibits p27Kip1 IRES activity. Among ITAFs, PTB is the most extensively studied. In addition to a role in translation, PTB is also involved in mRNA splicing, stability and localization within the cells (Sawicka et al., 2008). The data suggest that the majority of cellular IRESs require PTB for function, and PTB seems to be particularly important for the control of IRESs which are active during apoptosis (Mitchell et al., 2005; Bushell et al., 2006). PTB has been shown to upregulate many IRES translation, including HIF-1 α (Schepens et al., 2005) Apaf (Mitchell et al., 2001; Mitchell et al., 2003), and p53 (Grover et al., 2008) , but inhibit IRES translation of BiP (Kim et al., 2000). Therefore, PTB can either enhance or inhibit IRES-dependent translation depending on mRNAs. On the other hands, hnRNP A1 is involved in Cyclin D1 and c-Myc IRES translation (Damiano et al., 2013; Jo et al., 2008). ELAV protein HuD as a specific binding factor of the p27 5'UTR. Increased expression of HuD or the ubiquitously expressed HuR protein specifically inhibits p27 translation and p27 IRES activity (Kullmann et al., 2002).

3. Autophagy

3.1 Autophagy is an energy production mechanism of cells under stress

The term autophagy (Greek, “to eat oneself”) does not refer to a death process.

It denotes the process of self-cannibalization through a lysosomal degradation pathway. Autophagy is highly conserved from yeast to mammals. During starvation, autophagy is induced to recycle cellular components to produce amino acids and fatty acids which served as materials for mitochondrial energy production to survive (**Appendix VI**). It is the cell’s major regulated mechanism for degrading long-lived proteins and the only known pathway for degrading organelles (Klionsky and Emr, 2000; Levine and Klionsky, 2004). Under energy rich condition, autophagic process were inhibited by mTOR activation which inhibited ULK1 and Beclin-1 sequestered by Bcl-2 which inhibited phagophore formation. Under starvation condition, AMPK inhibited mTOR signaling which activate ULK1 and JNK phosphorylated Bcl-2 which released Beclin-1 to interact with Vps34 to induced autophagy. During autophagy, an isolated membrane forms, presumably arising from a vesicular compartment known as the preautophagosomal structure, invaginates and sequesters cytoplasmic constituents including mitochondria, endoplasmic reticulum, and ribosomes (Levine and Yuan, 2005). The edges of the membrane fuse to form a double or multimembranous



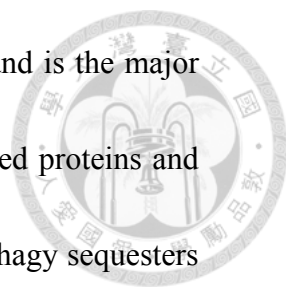
structure, known as the autophagosome or autophagic vacuole. The outer membrane of the autophagosome fuses with the lysosome (in mammalian cells) or vacuole (in yeast and plants) to deliver the inner membranous vesicle to the lumen of the degradative compartment. Degradation of the sequestered material generates nucleotides, amino acids, and free fatty acids that are recycled for macromolecular synthesis and ATP generation. Autophagy occurs at low basal levels in all cells to perform homeostatic functions (e.g., cytoplasmic and organelle turnover) but is rapidly upregulated when cells need to generate intracellular nutrients and energy (e.g., during starvation or trophic factor withdrawal), undergo architectural remodeling (e.g., during developmental transitions), or rid themselves of damaging cytoplasmic components (e.g., during oxidative stress, infection, and accumulation of protein aggregates). Nutritional status, hormonal factors, and other cues like temperature, oxygen concentrations, and cell density are important in the control of autophagy (Higgins et al., 2010; Gonzalez et al., 2011). Moreover, increasing evidence suggests that the deregulation of autophagy may contribute to a broad spectrum of mammalian diseases.

Two evolutionarily conserved nutrient sensors play roles in autophagy regulation: (a) the mammalian target of rapamycin (mTOR) kinase is the major inhibitory signal that shuts off autophagy during nutrient abundance (Lum et al.,

2005), and (b) the eukaryotic initiation factor 2α (eIF2 α) kinase Gcn2 and its downstream target Gcn4 (a transcriptional transactivator of autophagy genes) turn on autophagy during nutrient depletion (Talloczy et al., 2002). The class I PI3K/Akt signaling molecules link receptor tyrosine kinases to TOR activation and thereby repress autophagy in response to insulin-like and other growth factor signals (Levine and Yuan, 2005).

3.2 Classification of autophagy

There are different types of autophagy, including microautophagy, macroautophagy and chaperone-mediated autophagy (CMA) (**Appendix VII**). Microautophagy directly engulfs organelles by invagination or protrusion of arm-like structures of the lysosomal membrane. The sequestration of cargo occurs directly on the surface of vacuole (Muller et al., 2000; Sattler and Mayer, 2000). CMA is different from microautophagy and macroautophagy, and no vesicular traffic is required. CAM selectively degrades specific cytosolic proteins containing a pentapeptide motif (KFERQ) that is recognized by the heat shock cognate protein 70 (Hsc70), followed by unfolding and translocation of proteins through the lysosomal membrane by lysosome-associated membrane protein type 2A (LAMP2A) (Majeski and Dice, 2004). The final type of autophagy is



macroautophagy. Macroautophagy is the main type of autophagy and is the major cellular pathway to recycle cellular components including long lived proteins and organelles to provide energy under nutrient starvation. Macroautophagy sequesters protein and organelle in autophagosome, which is then fused with lysosome to form autolysosome (Mizushima et al., 2010). Furthermore, macroautophagy is formed by multistep process controlled by proteins termed autophagy-related (Atg) proteins (Klionsky et al., 2003). The formation of the phagophore requires the class III phosphatidylinositol 3-kinase (PI3K) Vps34 that forms a complex with Beclin 1. Inhibition of Vps34 by 3-methyladenine (3-MA) inhibits macroautophagy by prevention of the autophagosome nucleation (Wu et al., 2010). The elongation of the autophagosomal membrane is dependent on two ubiquitin-like conjugation systems (Ohsumi and Mizushima, 2004). Atg7 (ubiquitin-activating-enzyme (E1)-like) and Atg10 (ubiquitin-conjugating-enzyme (E2)-like) is required in Atg5-Atg12 conjugation, which controls autophagy formation. The Atg5-Atg12 conjugation depends on Vps34 activity and is localized onto the phagophore where it dissociates upon formation of the autophagosome. Atg5-Atg12 forms a complex with Atg16L that modulates the ubiquitin-like conjugation of LC3-I. The protein LC3 is proteolytic activated by cleavage of the C-terminus of LC3 by Atg4 to generate a cytosolic LC3-I. LC3-I subsequently conjugates with

phosphatidylethanolamine (PE) to form membrane associated LC3-II, and this lipidation process requires Atg7 and Atg3 (Tanida et al., 2004).



3.3 Autophagy regulates HIF-1 α expression

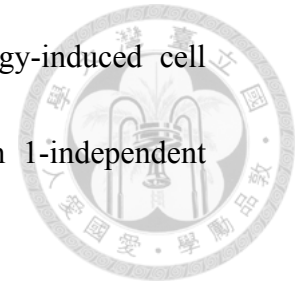
In addition to proteasome, some evidence shows that HIF-1 α is also degraded through autophagy-dependent pathway (Olmos et al., 2009; Ferreira et al., 2013; Hubbi et al., 2013). 15-Deoxy-Delta(12,14)-prostaglandin-J(2) induced HIF-1 α accumulation by an inhibition of lysosome activity (Olmos et al., 2009). Inhibition of lysosome activity by bafilomycin A1, chloroquine and ammonium chloride induces HIF-1 α accumulation in HeLa and Hep3B cells. Furthermore, HIF-1 α is degraded through CMA-dependent pathway. 6-Aminonicotinamide (6-AN), a commonly used activator of CMA, inhibits hypoxia-induced HIF-1 α accumulation and overexpression of Hsc70 or LAMP2A, CMA-dependent molecules, decreased hypoxia-induced HIF-1 α level (Hubbi et al., 2013). This CMA mediated HIF-1 α degradation is E3 ubiquitin ligase STIP1 homology and U-box containing protein 1 (STUB1) dependent (Ferreira et al., 2013). In Hubbi's paper, they also found that silence of Atg6 abolished hypoxia-induced HIF-1 α accumulation (Hubbi et al., 2013). The reason is unknown. However, it raises the possibility that autophagy might positively regulates HIF-1 α expression.



3.4 Alternative macroautophagy

Although macroautophagy has been studied for decades, it was not proved to contain subtype macroautophagy until recent years. In addition to conventional macroautophagy, there are at least two alternative macroautophagic pathways that have been discovered (Juenemann and Reits, 2012) (**Appendix VIII**): Beclin 1-independent macroautophagy which is the so-called noncanonical macroautophagy (Zhu et al., 2007; Scarlatti et al., 2008a, 2008b; Smith et al., 2010; Tian et al., 2010; Grishchuk et al., 2011; Zhou et al., 2012) and ATG5/ATG7-independent macroautophagy (Nishida et al., 2009). The Beclin 1-independent macroautophagy was first reported in 1-methyl-4-phenylpyridinium (MMP^+) treated neuronal cells (Zhu et al., 2007). The Beclin 1-independent macroautophagy was reported to induce cell apoptosis. Staurosporine was shown to induce apoptosis in cortical neurons through Beclin 1-independent macroautophagy (Grishchuk et al., 2011). Moreover, Beclin 1-independent macroautophagy was induced by resveratrol in human breast cancer cells, arsenic trioxide in ovarian cancers, Zinc protoporphyrin IX in HeLa cells to involve in cell apoptosis (Scarlatti et al., 2008a, 2008b; Smith et al., 2010; Zhou et al., 2012). Although the noncanonical macroautophagy is Beclin 1 independent, some data

shown that 3-MA can reverse this noncanonical macroautophagy-induced cell apoptosis (Grishchuk et al., 2011). It indicates that the Beclin 1-independent macroautophagy may be more complicated than we expect.



The ATG5/ATG7-independent macroautophagy was first discovered in mouse embryonic fibroblasts (MEF) lacking ATG5 and ATG7 under the treatment of cytotoxic stressor etoposide (Nishida et al., 2009). They found out that etoposide induced autophagic vacuoles in ATG5 or ATG7 knockout MEF cells by electron microscopy. Interestingly, the lipidated conjugate LC3-II, which is an important elongation process in autophagosome formation and is the most widely used detection indicator of autophagic formation, is not accumulated in ATG5/ATG7-independent macroautophagy. However, silenced of the upstream initiation protein like Beclin-1, Vps34 or ULK1 decreased the amount of ATG5/ATG7-independent macroautophagy.



Specific Aims

Hypoxia and nutrient deprivation widely exist in solid tumors because of the poor blood supply (Mueller-Klieser et al., 1988; Vaupel et al., 1989). In contrast to well-studied hypoxia, the role of nutrient deprivation in cancer cell metabolism, however, has not been fully elucidated. Thus, in this study, we explored the influence of nutrient deprivation on the cell metabolism and HIF-1 α expression as well as the regulatory mechanism. To achieve these aims, HBSS was used as the nutrient deprivation model.

1. To investigate the effect of nutrient deprivation on Warburg effect.
2. To explore the mechanism of the nutrient deprivation-affected Warburg effect.
3. To evaluate the effect of nutrient deprivation-induced Warburg effect on cell viability.
4. To investigate the effect on nutrient deprivation on HIF-1 α expression.
5. To explore the role of autophagy on nutrient deprivation-induced HIF-1 α expression.



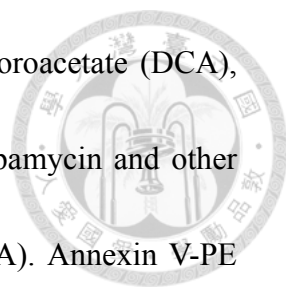
Materials and methods

Cell culture

HeLa and A431 cells were obtained from the American Type Culture Collection (Manassas, VA, USA), and CL1.5 was provided by Dr. Zhixin Yang (National Taiwan University, Taipei, Taiwan). Mouse embryonic fibroblasts (MEF) after immortalization were cultured in Dulbecco's modified Eagle medium complete medium supplemented with 10% (v/v) heated-inactivated fetal bovine serum, 100 U/ml penicillin, and 100 µg/ml streptomycin. Human umbilical vein endothelial cells (HUVEC) were purchased from ScienCell (Carlsbad, CA, USA). Cells were incubated at 37 °C in a humidified atmosphere of 5% CO₂ in air.

Reagents

HBSS (containing 5 mM glucose, 1.26 mM CaCl₂, 0.493 mM MgCl₂, 0.407 mM MgSO₄, 5.33 mM KCl, 0.441 mM KH₂PO₄, 4.17 mM NaHCO₃, 137.93 mM NaCl, and 0.338 mM Na₂HPO₄), dichlorodihydrofluorecein diacetate (DCFH₂-DA), 2-(N-(7-nitrobenz-2-oxa-1,3-diazol-4-yl)amino)-2-deoxyglucose (2-NBDG), and MitosoxRed were obtained from Invitrogen (Rockville, MD, USA). zVAD-fmk, compound C, and bafilomycin A1 were from Calbiochem (San Diego, CA, USA).



Butylated hydroxyanisole (BHA), N-acetyl-cysteine (NAC), dichloroacetate (DCA), propidium iodide (PI), 3-Methyladenine (3-MA), chloroquine, Rapamycin and other chemicals were obtained from Sigma Aldrich (St Louis, MO, USA). Annexin V-PE and 7-Aminoactinomycin D (7-AAD) were obtained from BioVision (Milpitas, CA, USA). Mito-TEMPO was purchased from Santa Cruz Biotechnology (Santa Cruz, CA, USA). The anti-HIF-1 α (for immunoblot) and Beclin 1 antibodies were from Becton Dickinson. The anti-LC3 polyclonal antibody was from MBL (Woburn, MA, USA). Specific anti-phospho-PDH E1 (Ser293) was obtained from NOVUS Biologicals (Littleton, CO, USA). Specific antibodies for phosphorylated AMPK (Thr172), PKM2 (Tyr105), JNK, p38, Akt, p70S6K (Thr389), 4E-BP1 (Ser65), total AMPK, caspase-3, PARP, PDK1, PDH, PKM2, p62, Akt, p70S6K and 4E-BP1 were purchased from Cell Signaling Technology (Beverly, MA, USA). Antibodies specific to HIF-1 α (for immunoprecipitation), PTB1, p38, JNK and normal rabbit IgG were from Santa Cruz Biotechnology (Santa Cruz, CA, USA). The anti-ATG5 antibody was from Abcam (Cambridge, UK). The anti- β -actin antibody was from Merck Millipore (Billerica, Ma, USA). Recombinant human PDHA1 which is a member of PDH complex and can be phosphorylated by PDK on Ser293 was obtained from SignalChem (Richmond, BC, Canada). All siRNAs and DharmaFECT Transfection Reagents were from Dharmacon (Lafayette, CO, USA). [γ -³²P]ATP was purchased from NEN (Boston, MA, USA).

[³⁵S]Methionine was purchased from GE Healthcare (Lafayette, CO, USA).



Plasmids transfection

Wild type (WT) and dominant negative (DN) AMPK plasmids were gifts from Dr. Kelly A. Wong (Whitehead Institute for Biomedical Research, Cambridge, MA, USA). The dual-tagged GFP-mRFP-LC3 plasmid was obtained from Addgene (Cambridge, MA, USA). The constitutive active Akt plasmid was kindly provided by Dr. Bing-Chang Chen (School of Respiratory Therapy, College of Medicine, Taipei Medical University, Taiwan). The pBIC-HIF-1 α (Galban et al., 2008) plasmid was a gift from Dr. Martin Holcik (Children's Hospital of Eastern Ontario Research Institute, Canada). Plasmids were transfected by Lipofectamine 2000 (Invitrogen) according to the manufacturer's instructions.

ROS detection

After starvation for the indicated time periods, cells were incubated in PBS containing 10 μ M DCFH₂-DA or 5 μ M MitoSoxRed for 30 min, and then washed with PBS, and immediately submitted to a flow analysis using a FACScan flow cytometer (Becton Dickinson, NJ, USA). Data were analyzed with the CellQuest program.



Annexin V/7-AAD staining

After starvation for the indicated time periods, cells were collected and washed with ice-cold PBS, and then incubated in calcium-containing PBS with Annexin V and 7-AAD for 30 min. After incubation, cells were immediately submitted to a flow analysis using a FACScan flow cytometer.

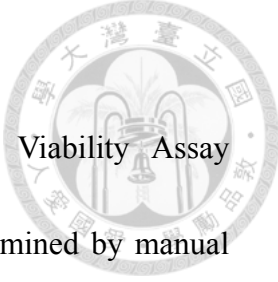
Cell cycle determination

After starvation for the indicated time periods, HeLa cells were collected and washed with ice-cold PBS, and then fixed with 70% (v/v) ethanol overnight at -20 °C. Fixed cells were washed with PBS, and then stained with 80 µg/ml PI. The cell cycle was measured by a FACScan flow cytometer.

Glucose uptake assay

2-NBDG is a fluorescent-labeled glucose analog that is incorporated into cells and allows quantification of glucose uptake. 2-NBDG was co-treated with HBSS starvation for 1 h, and the excess 2-NBDG was removed by washing with PBS. Cells were immediately submitted to a flow analysis using a FACScan flow cytometer.

ATP, LDH, pyruvate, lactate, and oxygen consumption assays

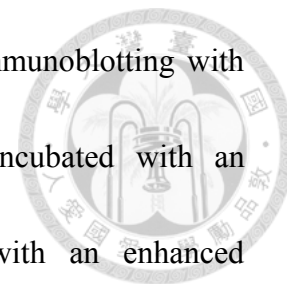


ATP was detected with a CellTiter-Glo[®] Luminescent Cell Viability Assay (Promega, Madison, WI, USA). Cytosolic LDH activity was determined by manual instructions of the CytoTox 96[®] Non-Radioactive cytotoxicity assay (Promega). Concentrations of intracellular total and cytoplasmic pyruvate and lactate in the culture medium were respectively determined with a Pyruvate Assay Kit and Lactate Assay Kit (BioVision, Milpitas, CA, USA). For cytoplasmic pyruvate assay, starved HeLa cells were swelled in Buffer A (0.05 mM PMSF, 10 mM HEPES, 1.5 mM MgCl₂, 100 mM KCl and 0.5 mM DTT) for 10 min and cell membrane was broken by dounce homogenizer. To remove mitochondria, cell lysate was centrifuged at 15,000xg for 30 min. The supernatant was determined as cytosol fraction. For oxygen consumption, HeLa cells were seeded in 3.5-cm dishes. After the indicated treatment, cells were collected, and the oxygen consumption rate was measured with MitoCell (MT200, Strathkelvin Instruments, North Lanarkshire, Scotland).

Immunoblot analysis

Cells were lysed in lysis buffer. After sonication, protein concentrations were determined using the Bio-Rad protein assay. Equal amounts of soluble protein were electrophoresed on 8%~12% SDS-PAGE, and transferred to Immobilon-P membranes.

Nonspecific binding was blocked with 5% nonfat milk. After immunoblotting with the first specific antibodies, membranes were washed and incubated with an HRP-conjugated secondary antibody. Protein was detected with an enhanced chemiluminescence detection reagent.



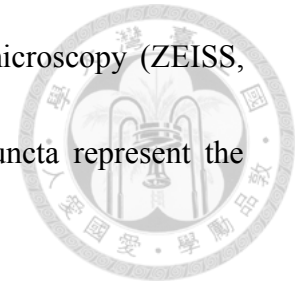
In vitro PDK kinase assay

To evaluate kinase activity of PDK, total protein extracts from the stimulated cell lysates were pre-cleaned at 4 °C for 1 h and then immunoprecipitated with 1 µg of the anti-PDK1 antibody for 4 h. Afterwards 10 µl protein A-agarose beads were added and rocked for another 30 min at 4 °C. The immunocomplexes were washed with cold lysis buffer, and then with kinase reaction buffer (20 mM Tris-HCl at pH 7.5, 10 mM MgCl₂, 2 mM DTT, and 10 µM ATP). Beads were incubated at 30 °C for 30 min in 25 µl kinase reaction buffer supplemented with 10 µCi of [γ -³²P]ATP and 1 µg recombinant human PDH protein. Reaction products were run on SDS-PAGE and transferred to polyvinylidene difluoride membranes, followed by autoradiography.

Microscopic detection of autophagosome

The tandem fluorescent-tagged LC3 construct (tfLC3) was transfected to cells by means of MicroPorator (Promega, USA). After HBSS starvation for 2 h, cells were

fixed with 4% paraformaldehyde and examined by a confocal microscopy (ZEISS, LSM 510 META Confocal Microscope). The yellow and red puncta represent the formation of autophagosome and autolysosome, respectively.



Quantitative real-time PCR

The cells were harvested using TriPure reagents (Roche) and total RNA was extracted by following the manufacturer's protocol. cDNAs were synthesized by using MMLV reverse transcriptase (Promega) and PCR was performed by using FastStart SYBR Green Master (Roche) and ABI Prism 7900 (Applied Biosystems). Each PCR reaction contained the cDNA, the Master Mix, and the following primers: HIF-1 α (forward: 5'- TGCTCATCAGTTGCCACTTC-3', reverse: 5'- TCCTCACACGCAAATAGCTG-3), and β -actin (forward: 5'- CGGGGACCTGACTGACTACC -3', reverse: 5'- AGGAAGGCTGGAAGAGTGC -3').

De novo translation

HeLa cells were cultured with methionine-free DMEM containing dialysed FBS for 2 h, and then 1 mCi [³⁵S]methionine was added for 30 min. After starvation by HBSS or CoCl₂ treatment, cells were lysed with RIPA buffer and precleaned with normal IgG.

Immunoprecipitation was performed by HIF-1 α antibody. Immunoprecipitated protein complexes were subjected to electrophoresis and expose to x-ray film.



Polysome analysis

Polysome analysis was conducted as described (Bor et al., 2006). Briefly, cycloheximide was added 30 min before HeLa cells were collected. Cells were scraped, resuspended with RSB buffer (10 mM Tris-HCl at pH 7.4, 10 mM NaCl, 3 mM MgCl₂ and 1000 U/ml RNasin) and lysed in equal volume of polysome extraction buffer (RSB buffer containing 1 % Triton X-100, 1 % deoxycholate, and 2 % Tween 20). After centrifuging, the cell extract was layered onto a 4 ml discontinuous 10% to 50% sucrose gradient. Fractionation was obtained with centrifugation at 36,000 rpm for 2 h at 4°C in a Beckman SW50 rotor. The gradient was monitored at 254 nm with ISCO UA-6 absorbance detector. The polysomal and nonpolysomal fractions were separated and subjected to mRNA isolation. cDNA was synthesized from equal volume of fractionated RNA and then PCR was performed with the following primers: HIF-1 α (forward: 5'-CTGGATGCTGGTGATTGGA-3', reverse: 5'- TTCATATCCAGGCTGTGTCG-3') and β -actin (forward: 5'-GCTGGAAGGTGG ACAGCGAG-3', reverse: 5'-TGGCATCGTGATGGACTCCG-3'). The PCR products were separated on a 3%

agarose gel and quantified by ImageJ.



***Xbp-1* splicing**

Xbp-1 splicing was analyzed by reverse transcription-PCR with the following primers:

Xbp-1 (forward: 5'-GAGTTAAGACAGCGCTTGGG-3', reverse: 5'-ACTGGGTCCAAGTTGTCCAG-3') and β -actin (forward: 5'-GCTGGAAGGTGGACAGCGAG-3', reverse: 5'-TGGCATCGTGATGGACTCCG-3'). The PCR products were separated on a 9% acrylamide gel and quantified by ImageJ.

IRES activity assay

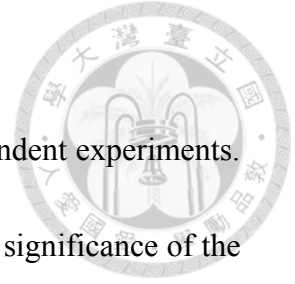
IRES activity was assayed by bicistronic reporter plasmid pBIC-HIF-1 α contains 2 to 352 bp of human HIF-1 α 5'UTR which has been ruled out the possibility of cryptic promoter activity and splicing of the bicistronic mRNA. Cells were transfected with pBIC-HIF-1 α . After indicated treatment, the amount of chloramphenicol acetyltransferase (CAT) was determined by CAT ELISA (Roche) according to the manufacturer's instructions. β -Galactosidase (β -Gal) enzymatic activity was determined by spectrophotometric assay using *o*-nitrophenyl- β -D-galactopyranoside. The relative IRES activity was calculated as the CAT/ β -Gal ratio.

Statistical evaluation

Values were expressed as the mean±S.E.M. of at least three independent experiments.

An analysis of variance (ANOVA) was used to assess the statistical significance of the

differences, and p values of < 0.05 were considered statistically significant.





Part I

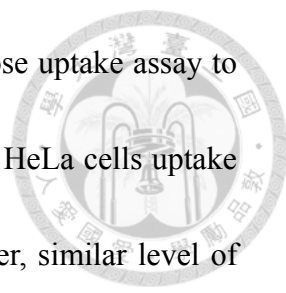
Nutrient deprivation induces the Warburg effect through ROS/AMPK-dependent activation of pyruvate dehydrogenase kinase



Results

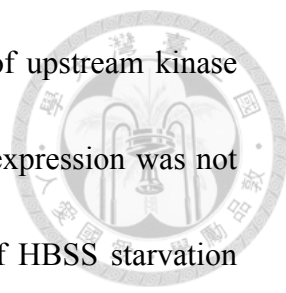
Nutrient deprivation induced the Warburg effect through the PDK/PDH pathway

In order to determine the effect of HBSS starvation on the Warburg response, the concentrations of lactate in the culture medium, the end product of glycolysis and the most important indicator of the Warburg effect, was detected. As shown in Fig. 1-1A, the extracellular level of lactate was significantly enhanced by HBSS starvation at 0.5~12 h in HeLa cells. Considering implanted tumor cells react differently to starvation condition (Kalaany and Sabatini, 2009) and this effect might be specific to cancer cell types, we tested various cancer cells and normal cells. We found that HBSS can also induce lactate production in A431, CL1.5, and HUVEC, but not in MEF (Fig. 1-1A). In contrast, HBSS starvation significantly reduced oxygen consumption in HeLa cells (Fig. 1-1B), suggesting that HBSS starvation not only induced the Warburg effect but also reduced mitochondrial oxidative phosphorylation. To determine if HBSS starvation exerts any effect on metabolic pathways responsible for the increased Warburg effect, glucose uptake, intracellular LDH activity, and pyruvate content were determined. Considering the status of different glucose concentrations containing in HBSS (i.e. 5 mM glucose) and DMEM (i.e. 25 mM



glucose), low glucose DMEM (5 mM) was also compared in glucose uptake assay to avoid an artificial effect from competition. As shown in Fig. 1-1C, HeLa cells uptake more glucose in HBSS than DMEM with 25 mM glucose; however, similar level of glucose uptake was observed in HBSS and DMEM with 5 mM glucose. We conclude that nutrient deprivation does not enhance glucose uptake within 1 h. In addition, LDH activity was not affected by nutrient deprivation (Fig. 1-1D). In the aspect of pyruvate, although the total amount of intracellular pyruvate was not changed by HBSS, the cytoplasmic pyruvate level was increased under nutrient deprivation (Fig. 1-1E).

Moreover, we also determined levels of PKM2 and PDH, two major enzymes which control the metabolism of pyruvate through either mitochondrial oxidative phosphorylation or the lactate pathway. As shown in Fig. 1-2A, HBSS starvation rapidly induced PDH E1 (Ser293) phosphorylation which is an inactivate form of PDH within 15~120 min, while PKM2 phosphorylation was not affected. Similar results of PDH phosphorylation by HBSS were also observed in A431, CL1.5 and HUVEC, but not in MEF (Fig. 1-2B). Since PDK is the only well-known enzyme to phosphorylate PDH, we tested the effect of a PDK inhibitor. We found that DCA, a PDK inhibitor (Whitehouse et al., 1974; Knoechel et al., 2006), significantly inhibited HBSS starvation-induced PDH phosphorylation (Fig. 1-2C). To understand if

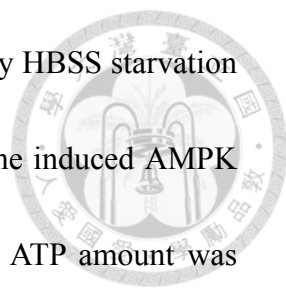


increased PDH phosphorylation results from the activity change of upstream kinase PDK, we first examined its protein expression. As a result, PDK expression was not affected under HBSS treatment (Fig. 1-2A). To further confirm if HBSS starvation affected PDK activity, an in vitro kinase assay was conducted by immunoprecipitating PDK followed by incubation with the recombinant PDHA1 protein. As shown in Fig. 1-2D, PDK activity following HBSS starvation increased within 2 h. All these results suggest that nutrient deprivation can induce the Warburg effect through the PDK/PDH pathway.

To further understand what nutrient component deficiency is involved in the HBSS-induced Warburg effect, we supplemented glucose, amino acids and/or FBS in HBSS. As a result, we found that 25 mM glucose delayed HBSS-induced PDH phosphorylation, while 10% FBS had no significant effect on PDH phosphorylation. Among the 5 amino acids tested (glutamine, leucine, arginine, histidine and cysteine), only cysteine significantly inhibited HBSS-induced PDH phosphorylation (Fig. 1-2E).

Nutrient deprivation activates AMPK to induce Warburg effect

Since nutrient deprivation is a condition of an energy crisis, we wondered if AMPK, an intracellular energy sensor, is involved in the HBSS starvation-induced Warburg effect. First, we determined if HBSS can induce AMPK (Thr172) phosphorylation. As



shown in Fig. 1-3A, AMPK phosphorylation was rapidly induced by HBSS starvation at 15 min and lasted for more than 2 h. Second, to understand if the induced AMPK phosphorylation is correlated with energy levels, the intracellular ATP amount was measured in HBSS-starved HeLa cells. As expected, the ATP level gradually decreased with time (Fig. 1-3B). Third, to understand if activated AMPK is responsible for energy conservation upon nutrient depletion, the AMPK inhibitor compound C and AMPK-DN were tested. We found that compound C and AMPK-DN further enhanced intracellular ATP loss after HBSS starvation (Fig. 1-3B).

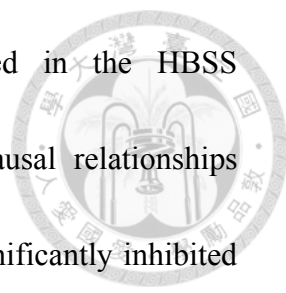
Next, we were interested to determine if AMPK is involved in the HBSS starvation-induced Warburg effect. As shown in Fig. 1-3C, compound C alone unexpectedly induced moderate PDH phosphorylation, and under this condition, HBSS starvation-induced PDH phosphorylation could not be further detected. These results suggest that AMPK plays a role in PDH phosphorylation induced by HBSS starvation. To confirm this notion, gene manipulation of AMPK activity was conducted by overexpressing AMPK-WT or AMPK-DN. As shown in Fig. 1-3D, AMPK-WT and AMPK-DN alone did not show significant effects on basal PDH phosphorylation. AMPK-DN significantly reduced HBSS starvation-induced PDH phosphorylation, while AMPK-WT did not have such effect. To understand if inhibition of PDH phosphorylation by compound C and AMPK-DN are functionally

associated with the outcome in energy regulation, lactate production was measured.

As shown in Fig. 1-3E, compound C and AMPK-DN indeed inhibited HBSS starvation-induced lactate production. All these results suggest that the HBSS starvation-induced Warburg effect is mediated by AMPK activation.

ROS production induced by nutrient deprivation promotes Warburg effect and is an upstream signal of AMPK

Since ROS are known to induce AMPK activation (Park et al., 2006; Farfariello et al., 2012), we explored if ROS are involved in the HBSS starvation-induced Warburg effect and is the upstream molecule for AMPK activation. First, DCFH₂-DA and MitoSoxRed staining were respectively used to detect cytosolic and mitochondrial ROS. We found that HBSS starvation induced a rapid but mild increase in cytosolic ROS at 0.5~4 h, which was then gradually reduced after starvation for 8 h (Fig. 1-4A). In contrast to cytosolic ROS, the level of mitochondrial ROS slowly increased, and achieved a marked and sustained response at 8~24 h (Fig. 1-4A). Next, we found that NAC which reduced cytosolic ROS increase (Fig. 1-4B) can significantly inhibit both basal and HBSS starvation-induced lactate production (Fig. 1-4C) as well as PDH phosphorylation (Fig. 1-4D). These results suggest that the HBSS starvation-induced Warburg effect is mediated by ROS production.



After observing that both ROS and AMPK are involved in the HBSS starvation-induced Warburg effect, we next determined their causal relationships using a pharmacological approach. Results revealed that NAC significantly inhibited HBSS starvation-induced AMPK phosphorylation (Fig. 1-4E). In contrast, inhibition of AMPK phosphorylation by compound C and AMPK-DN had no significant effect on cytosolic ROS production (Fig. 1-4F). These data indicated that ROS are the upstream signal for AMPK activation upon HBSS starvation. Finally, since HBSS starvation induced PDK-dependent PDH phosphorylation, we were interested in exploring if the ROS/AMPK signal affects PDK activation. As shown in Fig. 1-4G, inhibition of AMPK and ROS by compound C and NAC respectively significantly inhibited HBSS starvation-induced PDK activity. Thus, we concluded that the HBSS starvation-induced Warburg effect acts through the ROS/AMPK/PDK/PDH pathway.

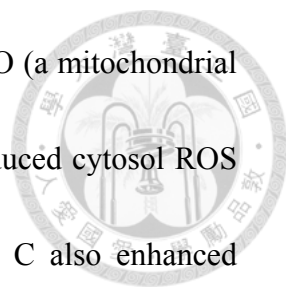
The Warburg effect reduces cell apoptosis upon nutrient deprivation

Next, we were interested in clarifying the role of increased Warburg effect in cell viability under nutrient deprivation stress. First, we characterized the death phenomenon of apoptosis in HBSS starvation. We found that HBSS starvation significantly induced apoptosis of HeLa cells (Fig. 1-5A), and this action was inhibited by zVAD, a pan-caspase inhibitor (Fig. 1-5B). In addition, HBSS starvation

time-dependently increased the cell population at the sub-G₁ phase at 6~24 h (Fig. 1-5C). To verify if HBSS starvation induced caspase-dependent cell death, immunoblotting was conducted to analyze caspase-3 cleavage. As a result, caspase-3 was cleaved to an active form after HBSS starvation for 8 h (Fig. 1-5D). Consistent with caspase-3 activation, PARP-1, a substrate of caspase-3, was time-dependently cleaved after HBSS starvation (Fig. 1-5E).

It has been reported that in dead cells MitoSOXRed can be released from the mitochondria and bind to nuclear DNA, giving a large artificial signal (Mukhopadhyay et al., 2007). To clarify if HBSS-induced mitochondrial ROS production at 8~24 h (Fig. 1-4A) is because of cell death, excluding signal of annexin V-positive dead cells and inhibition of cell death by zVAD were conducted. As shown in Fig. 1-5F, HBSS still can induce significant mitochondrial ROS production in annexin V negative cells and zVAD-treated cells. These results suggest that HBSS indeed can increase mitochondrial ROS production at the later time point.

Next, we like to understand if ROS/AMPK/PDK/PDH pathway is involved in the regulation of cell viability. Thus, we tested the effects of pharmacological inhibitors of ROS, AMPK and PDK on HBSS starvation-induced cell apoptosis. Results of Fig. 1-5G showed that DCA, a well-known inhibitor of PDK and thereby the Warburg effect, can concentration-dependently enhance HBSS starvation-induced cell



apoptosis. Similarly, the antioxidants BHA, NAC and Mito-TEMPO (a mitochondrial specific ROS scavenger), which can respectively inhibit HBSS-induced cytosol ROS (Fig. 1-4B) and mitochondrial ROS (Fig. 1-5H), and compound C also enhanced HBSS starvation-induced cell apoptosis at 12 h (Fig. 1-5I). Notably, BHA, NAC and compound C treatment alone induced moderate cell apoptosis. These results suggest that HBSS starvation-induced ROS production and AMPK phosphorylation play a protective role in cell viability. In addition, similar to the effect of compound C, AMPK-DN expression significantly enhanced HBSS-induced cell apoptosis at 12 h (Fig. 1-5J). Taken together, these results suggest that the HBSS starvation-induced Warburg effect can delay cell death.

PDK is not involved in nutrient deprivation-induced autophagy

Autophagy was found to be induced when cells suffer from nutrient and energy deprivation, and can delay cell death by recycling protein and organelles to amino acids which support energy production. Since ROS increase induced by Earle's balanced salt solution, a low nutrient buffer similar to HBSS, leads to autophagy (Scherz-Shouval et al., 2007), and AMPK was also evidenced to induce autophagy by inhibition of mTOR (Meley et al., 2006), we wondered if PDK activity is involved in HBSS starvation-induced autophagy. First we determined HBSS starvation-induced

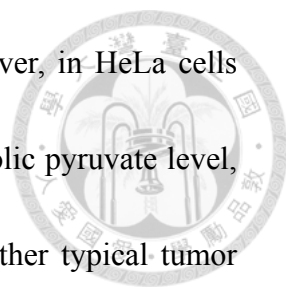
autophagy by Western blotting and confocal microscopy. Results of Fig. 1-6A showed a higher signal of LC3-II than that of LC3-I in resting HeLa cells, and after inhibition of lysosome activity by bafilomycin A1, the LC3-II level significantly and time-dependently accumulated within 1~6 h. Under bafilomycin A1 treatment, the increased LC3-II/LC3-I ratio induced by HBSS was higher than normal medium. We also used a dual-tagged GFP-mRFP-LC3 construct to monitor the maturation process of autophagosomes and autolysosomes. Results showed the significant appearance of red dots (i.e., a signal of autolysosome) and yellow dots (i.e., a signal of autophagosome) in cells receiving HBSS starvation (Fig. 1-6B), suggesting the ability of HBSS starvation to induce autophagic flux. Next, we determined if PDK activation is involved in HBSS starvation-induced autophagy. To this end, we used DCA to inhibit PDK activity. As shown in Fig. 1-6C, DCA did not have a significant effect on HBSS starvation-induced LC3 conversion. This result suggests that PDK activity is not involved in HBSS starvation-induced autophagy.



Discussion

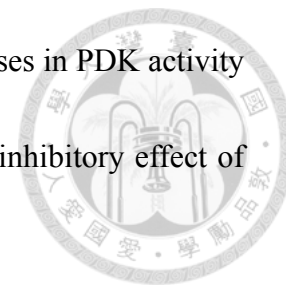
In addition to hypoxia, starvation is another characteristic of solid tumors. In contrast to hypoxia, the role of starvation in tumorigenesis still remains elusive. So far, starvation-induced autophagy is the most well-known mechanism to promote tumor cell survival (Kung, 2011; Mathew and White, 2011). In the present study, we tried to elucidate the effects and underlying molecular events of nutrient deprivation on metabolic changes, which thus affect cell viability. Therefore, we used HBSS as a starvation model and found that nutrient deprivation enhances the Warburg effect and delays cell apoptosis induced by HBSS starvation.

The Warburg effect is proven to enhance tumorigenesis and has garnered attention as a target for tumor treatment (Vander Heiden et al., 2009; Ponisovskiy, 2011). Lactate, the final product of the Warburg effect, is shown to impact various aspects of tumorigenesis, including immune escape (Gottfried et al., 2006; Fischer et al., 2007), cell migration (Baumann et al., 2009; Goetze et al., 2011), and radio-resistance (Groussard et al., 2000; Sattler et al., 2010). Our present data for the first time unveil a new cascade linking nutrient starvation and Warburg effect. In metabolic profiles, we found that HBSS starvation could induce lactate production in various cancer cell types and even in normal cells. However, in normal cells, Warburg effect exhibits the cell type specificity. Currently the reason why HBSS cannot induce Warburg effect in

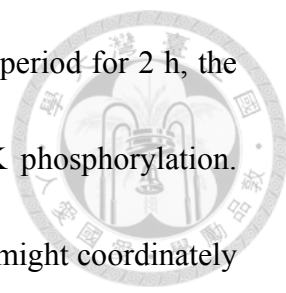


MEF unlike that seen in HUVEC is not fully understood. Moreover, in HeLa cells HBSS starvation cannot affect glucose uptake, but increases cytosolic pyruvate level, while inhibits oxygen consumption. Notably, unlike hypoxia, another typical tumor environment that facilitates the Warburg effect by upregulating enzymes expression of PKM2 and LDH (Brahimi-Horn et al., 2007; Porporato et al., 2011), we did not observe any changes in LDH activity, PKM2 Tyr105 phosphorylation or PKM2 protein expression after HBSS starvation for 2 h. Nevertheless, similar to hypoxia (Kim et al., 2006), HBSS starvation also induced PDH phosphorylation and inactivated PDH, leading to the inhibition of the conversion of pyruvate to acetyl-CoA, but the increase of pyruvate metabolism to lactate by LDH. Since PDH condenses the pyruvate into acetyl-CoA in mitochondria, the inhibition of PDH activity by nutrient deprivation should be responsible for the elevated cytosolic pyruvate level. For hypoxia-induced PDH phosphorylation, transcriptional upregulation of PDK expression via the HIF-1 α pathway is suggested (Wu et al., 2000). On the other hand, long-term starvation for 48 h was also reported to induce PDH phosphorylation by upregulation of PDK expression in the rat heart and skeletal muscle (Sugden et al., 2000; Wu et al., 2000). In this aspect, we did not detect any changes in PDK expression in HeLa cells undergoing HBSS starvation within 2 h. In our case, however, we found that starvation increases PDH phosphorylation via PDK

activation. This notion is supported by the parallel and rapid increases in PDK activity and PDH phosphorylation after nutrient starvation, as well as the inhibitory effect of DCA in this event.



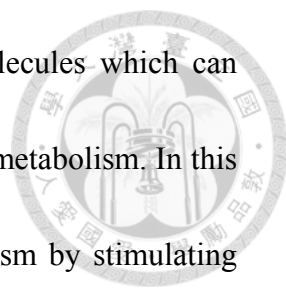
HBSS starvation also concomitantly and rapidly reduces intracellular ATP content and induces AMPK activation within 15 min. Since an increased AMP/ATP ratio induces AMPK phosphorylation, the reduced ATP level is at least one of the possibilities for inducing AMPK activation in cells subjected to HBSS conditioning. Moreover, besides ATP loss, we also showed the involvement of cytosolic ROS in AMPK activation at least at the early stage of HBSS starvation. The ROS scavenger NAC significantly inhibited HBSS starvation-induced AMPK phosphorylation, while the AMPK inhibitor had no significant effect on HBSS starvation-induced cytosolic ROS. Consistently, ROS were found to be upstream molecules of AMPK (Jorgensen and Rose, 2008; Jung et al., 2008). Regarding cytosolic ROS increase, we suggest it is generated from NADPH oxidase, because previous studies showed that serum starvation and growth factor starvation induced ROS production through NADPH oxidase (Rygiel et al., 2008; Liu et al., 2012). Moreover, aberrant ROS generation initially occurring through NADPH oxidase was reported to facilitate mitochondrial damage (Herrera et al., 2001). Therefore, we suggest that the early cytosolic ROS production caused by HBSS starvation might lead to remarkable ROS production



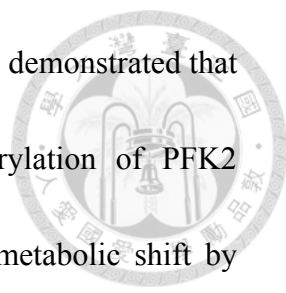
from mitochondria at late stage. Moreover, under our examination period for 2 h, the time course of cytosol ROS production is correlated with AMPK phosphorylation. Thus we suggest that both ATP loss and cytosolic ROS production might coordinately mediate the HBSS starvation-induced AMPK pathway. Nevertheless, we still cannot rule out the possible regulation between AMPK and mitochondrial ROS at late stage of HBSS starvation and subsequent outcomes in terms of Warburg effect and cell death, for example after 8 h upon an apparent mitochondrial ROS being increased.

Previous studies showed the ability of AMPK to induce glycolysis via activation of PFK2 (Mukhtar et al., 2008; Wu and Wei, 2012); however, the metabolic outcome in terms of the Warburg effect remains unknown. In this study, we found the intracellular pyruvate level after short-term treatment with HBSS starvation is not changed, but we did detect an increased cytosolic pyruvate level, which might contribute to the rapid production of lactate. In this study, we for the first time demonstrated the involvement of ROS-dependent AMPK in PDK activation. Due to significant inhibition of PDH phosphorylation by compound C, NAC, and expression of AMPK-DN, we suggest that ROS production and AMPK activation induced by HBSS starvation mediate PDH phosphorylation. In agreement with these findings, NAC and compound C can reduce PDK activity.

Since PDH is a key enzyme controlling pyruvate catabolism by shifting pathways

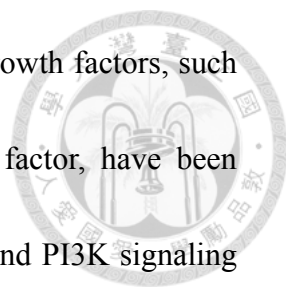


between mitochondrial phosphorylation and LDH formation; molecules which can modulate PDH phosphorylation should have an effect on pyruvate metabolism. In this aspect, NAC was shown to improve mitochondrial TCA metabolism by stimulating carbon flux through PDH, while the underlying molecular event has never been elucidated (Zwingmann and Bilodeau, 2006). Our current results not only support previous findings, but also highlight the role of ROS in shifting energy-producing processes from mitochondrial metabolism to the Warburg effect. We showed that NAC treatment alone in normal medium can alter the Warburg effect and mitochondrial metabolism in a reverse manner, i.e., reducing lactate formation but increasing oxygen consumption (data not shown). Likewise, HBSS starvation-induced lactate production is significantly inhibited by NAC. Similar to NAC, cysteine significantly inhibits HBSS-induced PDH phosphorylation. It may be because of cysteine is a precursor of glutathione and possesses the antioxidant activity (Droge, 2005). AMPK was shown to exert multiple effects on metabolic changes, and in the present study, we demonstrated that HBSS starvation-induced AMPK activation led to PDH phosphorylation and lactate production. However, we also observed that compound C itself induced moderate PDH phosphorylation without affecting PDK activity. Currently we cannot provide explanation for this discrepancy, and the effects of compound C on PDH phosphatase and/or other unidentified kinases of PDH still



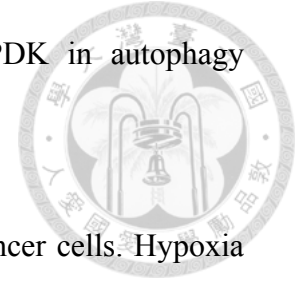
need to be investigated in the future. Therefore, we for the first time demonstrated that AMPK controls not only the glycolysis pathway by phosphorylation of PFK2 (Mukhtar et al., 2008; Wu and Wei, 2012) but also a pyruvate metabolic shift by regulation of PDK activity. Furthermore, due to PDK is a mitochondrial protein and AMPK locates in cytosol, we speculate the AMPK-dependent regulation of PDK occurs in an indirect manner.

Starvation was shown to induce apoptosis in different cell types (Braun et al., 2011), and our results also support this notion. In our study, HBSS starvation induces apoptosis and the active form of caspase-3 is induced in a time course correlated with PARP-1 cleavage, an index of caspase-3 activation. Furthermore, we found that inhibition of the Warburg effect by DCA enhances HBSS starvation-induced cell death. Inhibition of PDK upstream molecules, ROS and AMPK, produces similar results as with DCA. These data suggest that an increased Warburg effect upon HBSS starvation confers greater resistance to the death process upon cells. However, BHA and NAC itself slightly induced cell apoptosis. Although, ROS were thought as toxic by directly damage cellular proteins and DNA. Accumulation of oxidative damages has been shown to relate to neurodegenerative diseases, diabetes, cancer, and aging (Sena and Chandel, 2012; Liochev, 2013; Nogueira and Hay, 2013). Paradoxically, more and more evidence indicated that ROS also served as critical signaling



molecules in cell proliferation and survival (Ray et al., 2012). Growth factors, such as insulin, Platelet-derived growth factor and epidermal growth factor, have been demonstrated to induce ROS production which regulated MAPK and PI3K signaling by transiently oxidized and inhibited protein tyrosine phosphatase (Bennett et al., 1996; Meng et al., 2002; Meng et al., 2004). Inhibition of physiological ROS may induce cell death. Moreover, NAC has been widely investigated for its anticancer efficacy in clinical, and the effectiveness of NAC is believed to depend on the antioxidant properties (Zahid et al., 2010; De Flora et al., 2001). NAC has been shown to regulate cell cycle progression, differentiation, migration, and angiogenesis by targeting cyclin D1, I B, metalloproteinases 2/9, and angiostatin. Furthermore, NAC induced growth arrest and apoptosis by expression of HMG boxcontaining protein 1, a transcription suppressor, and decreased EGFR/Akt activation in oral cancers (Lee et al., 2013). In that case, we proposed that BHA and NAC induced cell death is because of the inhibition of physiological ROS which is important in cellular signaling. Besides the Warburg effect, autophagy is an evolutionarily conserved phenomenon for maintaining homeostatic functions such as protein degradation and organelle turnover. Nutrient deprivation was shown to induce autophagy which can delay nutrient deprivation-induced cell death (Jin and White, 2007). In the present study, autophagy indeed is induced upon HBSS starvation;

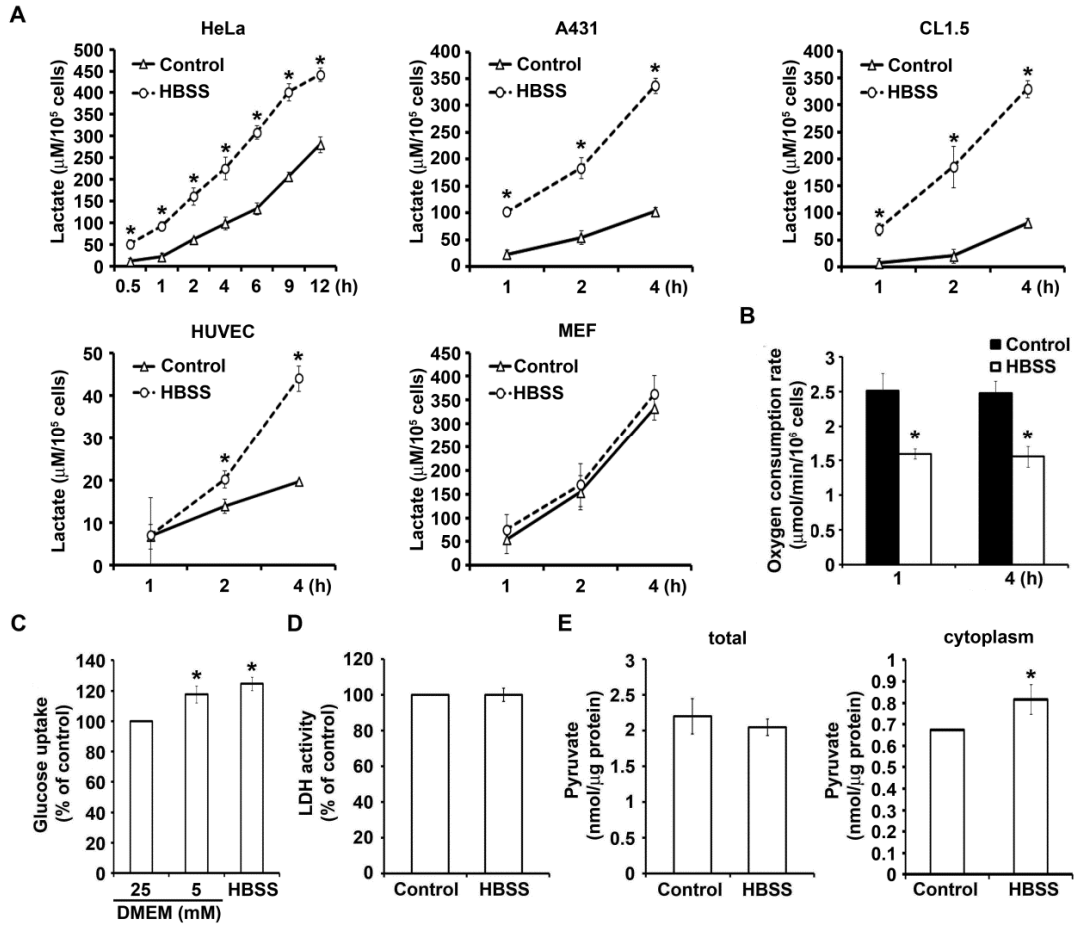
however, our data using DCA rule out the involvement of PDK in autophagy induction in the case of nutrient deprivation.



The Warburg effect provides several growth advantages for cancer cells. Hypoxia is well known to induce the Warburg effect through HIF-1 α accumulation. In the present study, we demonstrated that nutrient deprivation, another characteristic of solid tumors, also induces the Warburg effect to support cell viability upon starvation stress (Fig. 1-7). Unlike HIF-1 α which induced expression of PDK, we for the first time demonstrated that a low-nutrient condition drives cancer cells to utilize glycolysis to produce ATP, and this increased Warburg effect is through a novel mechanism involving ROS/AMPK-dependent activation of PDK. In addition, autophagy provides an alternative mechanism in accompany with Warburg effect to protect cells against nutrient stress.



Figure 1-1



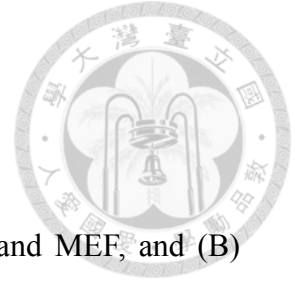


Figure 1-1. Nutrient deprivation induces the Warburg effect.

(A) Extracellular lactate levels in HeLa, A431, CL1.5, HUVEC and MEF, and (B)

oxygen consumption were detected after cells were treated with HBSS for the

indicated time periods. (C) Glucose uptake, (D) LDH activity, and (E) total and

cytoplasmic pyruvate were detected after HeLa cells were treated with HBSS for 1 h.

Data were the mean \pm S.E.M. from at least three independent experiments. * $p < 0.05$,

indicating significant effects of HBSS starvation and low glucose (5 mM).



Figure 1-2

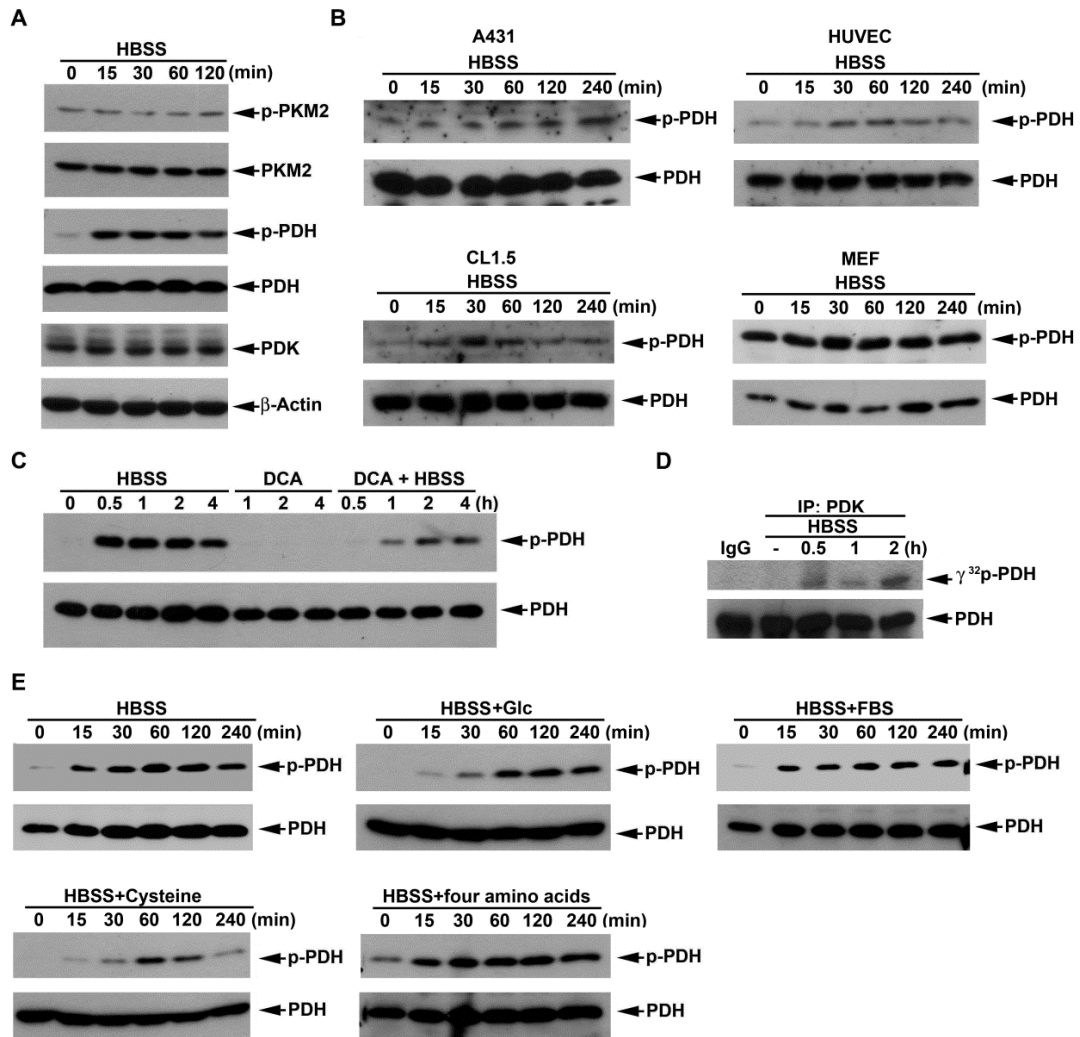


Figure 1-2. Nutrient deprivation activates the PDK/PDH pathway.

(A, C, E) HeLa cells and (B) A431, CL1.5, HUVEC and MEF were treated with HBSS for the indicated time periods, either in the presence or absence of DCA (10 mM), glucose (25 mM), 10% FBS, four amino acids (4 mM glutamine, 0.8 mM leucine, 0.4 mM arginine, 0.2 mM histidine) or 0.2 mM cysteine. Total cell lysates were collected and subjected to Western blot analysis using the indicated antibodies.

(D) After treatment with HBSS for the indicated time periods, PDK was immunoprecipitated and subjected to kinase assay. Results were representative of three independent experiments.

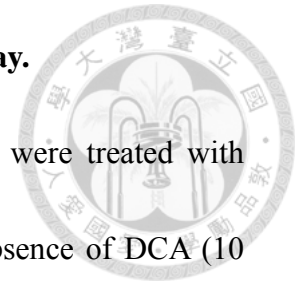




Figure 1-3

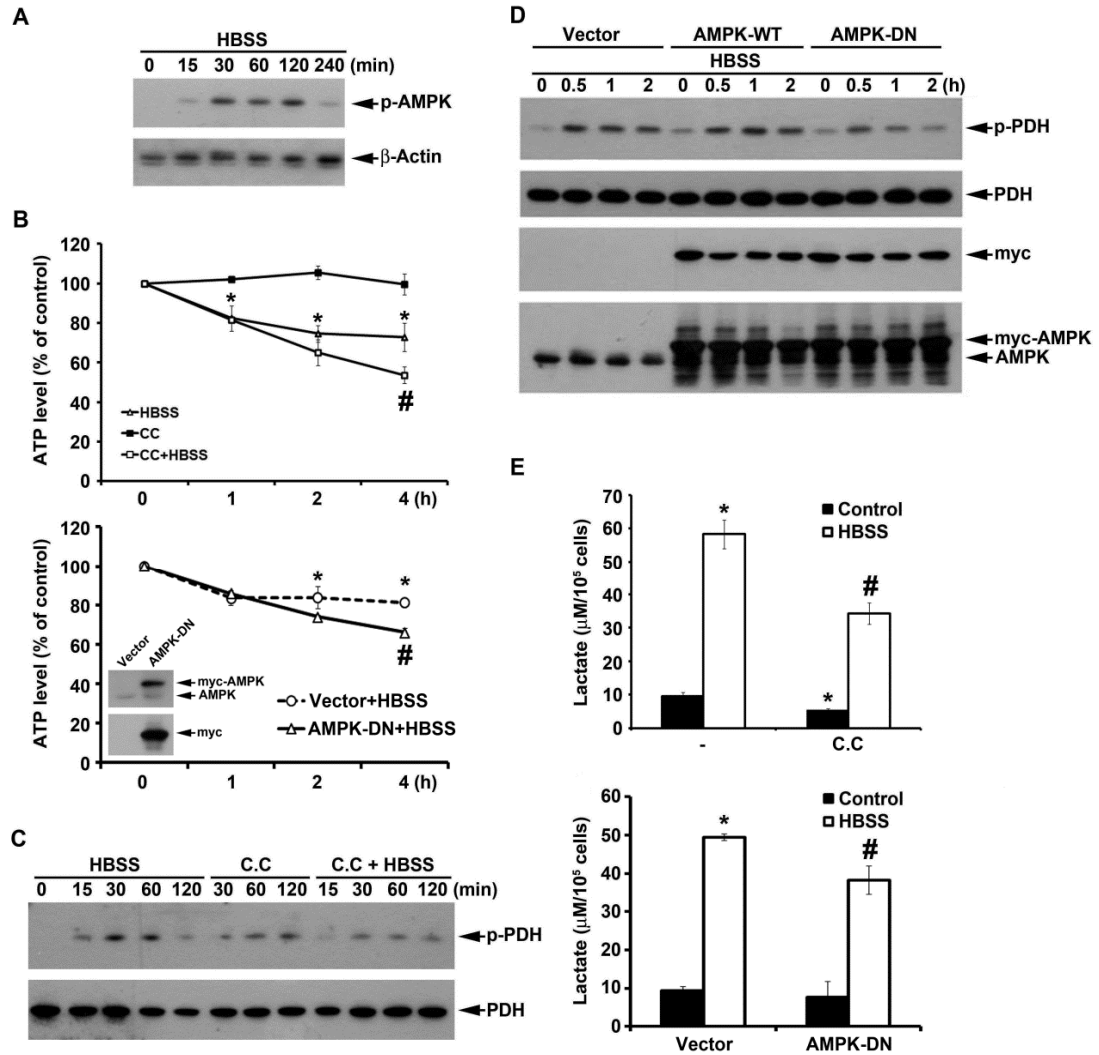




Figure 1-3. AMPK is involved in the nutrient deprivation-induced Warburg effect.

(A) HeLa cells were treated with HBSS for the indicated time periods, and AMPK was determined by immunoblotting. (B) After pretreatment with 10 μ M compound C or overexpression of AMPK-DN, cells underwent HBSS starvation, and intracellular ATP levels were determined at the indicated time points. (C) Cells were pretreated with compound C followed by HBSS starvation. PDH phosphorylation was determined by immunoblotting. (D) Cells were transfected with myc-tagged AMPK-WT or AMPK-DN, followed by HBSS starvation. Total cell lysates were collected and subjected to a Western blot analysis using the indicated antibodies. (E) Extracellular lactate was detected in HeLa cells which were treated with 10 μ M compound C or AMPK-DN, followed by HBSS starvation for 1 h. Data in (B) and (E) were the mean \pm S.E.M. from at least three independent experiments. * $p < 0.05$, indicating significant effects of HBSS starvation and compound C compared to control cells. # $p < 0.05$, indicating significant inhibition of HBSS starvation-induced intracellular ATP loss and lactate formation by compound C and AMPK-DN.



Figure 1-4

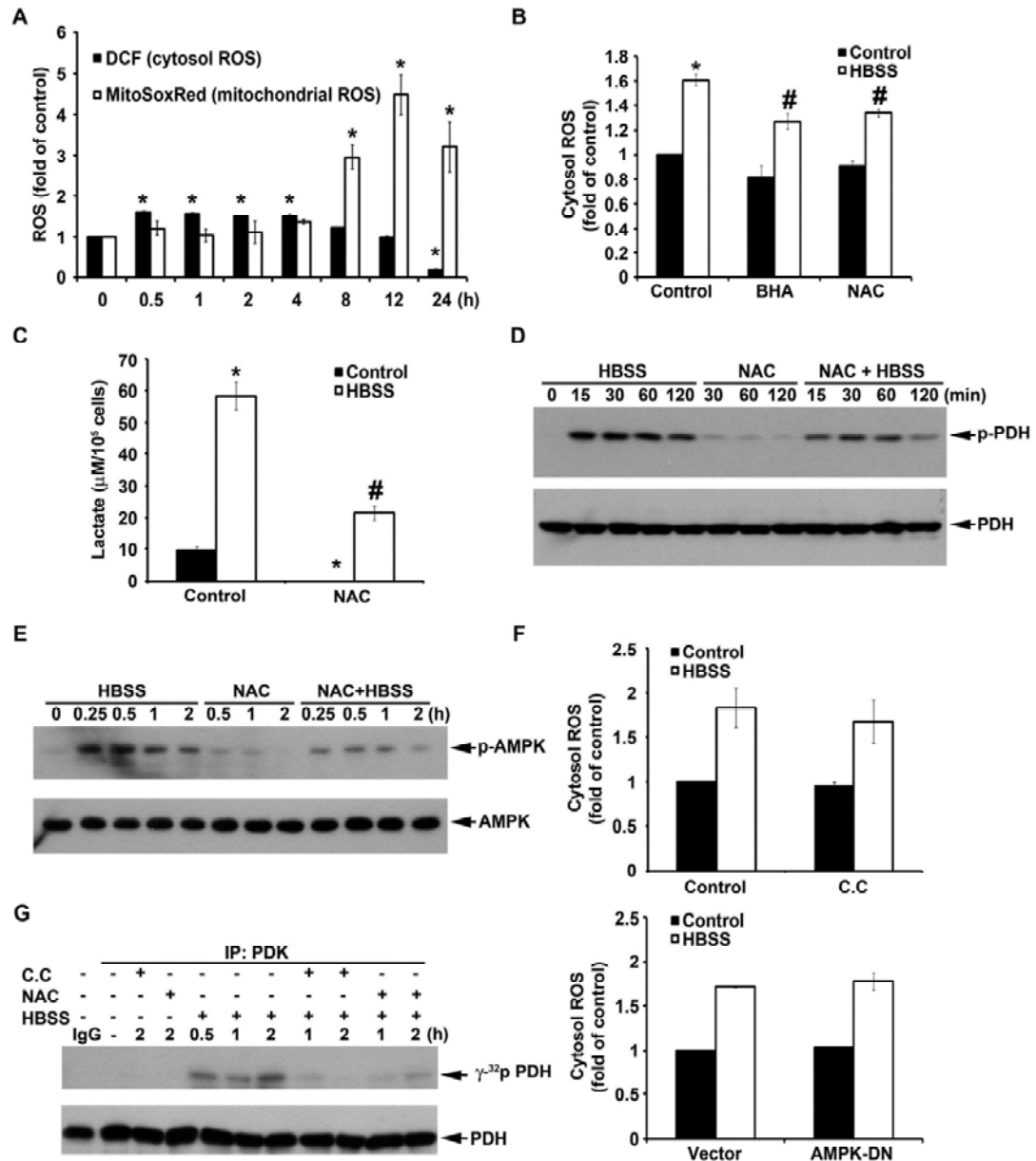


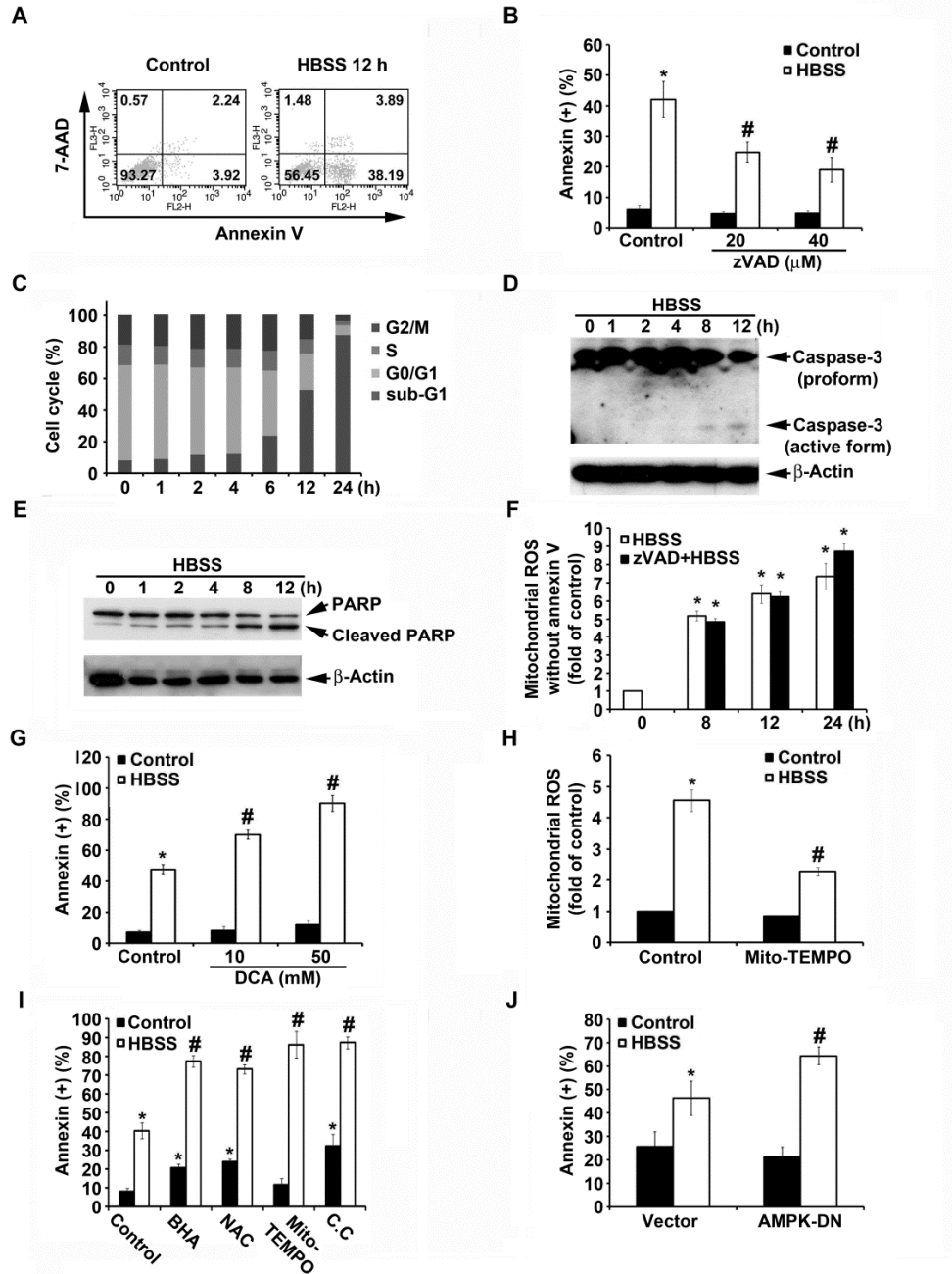


Figure 1-4. ROS are involved in the nutrient deprivation-induced Warburg effect and are upstream signals of AMPK.

(A) Cytosolic and mitochondrial ROS were detected after HeLa cells were treated with HBSS for the indicated time periods. (B, C) Cytosolic ROS (B) and extracellular lactate (C) were detected after HeLa cells were treated with HBSS for 1 h in the absence or presence of BHA (100 μ M) or NAC (10 mM). (D, E) HeLa cells were treated with or without 10 mM NAC for 30 min followed by HBSS starvation for the indicated time periods. Phosphorylation of PDH (D) and AMPK (E) were detected by a Western blot analysis. (F) Cytosolic ROS were detected after HeLa cells were treated with HBSS for 1 h with 10 μ M compound C or overexpression of AMPK-DN. (G) After treatment with HBSS with or without 10 μ M compound C or 10 mM NAC for the indicated time periods, PDK was immunoprecipitated and subjected to a kinase assay. Data in (A), (B), (C), and (F) were the mean \pm S.E.M. from at least three independent experiments. * $p < 0.05$, indicating significant effects of HBSS starvation and NAC compared to control cells. # $p < 0.05$, indicating significant inhibition of HBSS starvation-induced cytosolic ROS and lactate formation by BHA or NAC.



Figure 1-5



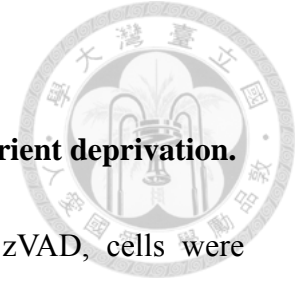
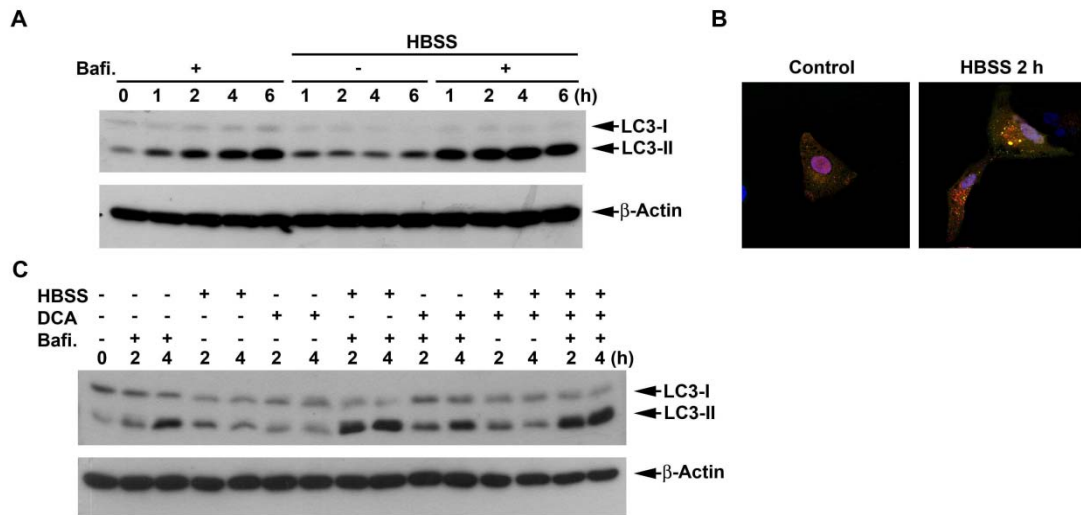


Figure 1-5. The Warburg effect reduces cell apoptosis upon nutrient deprivation.

(A, B) After treatment with HBSS for 12 h with or without zVAD, cells were collected for the cell death analysis using Annexin V/7-AAD double staining. (C) Cell cycle analysis using propidium iodide (PI) staining was conducted after HBSS starvation for the indicated time periods. (D) Caspase-3 activation and (E) PARP cleavage were detected by a Western blot analysis after HBSS starvation for the indicated time periods. (F) After treatment with HBSS for 8~24 h with or without zVAD, cells were stained with MitoSoxRed and annexin V. (G, I, J) After treatment with HBSS for 12 h with or without DCA (G), BHA (100 μ M), NAC (10 mM), Mito-TEMPO (500 μ M), compound C (10 μ M) (I), or overexpression of AMPK-DN (J), cells were collected for a cell death analysis using Annexin V/7-AAD double staining. (H) After treatment with HBSS for 12 h with or without Mito-TEMPO (500 μ M), cells were collected for mitochondrial ROS analysis using MitoSoxRed. Data in (B), (F)-(J) were the mean \pm S.E.M. from at least three independent experiments. * $p < 0.05$, indicating significant effects of HBSS starvation and the indicated agents compared to control cells. # $p < 0.05$, indicating significant inhibition of HBSS starvation-induced responses by various manipulations.



Figure 1-6



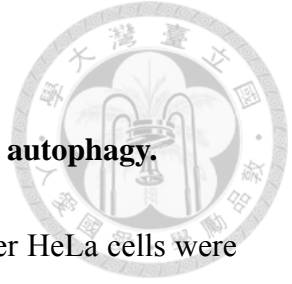


Figure 1-6. PDK is not involved in nutrient deprivation-induced autophagy.

(A, C) LC3 conversion was detected by a Western blot analysis after HeLa cells were treated with HBSS for the indicated periods, with or without the presence of 50 nM bafilomycin A1 (A, C) or 10 mM DCA (C). (B) Dual-tagged GFP-mRFP-LC3 was overexpressed in HeLa cells to monitor the maturation processes of autophagosomes (yellow puncta formation) and autolysosomes (red puncta formation).



Figure 1-7

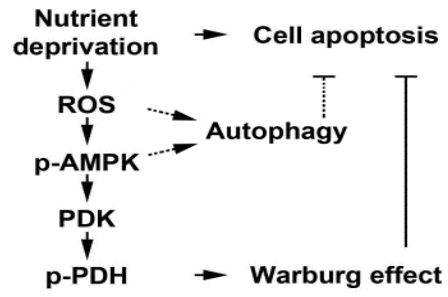




Figure 1-7. Schematic summary of the nutrient deprivation-induced Warburg effect and autophagy in HeLa cells.

HBSS starvation induces the cytoprotective Warburg effect by upregulating the PDK activity via an AMPK-dependent mechanism. The ROS-mediated AMPK pathway leads to PDK activation and PDH phosphorylation, which in turn loses its ability to convert pyruvate to acetyl-CoA, but increases pyruvate metabolism to lactate by LDH. In addition, nutrient starvation also induces autophagy, which provides an additional pathway independent of Warburg effect to protect cells against metabolic stress.



Part II

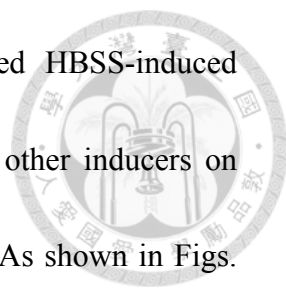
**Beclin-1-independent autophagy positively regulates internal
ribosomal entry site-dependent translation of hypoxia-inducible
factor 1 α under nutrient deprivation**



Results

HBSS induces HIF-1 α expression and potentiates the HIF-1 α responses of hypoxia and CoCl₂

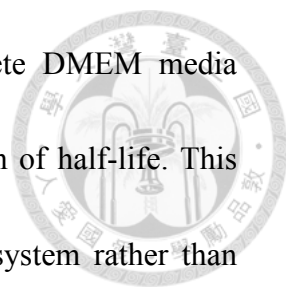
To understand the effect of nutrient deprivation on HIF-1 α expression, the medium HBSS containing 5 mM glucose in the absence of 10% FBS was used as a starvation model to treat different cancer cell lines. As shown in Fig. 2-1A, HBSS significantly induced HIF-1 α expression around 1 h treatment and sustained this effect over 5 h in HeLa cells. Considering the cell type-specificity of this effect, we tested various cancer and normal cell types. We found that HBSS still can increase HIF-1 α expression in A431 and A375 cancer cells as well as the primary HUVEC (Fig. 2-1A). To further understand what nutrient component(s) deficiency is involved in the HBSS-induced HIF-1 α expression, we supplemented glucose, amino acids or FBS in HBSS. As a result shown in Fig. 2-1B, we found that 25 mM glucose had no significant effect on HBSS-induced HIF-1 α expression, while 10% FBS totally reversed HBSS-induced HIF-1 α expression. Among the 5 amino acids (glutamine, leucine, arginine, histidine and cysteine) tested, which have been studied for nutrient deprivation (Armstrong et al., 2004; Drogat et al., 2007; Torii et al., 2011; Averous et al., 2012; Garcia-Navas et al., 2012), only cysteine, but not the combination of



glutamine, leucine, arginine and histidine, significantly inhibited HBSS-induced HIF-1 α expression (Fig. 2-1B). To test the effect of HBSS with other inducers on HIF-1 α expression, HBSS was co-treated with hypoxia or CoCl₂. As shown in Figs. 2-1C and 2-1D, the extent of HIF-1 α expression induced by HBSS was similar to that under CoCl₂ treatment, but is much less than that induced by hypoxia. Interestingly HBSS showed synergistic interaction with CoCl₂ and hypoxia, suggesting that nutrient deprivation-induced HIF-1 α expression is resulting from a mechanism different from CoCl₂ and hypoxia.

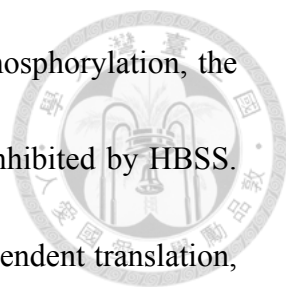
HBSS enhances HIF-1 α expression through IRES-dependent translation

To understand HBSS-induced HIF-1 α expression through regulating transcriptional, translational and/or protein stability levels, different experiments were conducted. In the aspect of transcription, we found that HBSS has no effect on HIF-1 α mRNA expression within 4 h (Fig. 2-2A). We conclude that HBSS-induced HIF-1 α expression is not at transcriptional level. Next, we used cycloheximide (CHX), a general translation inhibitor, to determine if HBSS-induced HIF-1 α expression is via affecting protein stability. After induction of HIF-1 α by HBSS treatment for 4 h, HBSS was changed to complete DMEM with 10% FBS or remained in HBSS with or without CHX, and the HIF-1 α protein degradation was determined. As shown in Fig.



2-2B, the HIF-1 α protein degradation rate measured in complete DMEM media regardless of CHX treatment or not was similar, i.e. around 5 min of half-life. This result suggests that the protein degradation through proteasome system rather than protein synthesis process plays immediate and almost the major role in controlling HIF-1 α protein expression. In cells with HBSS replacement and sustained HIF-1 α expression, CHX treatment also rapidly led to protein degradation by 56% at 5 min, suggesting that HBSS-induced HIF-1 α expression in major does not result from protein stabilization. To understand if HBSS-induced HIF-1 α expression is through HIF-1 α protein newly synthesis, de novo translation was conducted by [³⁵S]methionine labeling. As shown in Fig. 2-2C, HBSS can enhance de novo HIF-1 α translation. Similarly CoCl₂ exerts this action as previously reported (Galban et al., 2008). To directly demonstrate the ability of HBSS to enhance HIF-1 α translation, the relative associations of HIF-1 α mRNA with the polysomal and nonpolysomal fraction were determined. As shown in Fig. 2-2D, HBSS enhanced HIF-1 α mRNA binding to polysome by 20%, while hypoxia has no significant effect as previously reported (Lang et al., 2002).

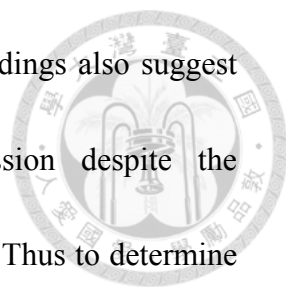
This finding drives us to determine if the cap-dependent translation signaling is induced by HBSS. As shown in Fig. 2-2E, p70S6K and 4E-BP1 phosphorylation, indexes of cap-dependent translation, however, were significantly inhibited by HBSS.



Consistent with the inhibition of cap-dependent translation, Akt phosphorylation, the upstream molecule of mTOR, was also significantly and rapidly inhibited by HBSS. After ruling out the induced HIF-1 α by HBSS is related to cap-dependent translation, we next determined if it is through IRES-dependent translation, as it has been reported that 5' UTR of HIF-1 α mRNA contains the IRES structure (Lang et al., 2002). IRES activity of HIF-1 α was measured by transfection of bicistronic plasmid containing β -gal and CAT, and controlled by CMV and 5' UTR of HIF-1 α , respectively. As shown in Fig. 2-2F, HBSS significantly increased IRES activity of HIF-1 α . All these results suggest that nutrient deprivation can induce HIF-1 α expression through IRES-dependent translation.

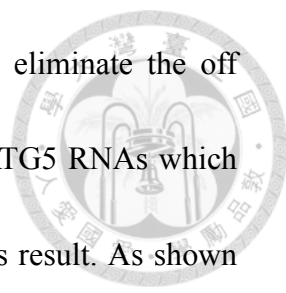
Beclin 1-independent macroautophagy positively regulates HBSS-induced HIF-1 α IRES activity

It has been demonstrated that HIF-1 α can be degraded through CMA and proteasome, thus we determined if bafilomycin A1, a lysosome inhibitor, and MG132, a proteasome inhibitor, can accumulate HIF-1 α protein in HeLa cells. Indeed as shown in Fig. 2-3A, both of bafilomycin A1 and MG132 can induce HIF-1 α protein accumulation significantly. In addition, the amount of HIF-1 α accumulated more by MG132 than by bafilomycin A1 treatment supports the notion that proteasome is the



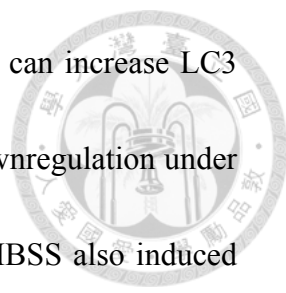
major degradation pathway of HIF-1 α . Paradoxically previous findings also suggest that macroautophagy can positively regulate HIF-1 α expression despite the underlying molecular mechanism is unknown (Hubbi et al., 2013). Thus to determine the role of macroautophagy in HBSS-induced HIF-1 α expression, we first confirmed the ability of HBSS to induce macroautophagy. As shown in Fig. 2-3B, although HBSS alone cannot significantly induce LC3-II accumulation, it indeed can enhance the response when combined with bafilomycin A1, an index of macroautophagic flux. Next, we used pharmacological and genetic approaches to verify the contribution of macroautophagy in HIF-1 α induction caused by HBSS. We found that 3-MA, an inhibitor of class III PI3K leading to the inhibition of macroautophagy (Seglen and Gordon, 1982; Wu et al., 2010), can prevent HBSS-induced HIF-1 α expression, p62 downregulation and LC3-II accumulation (Fig. 2-3C). Additionally we found another lysosome inhibitor chloroquine exerts similar effect as bafilomycin A1 (Fig. 2-3D). Chloroquine alone moderately increased HIF-1 α and p62 protein expression, but significantly reversed the effects of HBSS on HIF-1 α induction and p62 downregulation.

To exclude the possibility of non-specific effects of 3-MA and chloroquine, we further used siRNA approach to explore the role of macroautophagy in HBSS-induced HIF-1 α expression. As a result our data revealed that silence of ATG5 can reverse



HBSS-induced HIF-1 α expression in HeLa cells (Fig. 2-3E). To eliminate the off target effect of single si-ATG5 used, we used additional three si-ATG5 RNAs which target different sequences of ATG5 to strengthen confidence in this result. As shown in Fig. 2-3F, all si-ATG5 RNAs can significantly inhibit HBSS-induced HIF-1 α expression. Notably, silence of Beclin 1 failed to affect HBSS-induced HIF-1 α expression (Fig. 2-3G). Considering mTOR inhibition leads to macroautophagy and the ability of HBSS to inhibit Akt/mTOR signaling, we used mTOR inhibitor rapamycin to check the role of mTOR inhibition in HIF-1 α expression. As a result rapamycin treatment exerted a rapid p70S6K inactivation as HBSS, however, compare to the control, rapamycin had no significant effect on HIF-1 α expression (Fig. 2-3H). Furthermore, our data revealed no significant changes of HIF-1 α mRNA level by si-ATG5 and si-Beclin 1, confirming si-ATG5-reversed HIF-1 α expression is not because of the inhibition of HIF-1 α mRNA (Fig. 2-3I). Consistent to the effects on HIF-1 α protein expression, silence of ATG5 significantly suppressed HIF-1 α IRES activity, while silence of Beclin 1 had no effect (Fig. 2-3J). All these results suggest that the Beclin 1-independent macroautophagy is involved to upregulate HIF-1 α IRES translation under starvation stress.

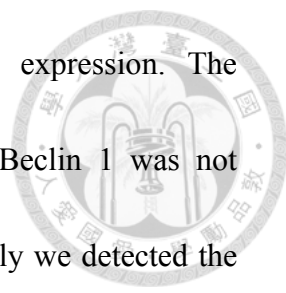
To understand if above findings observed in nutrient-deprived HeLa cells are cell types specific, we further determined the effects in A431 and A375 cells. Like in



HeLa cells, in condition of lysosomal function impairment, HBSS can increase LC3 conversion in A431 and A375 cells (Fig. 2-4A). Moreover, p62 downregulation under HBSS treatment was restored by chloroquine (Fig. 2-4A). Next, HBSS also induced significant HIF-1 α protein expression in A431 and A375 cells, and this effect can be reversed by 3-MA (Fig. 2-4B) and si-ATG5 (Fig. 2-4C). Accordingly HBSS increased HIF-1 α IRES activity in A431 and A375 cells (Fig. 2-4D). These results further suggest that macroautophagy involving in HIF-1 α expression through the IRES translation pathway is not cell type-specific.

Hypoxia-induced HIF-1 α expression also is partially through IRES activation and dependent on Beclin 1 but not ATG5

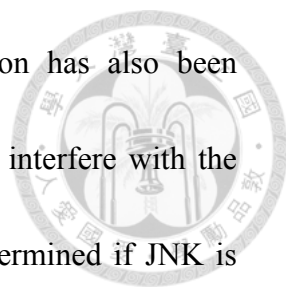
Since si-ATG6 has been shown to inhibit hypoxia-induced HIF-1 α (Hubbi et al., 2013), we interested to understand if macroautophagy also plays a role in hypoxia-induced HIF-1 α expression through IRES activation. Our data revealed that HIF-1 α expression induced by hypoxia was inhibited by 3-MA (Fig. 2-5A). Notably unlike HBSS, hypoxic effect on HIF-1 α protein expression was not changed by si-ATG5 (Fig. 2-5B), but was reduced by silence of Beclin 1 (Fig. 2-5C). To eliminate the off target effect, we used three si-Beclin 1 RNAs which target different sequences of Beclin 1 to strengthen confidence in this result. As shown in Fig. 2-5D, all



si-Beclin 1 RNAs partially reversed hypoxia-induced HIF-1 α expression. The inhibition of hypoxia-induced HIF-1 α protein expression by si-Beclin 1 was not because of interfering with HIF-1 α mRNA (Fig. 2-5E). Interestingly we detected the ability of hypoxia to increase HIF-1 α IRES activity, and this action in agreement with protein effect was inhibited by si-Beclin 1 but not by si-ATG5 (Fig. 2-5F). All these results suggest that hypoxia-induced HIF-1 α expression is partial dependent on macroautophagy-associated IRES activity. However, different from nutrient starvation it is through Beclin 1-, but not ATG5-, dependent pathway.

ROS, AMPK and JNK mediate HBSS-induced HIF-1 α expression

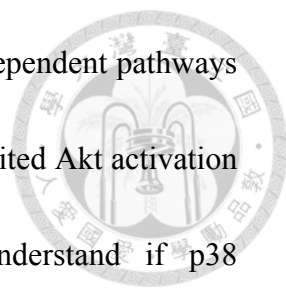
Our previous study showed that HBSS induces reactive oxygen species (ROS) production followed by AMPK activation and macroautophagy (Wu et al., 2013). Since macroautophagy induction contributes to HIF-1 α expression, we determined if ROS/AMPK signaling is also involved in HIF-1 α expression under starvation. As a result, ROS scavenger NAC abrogated HBSS-induced HIF-1 α expression (Fig. 2-6A) and macroautophagy (Fig. 2-6B). Similarly AMPK inhibitor compound C also significantly inhibited HBSS-induced HIF-1 α expression (Fig. 2-6A) and macroautophagy (Fig. 2-6B). These results demonstrated that ROS/AMPK signaling is involved in HBSS-induced macroautophagy and HIF-1 α expression. In addition to



ROS/AMPK signaling, nutrient starvation-induced JNK activation has also been shown to induce macroautophagy by phosphorylation of Bcl-2 to interfere with the interaction of Bcl-2 and Beclin 1 (Wei et al., 2008). Here we determined if JNK is involved in HBSS-induced HIF-1 α expression. As a result, JNK inhibitor SP600125 significantly suppressed HBSS-induced HIF-1 α expression (Fig. 2-6A) and autophagy (Fig. 2-6B). The findings that inhibition of the upstream molecules of macroautophagy all interferes with HBSS-induced HIF-1 α expression further confirmed the important role of macroautophagy in regulation of HIF-1 α expression. Furthermore, we determined if ROS/AMPK are the upstream molecules of JNK. We found that NAC and compound C had no significant effects on HBSS-induced JNK phosphorylation (Fig. 2-6C), but can suppress HIF-1 α IRES activity. Moreover, Iressa, as the control inhibitor, did not have significant effect on HIF-1 α IRES activity (Fig. 2-6D). Likewise, JNK inhibitor SP600125 also can suppress HIF-1 α IRES activity (Fig. 2-6D). All these results suggest that ROS/AMPK and JNK are bifurcated signaling cascades triggered by HBSS, and contribute to macroautophagy-dependent HIF-1 α IRES activation.

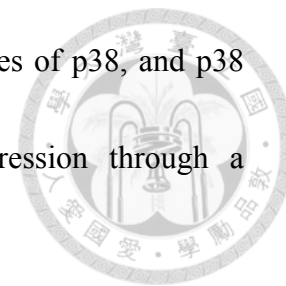
p38 also positively regulates HBSS-induced HIF-1 α expression

It has been demonstrated that inhibition of Akt leads to induce the



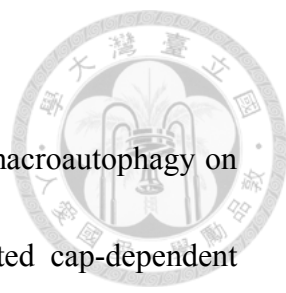
IRES-dependent translation of cyclin D1 and c-myc through p38 dependent pathways (Shi et al., 2005). Here we also found that HBSS significantly inhibited Akt activation (Fig. 2-2E) but induced p38 activation (Fig. 2-7A). To understand if p38 phosphorylation plays a role in HBSS-induced HIF-1 α expression and macroautophagy, HIF-1 α protein level was detected after inhibition of p38. As shown in Fig. 2-7B and 2-7C, SB203580, a well-defined p38 inhibitor, significantly blocked HBSS-induced HIF-1 α expression and IRES activity. However, inhibition of p38 did not have significant effect on macroautophagy (Fig. 2-7D). Considering above findings that ROS/AMPK signaling is involved in HBSS-induced HIF-1 α expression, we further determined if ROS/AMPK is the upstream signaling of p38. As shown in Fig. 2-7E, inhibition of ROS and AMPK by NAC and compound C, respectively, reduced HBSS-induced p38 phosphorylation. Considering that stimuli-triggered autophagy may also induce ER stress and subsequent p38 activation by IRE-1 signaling pathway (Yang et al., 2014), we tested if HBSS-induced p38 is related to activation of IRE-1. By detection of the splicing form of XBP1 mRNA which is the IRE-1 downstream signaling (Yoshida et al., 2001), we demonstrated that HBSS has no significant effect on XBP1 splicing while thapsigargin which is the well-known ER stressor significantly induced splicing form of XBP1 (Fig. 2-7F). In that case, we rule out the possibility that HBSS induced p38 is through IRE-1. All these results

suggest that ROS and AMPK are the upstream signaling molecules of p38, and p38 enhances HIF-1 α IRES activity and subsequent HIF-1 α expression through a macroautophagy-independent pathway.



Next, we wondered if Akt inhibition also mediates the HBSS-induced HIF-1 α expression. Since HBSS inhibited Akt phosphorylation, we over-expressed constitutively active Akt to determine the HIF-1 α expression under HBSS treatment. As a result, overexpression of constitutively active Akt did not reverse HBSS-induced HIF-1 α expression (Fig. 2-7G). In addition, it has been proved that p38 associated c-myc IRES activity in rapamycin-treated multiple myeloma cells is MNK1 dependent (Shi et al., 2013). By using MNK1 inhibitor CGP57380, we determined if this mechanism is involved in HBSS-induced HIF-1 α expression. As shown in Fig. 2-7H, CGP57380 only partially inhibited HBSS-induced HIF-1 α expression at 4 h, however, MNK1 phosphorylation which represents for its active form was inhibited under HBSS treatment. In that case, we rule out the contribution of MNK1 in HBSS-induced HIF-1 α expression. Finally, since PTB1, an IRES transacting factor (ITAF), has been reported to stimulate IRES-mediated HIF-1 α translation during hypoxia (Schepens et al., 2005), we further used siRNA approach to explore its role in our study. As a result our data revealed that silence of PTB1 did not reverse HBSS-induced HIF-1 α expression (Fig. 2-7I).

Discussion



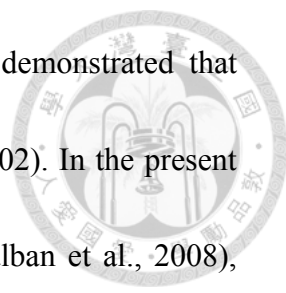
In this study, we for the first time demonstrate the effect of macroautophagy on HIF-1 α expression, and unravel that unlike growth factors-elicited cap-dependent translation and hypoxia-elicited stabilization of HIF-1 α , starvation-induced HIF-1 α expression is through cap-independent translation mechanism involving Beclin 1-independent macroautophagy. Such Beclin 1-independent macroautophagy controlled-translational process under starvation stress requires ROS/AMPK and JNK signaling. Furthermore, hypoxia also induces cap-independent HIF-1 α protein translation, which is controlled by macroautophagy. However, unlike starvation, it is Beclin 1-dependent, but ATG5-independent macroautophagy involved to regulate hypoxia-induced HIF-1 α . In addition, p38 also plays an important role in starvation-induced HIF-1 α expression (Fig. 2-8).

HIF-1 α is a transcription factor that has been reported to control more than 60 genes and has been demonstrated to play an important role in tumor angiogenesis, metastasis, growth and chemoresistance (Giaccia et al., 2003; Semenza, 2003; Dewhirst, 2007). Our present study shows that in addition to hypoxia, starvation, another environmental phenomenon in solid tumors, can also induce HIF-1 α expression. Thus HIF-1 α is suggested to play a crucial role in tumorigenesis under starvation condition. In addition, HBSS-induced HIF-1 α was reduced at 6 h, and it

may be due to cell apoptosis as demonstrated in our previous work (Wu et al., 2013).

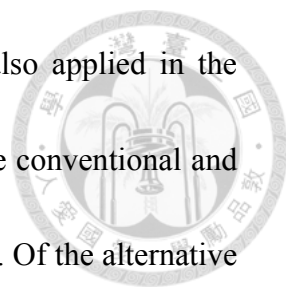
Notably although extent of HIF-1 α expression induced by starvation is much less than that induced by hypoxia, both responses display a synergistic effect, suggesting the differential molecular mechanisms for HIF-1 α induction by the two solid tumor-harboring metabolic microenvironments. Moreover, starvation also can induce HIF-1 α expression in HUVEC as well as in various cancer cell types examined, indicating that this effect is a general action, and not specific to cancer cells only. In addition, our previous work demonstrated that HBSS can induce ROS production within 30 min (Wu et al., 2013). In the present study, cysteine, a precursor of glutathione (Droge, 2005), can reverse HBSS-induced HIF-1 α expression, implying that ROS is involved in starvation-induced HIF-1 α expression, and our NAC result indeed supports this notion.

Unlike hypoxia-induced HIF-1 α majorly by inhibition of HIF-1 α protein degradation via proteasome system, the enhancement of HIF-1 mRNA binding to polysome by HBSS indicates that starvation induces HIF-1 α expression through enhancement of translation. Unlike cytokines and EGF, which induce HIF-1 α by Akt/mTOR-dependent translation (Liu et al., 2006), starvation deficient of growth factors inhibits Akt and mTOR downstream signaling including 4E-BP1 and p70S6K phosphorylation. Our data further show that starvation-induced HIF-1 α expression is



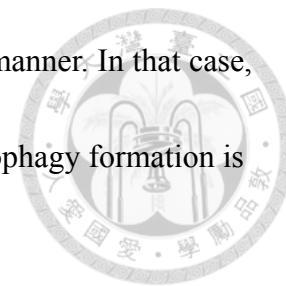
through IRES-dependent translation. In this aspect, it has been demonstrated that serum starvation can induce HIF-1 α IRES activity (Lang et al., 2002). In the present study, using reporter assay containing human HIF-1 α 5'UTR (Galban et al., 2008), we demonstrate the increased HIF-1 α IRES activity under HBSS starvation. The results of hypoxia are different from starvation; hypoxia induces HIF-1 α IRES activity but has no significant effect on the mRNA binding to polysome. These paradoxical data on HIF-1 α regulation by hypoxia might be because of the inhibition of cap-dependent translation, but the increased IRES-translation as reported previously (Lang et al., 2002).

It is well known that CMA is an additional pathway besides proteasome system to degrade HIF-1 α protein (Olmos et al., 2009; Ferreira et al., 2013; Hubbi et al., 2013). By comparing the effects of lysosome and proteasome inhibitors on HIF-1 α accumulation, we found that MG132 treatment can accumulate more HIF-1 α protein than bafilomycin A1. In addition, another lysosome inhibitor chloroquine also can induce HIF-1 α accumulation, further supporting the notion that HIF-1 α can be degraded through a lysosome-associated pathway. In our study we found the ability of HBSS to induce macroautophagy, but such stress-conferred protein degradation pathway seems not to regulate the protein stability of induced HIF-1 α . Instead it is interestingly to note that macroautophagy is involved to positively regulate



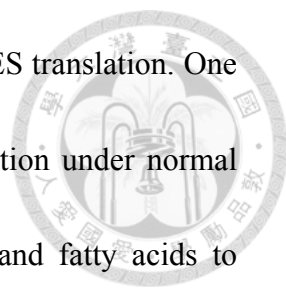
starvation-induced HIF-1 α expression. Moreover, such event is also applied in the case of hypoxia-induced HIF-1 α expression. Furthermore, there are conventional and alternative macroautophagy pathways (Juenemann and Reits, 2012). Of the alternative pathway, Beclin 1-independent macroautophagy can be induced by different stresses (Zhu et al., 2007; Scarlatti et al., 2008b; Smith et al., 2010; Grishchuk et al., 2011). Our data demonstrate that si-ATG5 but not si-Beclin 1 significantly reverses starvation-induced HIF-1 α expression. Conversely, si-Beclin 1 rather than si-ATG5 inhibits the response induced by hypoxia. Thus, it is suggested that the alternative macroautophagy is an essential event to trigger HIF-1 α IRES activity in cells facing different stresses like nutrient starvation and hypoxia. However, currently it remains unknown how alternative types of macroautophagy with independence on either ATG5 or Beclin-1 and relying on stress context are differentially regulated, but mediate the same effect on increasing HIF-1 α IRES activity. Considering that Beclin 1 interacts with Class III PI3K to induce macroautophagy formation, some papers demonstrated that 3-MA, a well-known Class III PI3K inhibitor, cannot interfere with Beclin 1-independent macroautophagy-induced effect (Zhu et al., 2007; Tian et al., 2010). However, 3-MA has also been reported to inhibit Beclin 1-independent macroautophagy-induced cell death induced by staurosporine (Grishchuk et al., 2011) as our finding in starvation condition. Thus we propose that Class III PI3K might be

involved in macroautophagy formation in a Beclin 1-independent manner. In that case, we suggest that the underlying mechanism of alternative macroautophagy formation is more complicated than we expect.



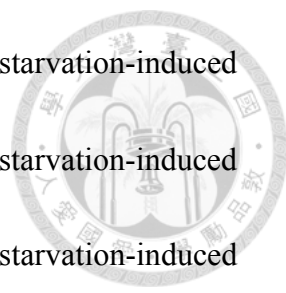
After showing the role of alternative macroautophagy in starvation-induced HIF-1 α expression, and knowing the crucial function of mTOR inhibition on macroautophagy initiation, we consider the contribution of mTOR signaling inhibition induced by nutrient starvation in HIF-1 α upregulation. Using rapamycin which is a specific mTOR inhibitor, our results show its inability to induce HIF-1 α expression. Thus, we conclude that it is not mTOR inhibition alone but requiring other signaling pathways and molecular events concomitantly provided by starvation to induce HIF-1 α IRES activity.

Finally, unlike well-studied mTOR signaling in the cap-dependent translation, the mechanism for IRES-mediated protein translation is unclear. Our results demonstrate that Beclin 1-independent macroautophagy can positively regulate starvation-induced HIF-1 α IRES translation. However, how macroautophagy regulates HIF-1 α IRES translation needs to be further studied. Considering that the important function of macroautophagy is to recycle proteins to provide amino acids and fatty acids to mitochondrial energy production under starvation condition (Kourtis and Tavernarakis, 2009), we suggest that macroautophagy functions through at least



two possible mechanisms to control starvation-induced HIF-1 α IRES translation. One is degradation of molecules which inhibited HIF-1 α IRES translation under normal condition. Another is recycling proteins to release amino acids and fatty acids to provide mitochondria energy production for HIF-1 α IRES translation. In the case of hypoxia, silence of ATG6 has been reported to inhibit hypoxia-induced HIF-1 α (Hubbi et al., 2013), implying that macroautophagy may positively regulate hypoxia-induced HIF-1 α expression. Our results also support this notion and further demonstrate that it is through ATG5-independent macroautophagy, an alternative autophagy (Nishida et al., 2009). Finally, according to our HBSS and hypoxia results, we for the first time demonstrate that Beclin 1- and ATG5-independent autophagy positively regulate HBSS- and hypoxia-induced HIF-1 α , respectively.

Akt and p38 have been demonstrated to regulate IRES-dependent protein translation, however, the role in regulation of IRES activity is more ambiguous. For example, inhibition of Akt and p38 reduce TNF- α -induced IRES-dependent HIF-1 α translation (Zhou et al., 2004). In contrast, inhibition of Akt activity induces IRES-dependent translation of cyclin D1 and c-myc through p38-dependent pathway (Shi et al., 2005). Despite the conflict role of Akt in IRES activity observed in previous studies, p38 seems to be a positive regulator in this effect. In the present study we showed that p38 can positively regulates starvation-induced HIF-1 α



translation, while Akt activity does not have significant effect on starvation-induced HIF-1 α translation. Moreover, since p38 are not involved in starvation-induced macroautophagy formation, the mechanism of p38 regulation of starvation-induced HIF-1 α IRES activity and protein expression is needed to be further investigated. Interestingly, ROS and AMPK are involved in starvation-induced p38 phosphorylation. It has been reported that AMPK can active p38 through a TAK1 dependent pathway (Chang et al., 2010). Although ROS-AMPK-p38 signaling cascade has been demonstrated to induce apoptosis, glucose uptake and cyclooxygenase-2 expression (Arsikin et al., 2012; Kim et al., 2013), we for the first time link this pathway to IRES activity.

In summary, HIF-1 α is an important protein to regulate tumorigenesis. In the present study, we demonstrate a novel mechanism responsible for nutrient starvation-induced HIF-1 α expression. This mechanism is through Beclin 1-independent macroautophagy to increase IRES-dependent HIF-1 α translation. Furthermore, ATG5-independent macroautophagy also can positively regulate the hypoxic-mediated cap-independent protein translation of HIF-1 α . Thus, it is a novel finding in this study to expand the multiple functions of macroautophagy under stress conditions to positively control the protein translation through cap-independent pathway.



Figure 2-1

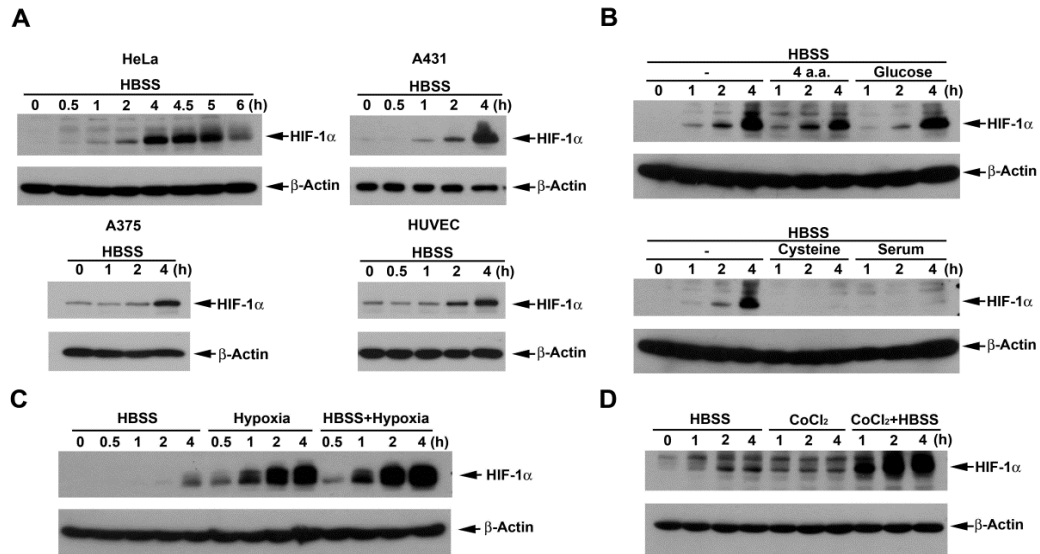




Figure 2-1. HBSS induces HIF-1 α expression and potentiates the HIF-1 α responses of hypoxia and CoCl₂.

(A) HeLa, A431, A375 and HUVEC were treated with HBSS. At indicated time points, cell lysates were evaluated for the HIF-1 α protein level. (B) HeLa cells were treated with HBSS for the indicated time periods, either in the presence or absence of four amino acids (4 mM glutamine, 0.8 mM leucine, 0.4 mM arginine, 0.2 mM histidine), glucose (25 mM), cysteine (0.2 mM) or 10% FBS. (C, D) HeLa cells were treated with HBSS for the indicated time periods, either in the presence or absence of hypoxia (C) or 200 μ M CoCl₂ (D). Total cell lysates were collected and subjected to Western blot analysis.



Figure 2-2

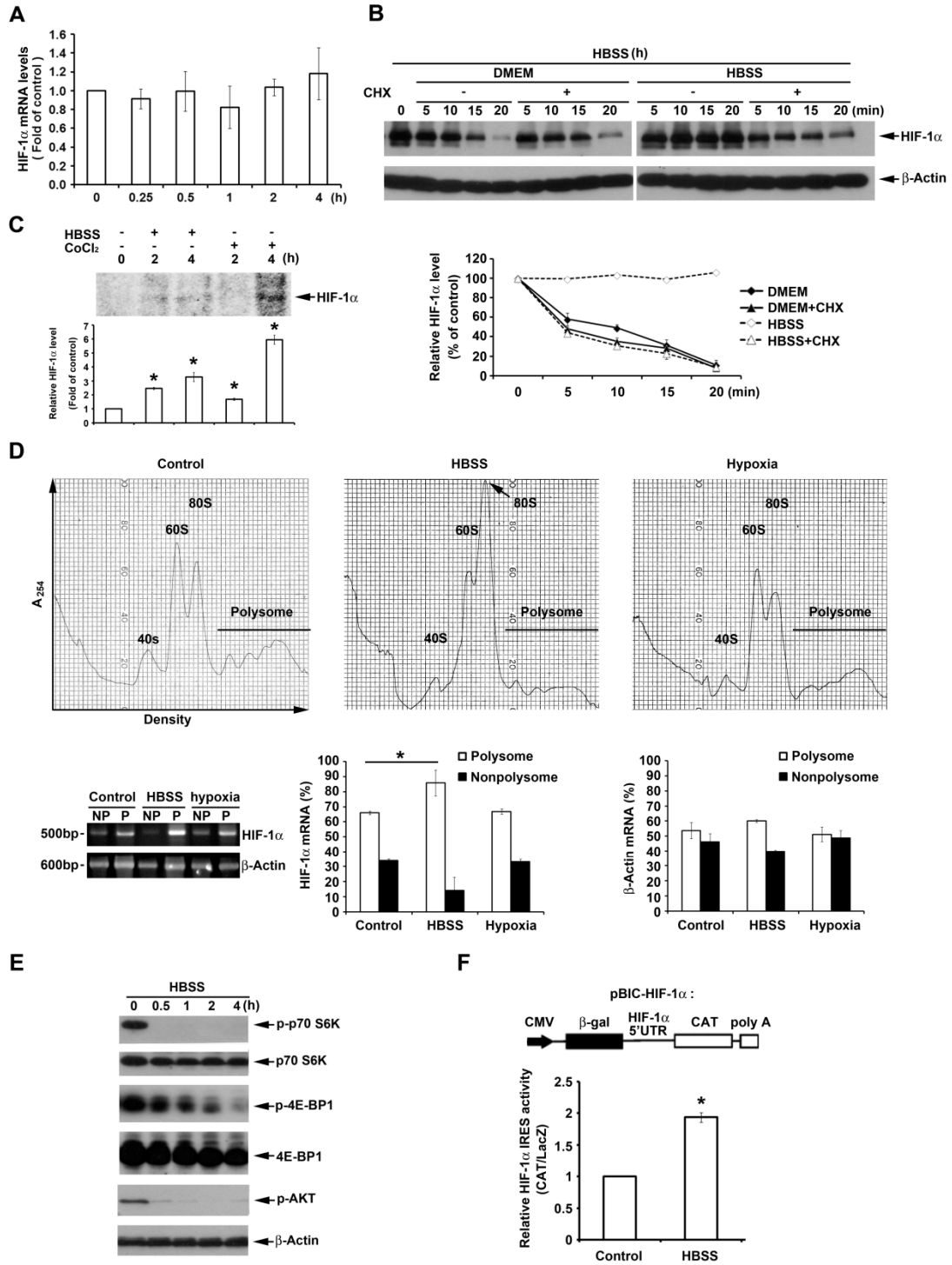


Figure 2-2. HBSS enhances HIF-1 α expression through IRES-dependent translation.



(A) HeLa cells were treated with HBSS. At indicated time points cells were collected and HIF-1 α gene expression was determined by real time PCR. (B) HIF-1 α was induced after treatment of HBSS for 4 h, and then HBSS was changed to complete DMEM or maintained in HBSS with or without 10 μ M cycloheximide (CHX). Cell lysates were evaluated for the HIF-1 α protein level. (C) [³⁵S]Methionine labeled HeLa cells were treated with HBSS or 200 μ M CoCl₂ for 2 or 4 h, and cell lysates were collected and immunoprecipitated by HIF-1 α antibody to determine *de novo* protein expression of HIF-1 α . (D) HeLa cells were treated with HBSS or hypoxia for 2 h. Polysomal (P) and nonpolysomal (NP) fractions were separated by discontinuous sucrose gradient (10%-50%). The amounts of HIF-1 α and β -actin mRNA were analyzed by reverse transcription-PCR. (E) HeLa cells were treated with HBSS for indicated time points. Total cell lysates were collected and subjected to Western blot analysis. (F) After transfection of pBIC-HIF-1 α plasmid, HeLa cells were treated with HBSS for 4 h. CAT and LacZ expression were detected, and the ratio CAT/LacZ represented HIF-1 α IRES activity. **p*<0.05, indicating significant increase of HIF-1 α translation (C), changes of HIF-1 α mRNA in polysomal and nonpolysomal fractions (D) and increase of IRES activity by HBSS.

Figure 2-3

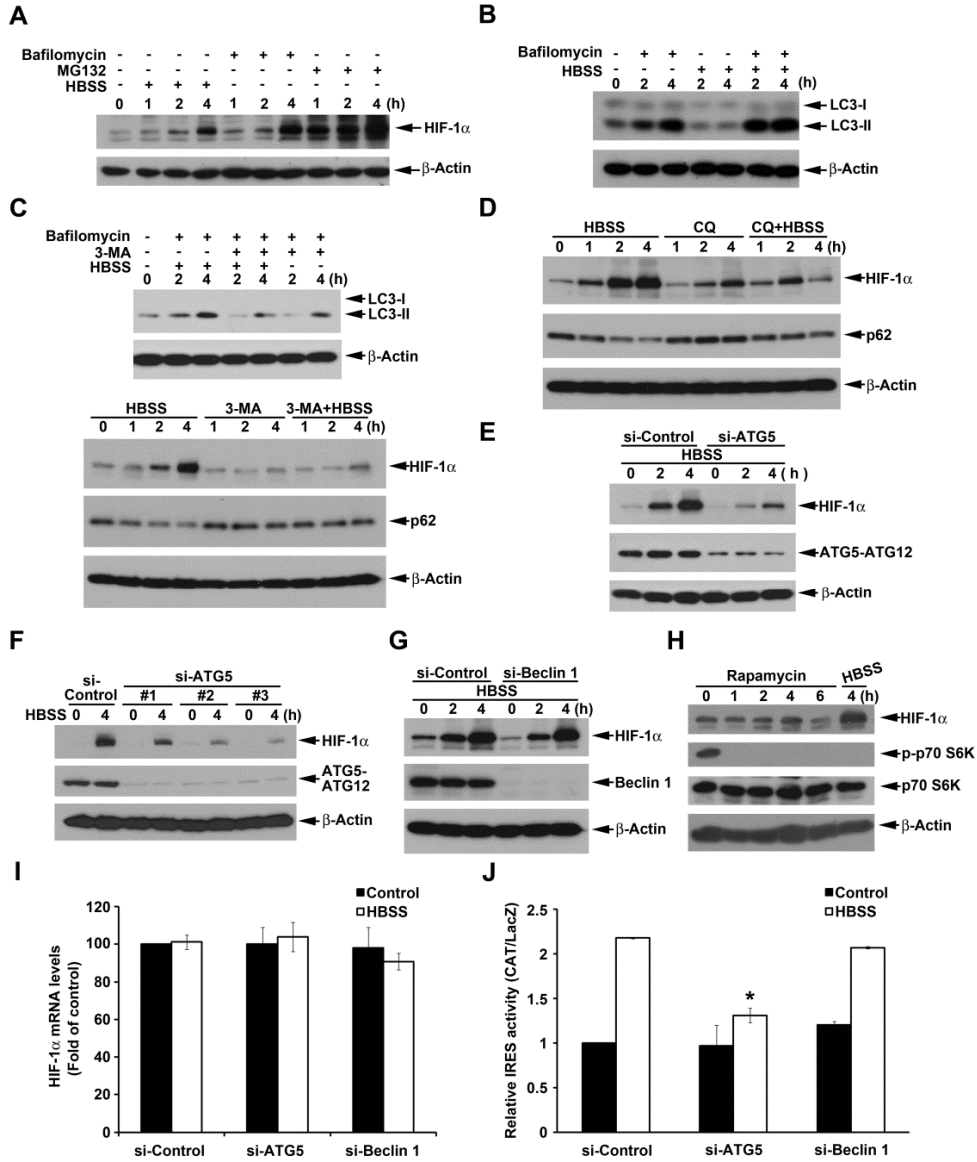




Figure 2-3. Beclin 1-independent macroautophagy positively regulates HBSS-induced HIF-1 α IRES activity in HeLa cells.

(A) HeLa cells were treated with HBSS, 100 nM bafilomycin A1 or 20 μ M MG132 for indicated time points. Total cell lysates were collected and subjected to Western blot analysis. (B-D, H) HeLa cells were treated with HBSS in the absence or presence of 100 nM bafilomycin A1 (B, C), 10 mM 3-MA (C), 100 μ M chloroquine (D) or 500 nM rapamycin (H) for indicated time points. Total cell lysates were collected and subjected to Western blot analysis using the indicated antibodies. (E, F, G) After silence of ATG5 (E, F) or Beclin 1 (G) for 72 h, HeLa cells were treated with HBSS for 2 or 4 h. Total cell lysates were collected and subjected to Western blot analysis. (I, J) After silence of ATG5 or Beclin 1, HeLa cells were treated with HBSS for 4 h to determine the HIF-1 α gene expression (I) or transfected with pBIC-HIF-1 α plasmid for 24 h and then treated with HBSS for 4 h to determine the IRES activity (J).

* $p < 0.05$, indicating significant inhibition of HBSS-induced IRES activity.



Figure 2-4

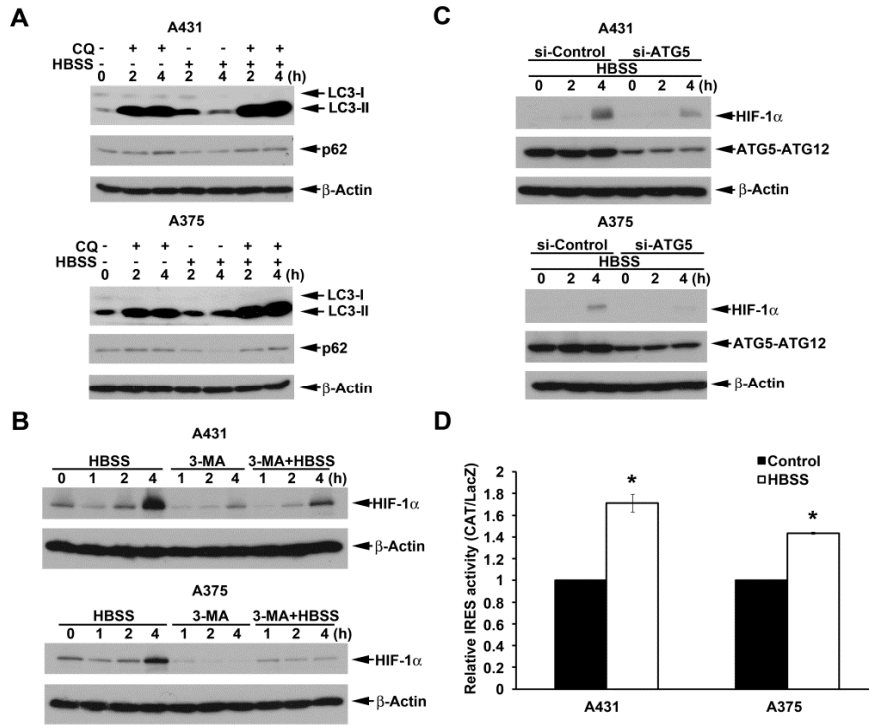




Figure 2-4. Beclin 1-independent macroautophagy also positively regulates HBSS-induced HIF-1 α IRES activity in A431 and A375 cells.

(A, B) A431 or A375 cells were treated with HBSS in the absence or presence of 100 μ M chloroquine (A) or 10 mM 3-MA (B) for indicated time points. Total cell lysates were collected and subjected to Western blot analysis. (C) After silence of ATG5 for 72 h, A431 or A375 cells were treated with HBSS for indicated time points. Total cell lysates were collected and subjected to Western blot analysis. (D) As described in Fig. 2-3I, HIF-1 α IRES activity was determined after 4 h treatment with HBSS. * p <0.05, indicating significant increase of IRES activity by HBSS.



Figure 2-5

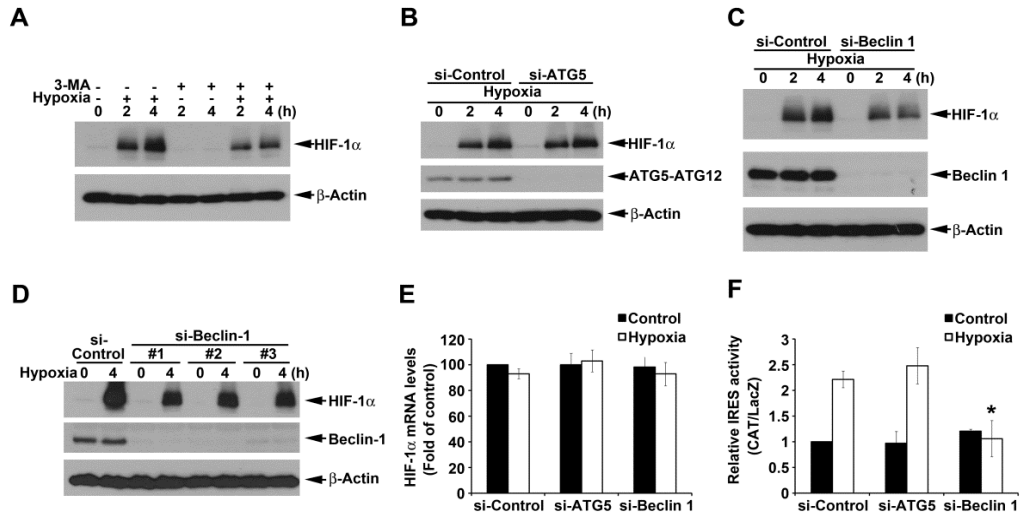




Figure 2-5. ATG5-independent macroautophagy positively regulates hypoxia-induced HIF-1 α .

(A) HeLa cells were cultured under hypoxia condition with or without 10 mM 3-MA for 2 or 4 h. Total cell lysates were collected and subjected to Western blot analysis.

(B-D) After silence of ATG5 (B) or Beclin 1 (C, D), HeLa cells were cultured under hypoxia condition for 2 or 4 h. Total cell lysates were collected and subjected to Western blot analysis. In some experiments, HeLa cells were cultured under hypoxia condition for 4 h to determine the HIF-1 α gene expression by PCR (E) or transfected with pBIC-HIF-1 α plasmid and cultured under hypoxia condition for 4 h to determine the IRES activity (F). * $p < 0.05$, indicating significant inhibition of HBSS-induced IRES activity.



Figure 2-6

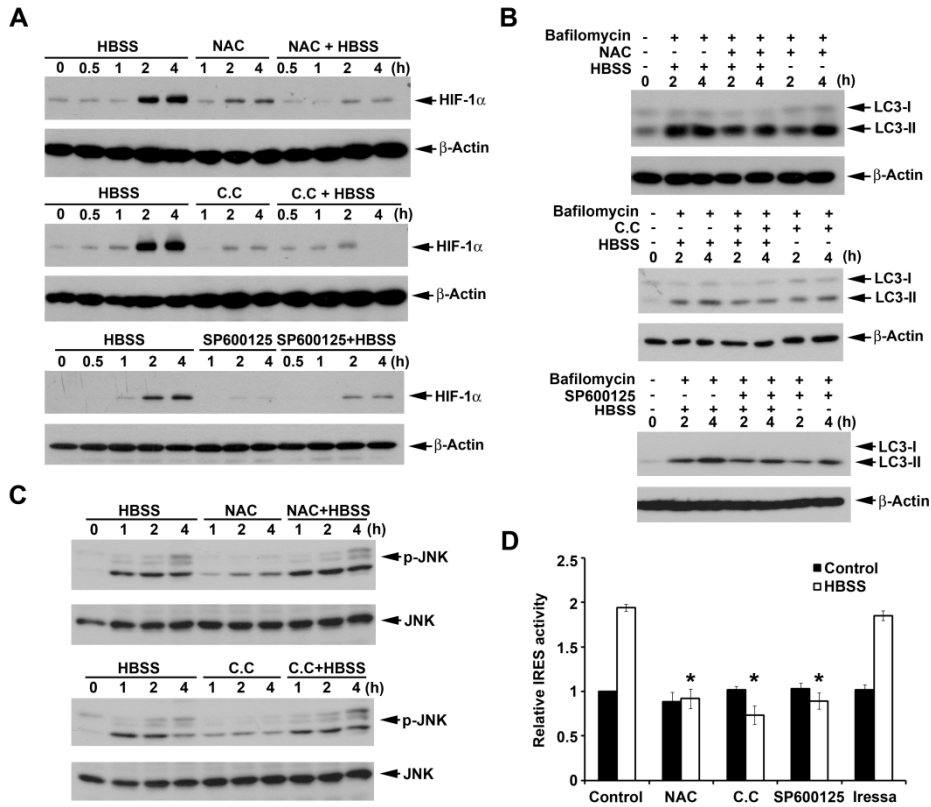




Figure 2-6. ROS, AMPK and JNK are involved in HBSS-induced HIF-1 α expression.

(A, C) HeLa cells were treated with HBSS for the indicated time periods, either in the presence or absence of NAC (10 mM), Compound C (10 μ M) or SP600125 (10 μ M). Total cell lysates were collected and subjected to Western blot analysis. (B) After treated with NAC (10 mM), Compound C (10 μ M) or SP600125 (10 μ M) for 30 min, HeLa cells were treated with HBSS with or without 100 nM bafilomycin A1 for the indicated time periods. Total cell lysates were collected and subjected to Western blot analysis. (D) HIF-1 α IRES activity was determined after treatment of HBSS for 4 h with or without NAC, Compound C, SP600125 or Iressa (1 μ M). * p <0.05, indicating significant inhibition of HBSS-induced IRES activity.



Figure 2-7

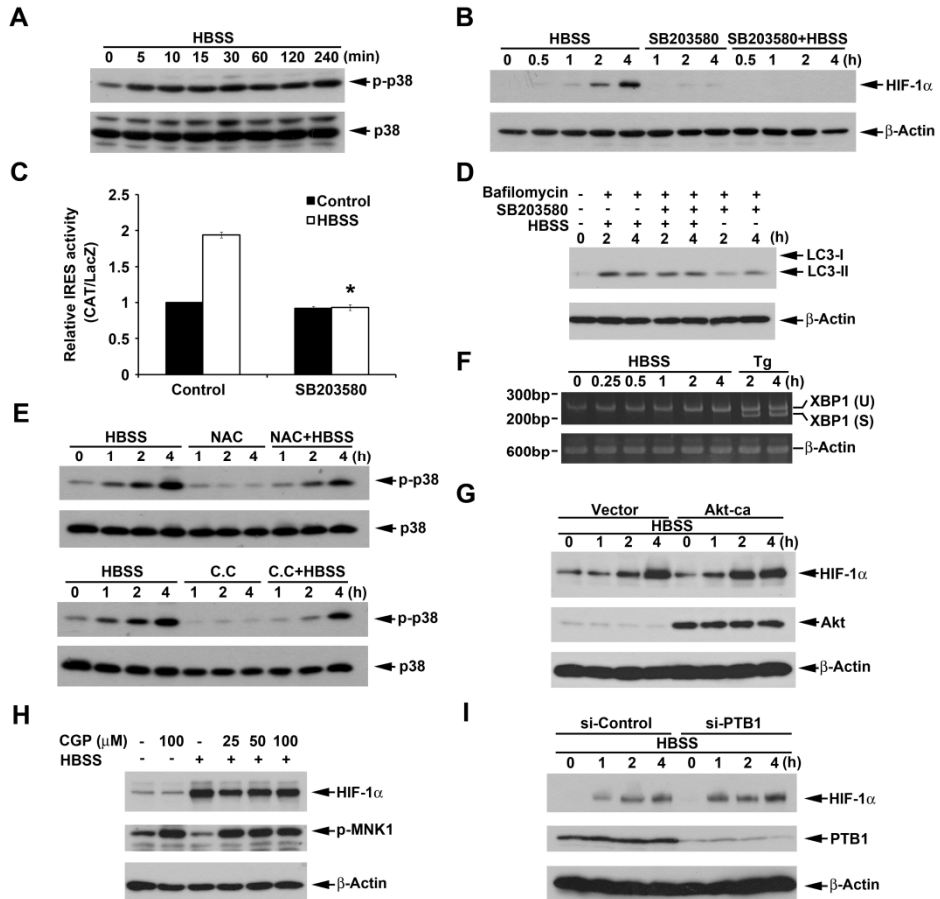




Figure 2-7. p38 mediates HBSS-induced HIF-1 α expression independent of macroautophagy.

(A-F, H) HeLa cells were treated with HBSS in the absence or presence of SB203580 (10 μ M) (B-D), bafilomycin A1 (100 nM) (D), NAC (10 mM) (E), Compound C (10 μ M) (E), thapsigargin (1 μ M) (F), CPG57380 (25, 50 or 100 μ M) (H) for indicated time points. Total cell lysates were collected and subjected to Western blot analysis.

(G, I) After transfection of constitutively active Akt for 24 h (G) or silence of PTB1 for 72 h (I), HeLa cells were treated with HBSS for indicated time points. Total cell lysates were collected and subjected to Western blot analysis. In (C), HIF-1 α IRES activity was determined after treatment of HBSS for 4 h. * $p < 0.05$, indicating significant inhibition of HBSS-induced IRES activity by SB203580.



Figure 2-8

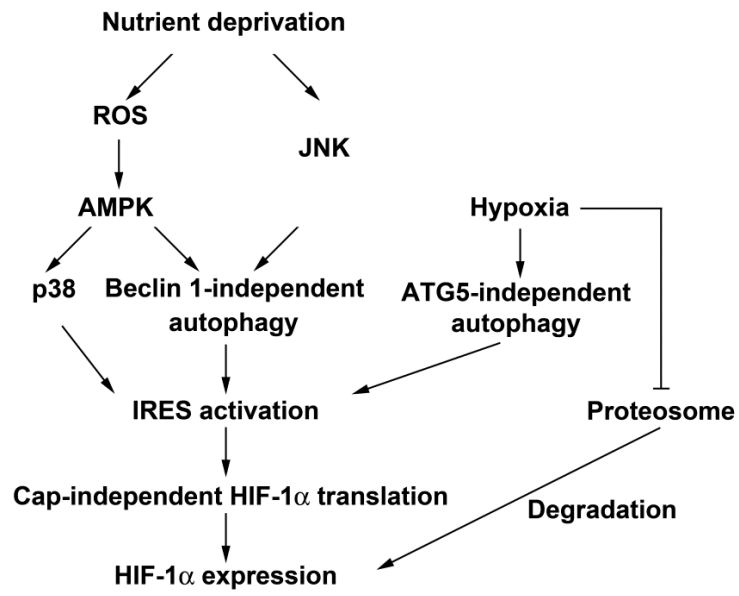


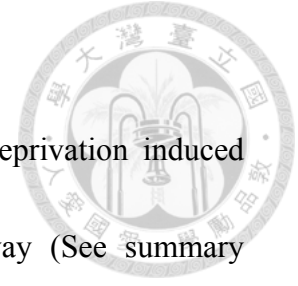


Figure 2-8. Schematic summary of nutrient deprivation- and hypoxia-induced

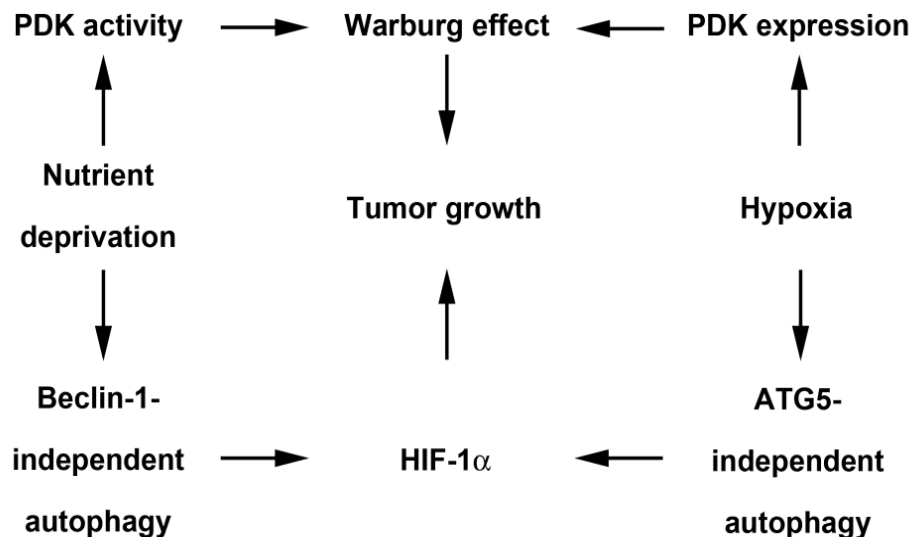
HIF-1 α expression.

HBSS starvation induces HIF-1 α protein expression through enhancement of IRES activity which is positively regulated by Beclin 1-independent macroautophagy. The Beclin 1-independent macroautophagy is controlled by ROS/AMPK and JNK signaling pathways. Furthermore, p38 which is activated by ROS-mediated AMPK also positively regulates HBSS-induced HIF-1 α IRES activity but in a macroautophagy-independent manner. In addition, hypoxia not only stabilizes HIF-1 α through inhibition of proteasome degradation pathway, but also induces IRES activity through an ATG5-independent macroautophagy pathway.

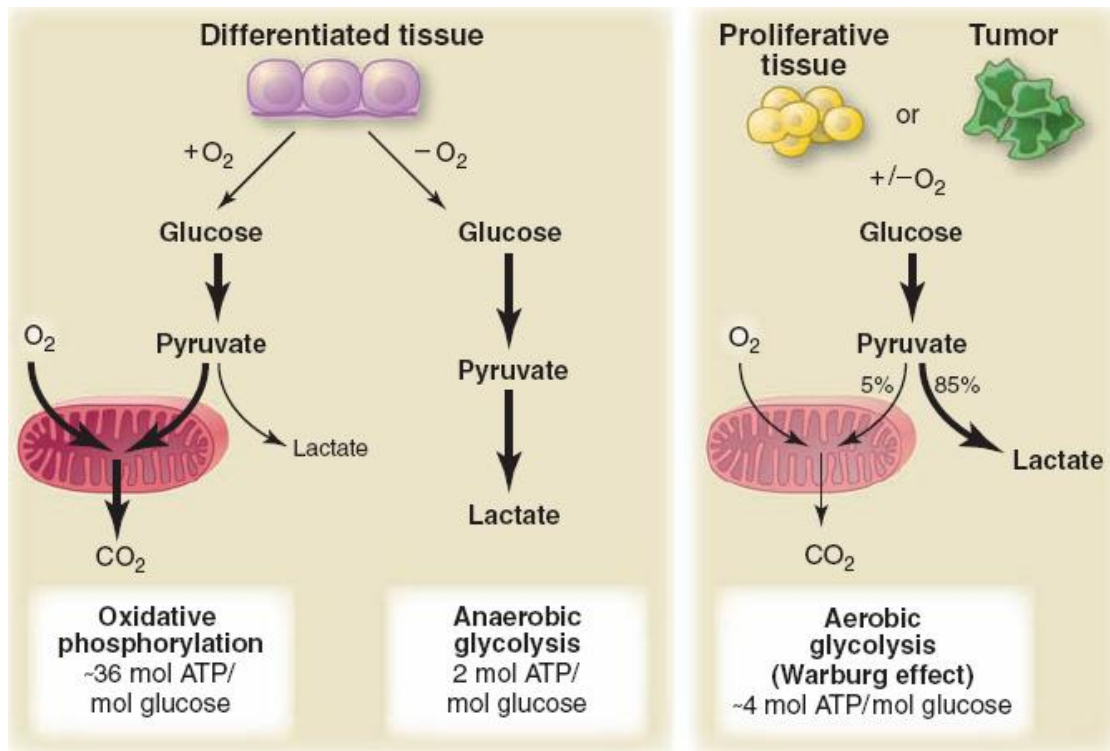
Conclusion



Our results demonstrated that both hypoxia and nutrient deprivation induced Warburg effect and HIF-1 α , however, through different pathway (See summary Figure). Hypoxia induced Warburg effect by over-expression of PDK through accumulation of HIF-1 α . However, nutrient deprivation induced Warburg effect by promotion of PDK activity through ROS/AMPK signaling. In addition to inhibition of protein degradation, hypoxia induced ATG5-independent autophagy to regulated HIF-1 α IRES activity. However, nutrient deprivation induced HIF-1 α through induction of protein expression by activation of HIF-1 α IRES translation which is positively regulated by Beclin-1-independent autophagy.



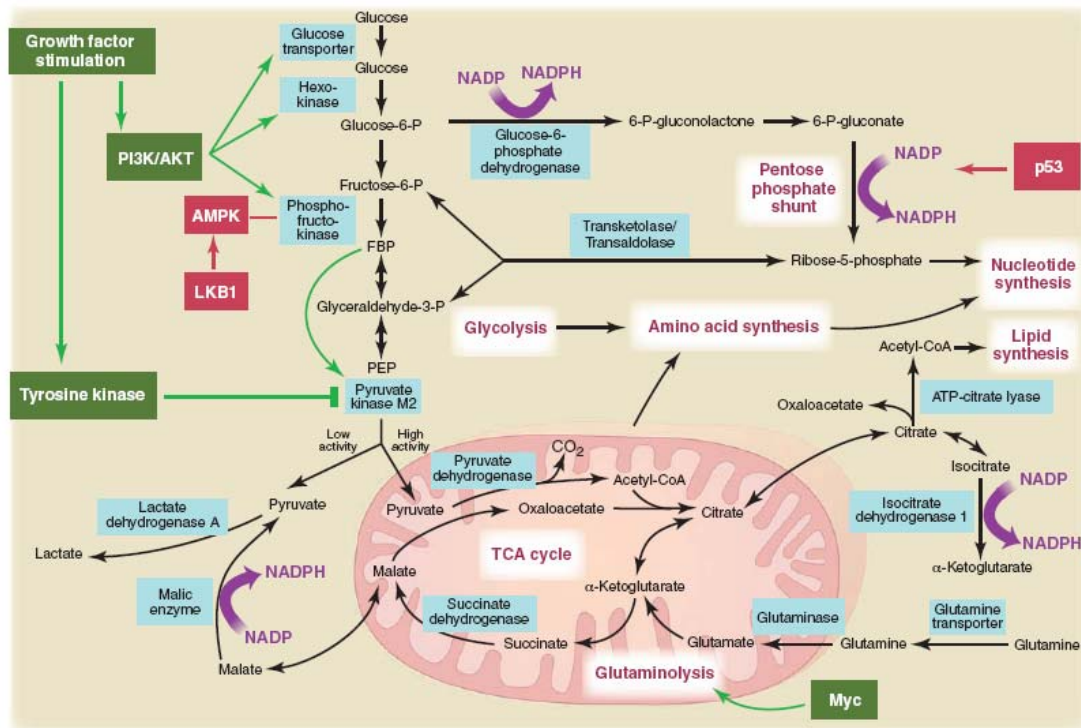
Appendix I



Schematic representation of the differences between oxidative phosphorylation, anaerobic glycolysis, and aerobic glycolysis (Warburg effect).

(cited from Science 324, 1029, 2009)

Appendix II



Metabolic pathways active in proliferating cells are directly controlled

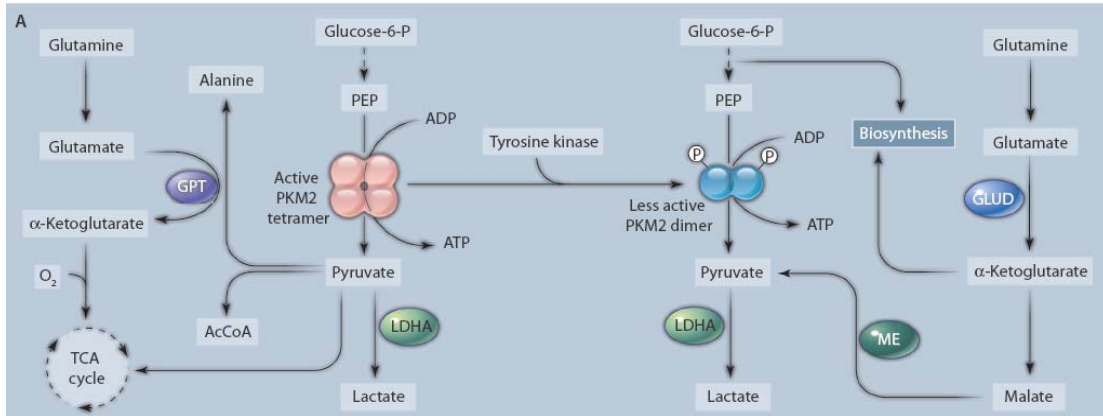
by signaling pathways involving known oncogenes and tumor suppressor

genes.

(cited from Science 324, 1029, 2009)



Appendix III

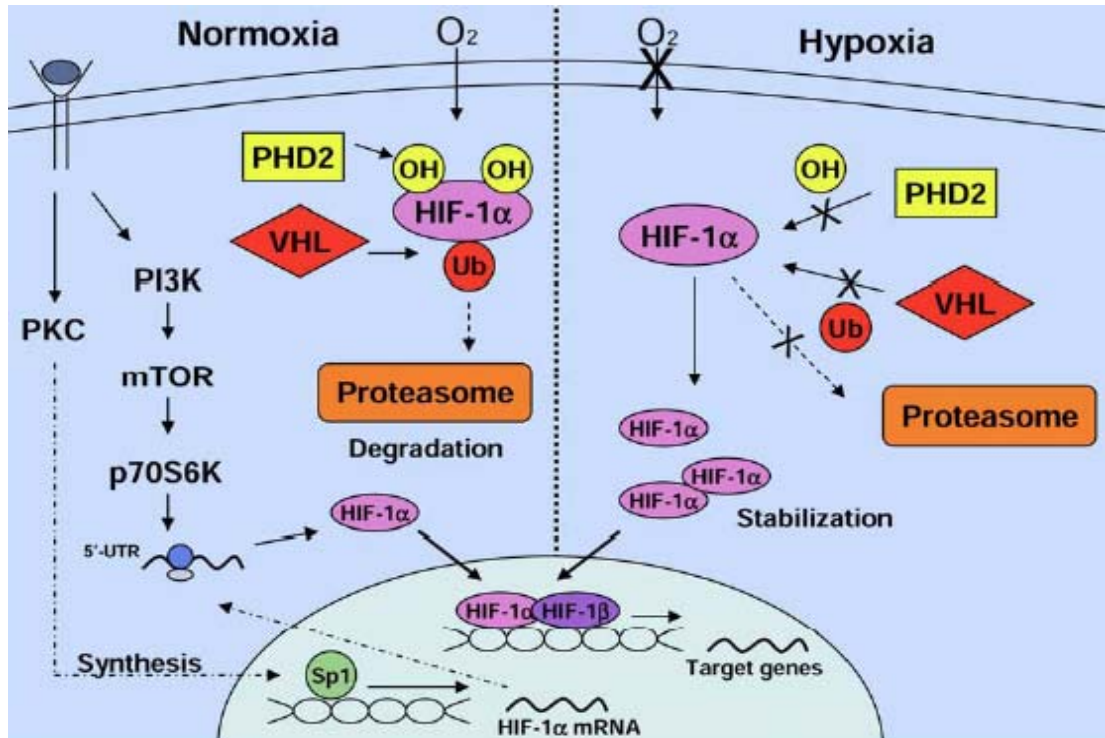


Schematic depiction of tyrosine kinase phosphorylation of active PKM2

tetramer to a less active dimer of PKM2.

(cited from Science Signaling 2, 1, 2009)

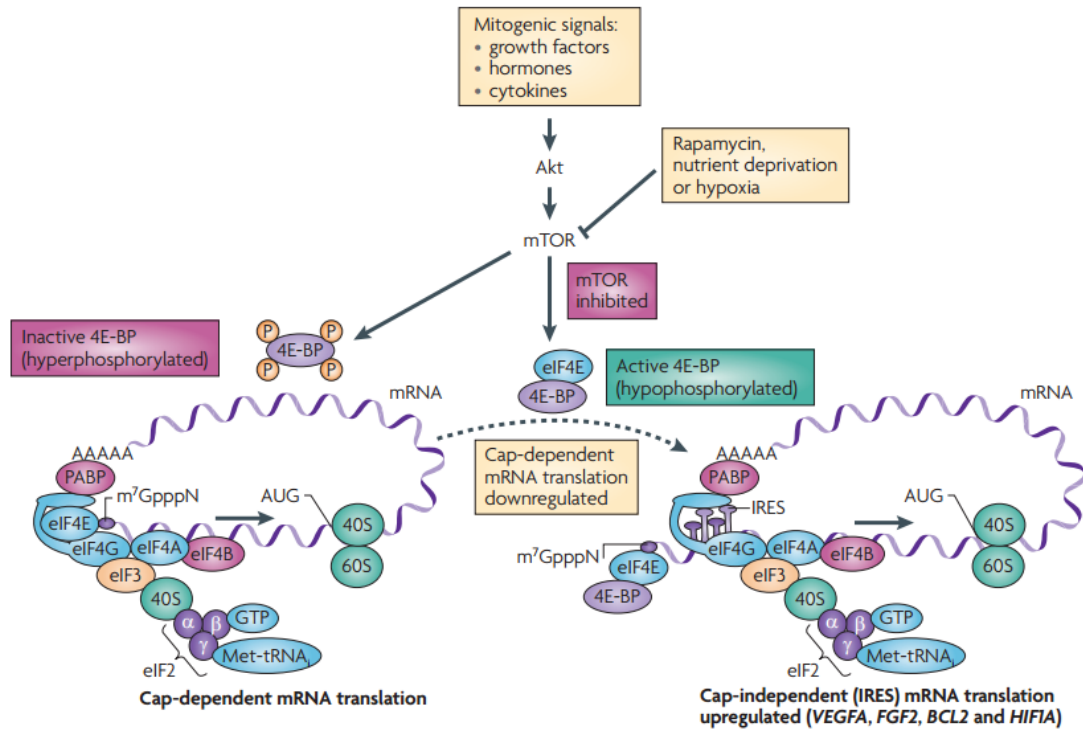
Appendix IV



Oxygen-dependent and independent regulation of HIF-1

(cited from International Journal of Biochemistry and Cell Biology 37, 533, 2005)

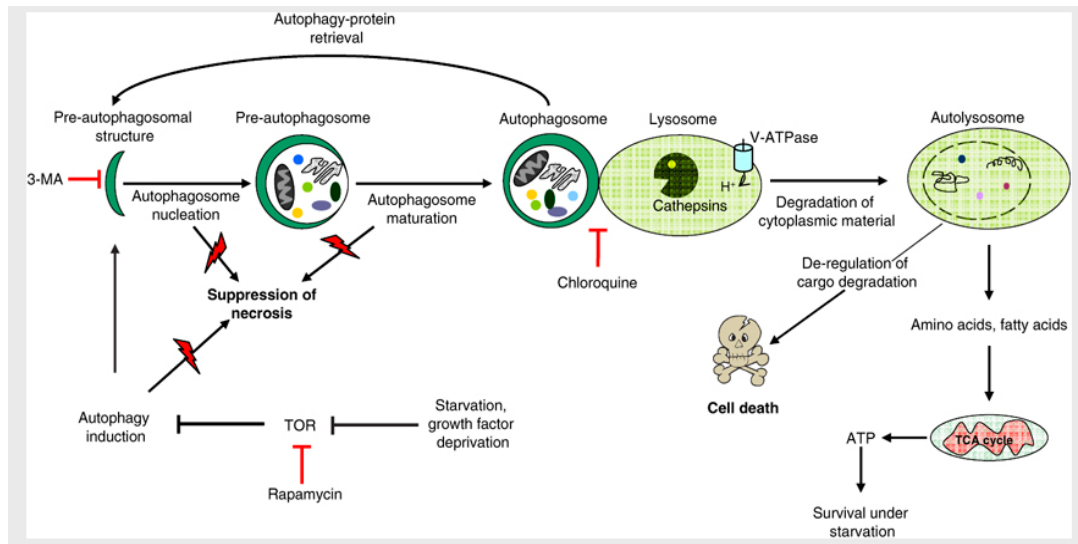
Appendix V



Cap-dependent and cap-independent translation.

(cited from Nature Reviews Cancer 10, 254, 2013)

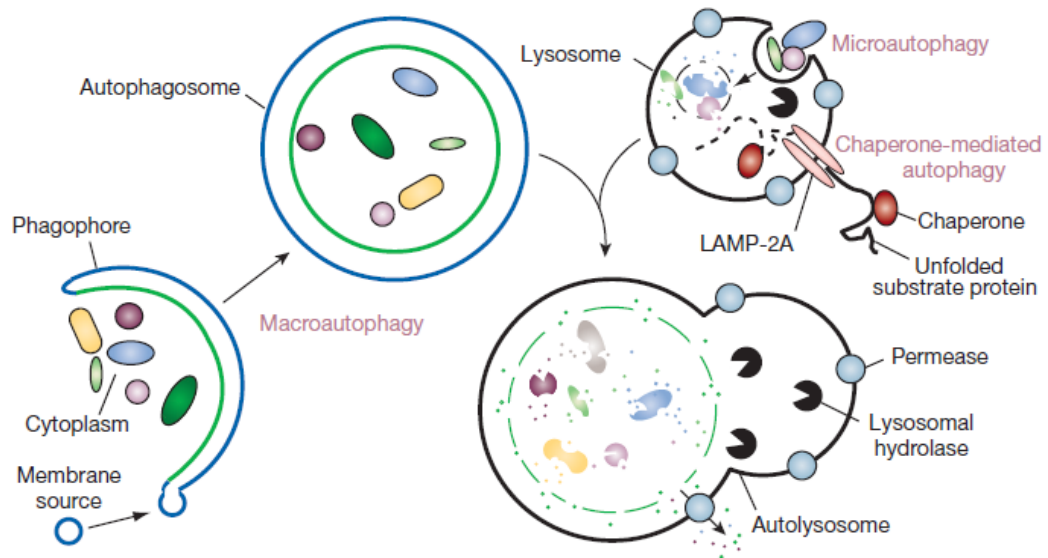
Appendix VI



Interfacing the core autophagic pathway with cell death mechanisms.

(cited from *Cell Death and Differentiation* 126, 21, 2009)

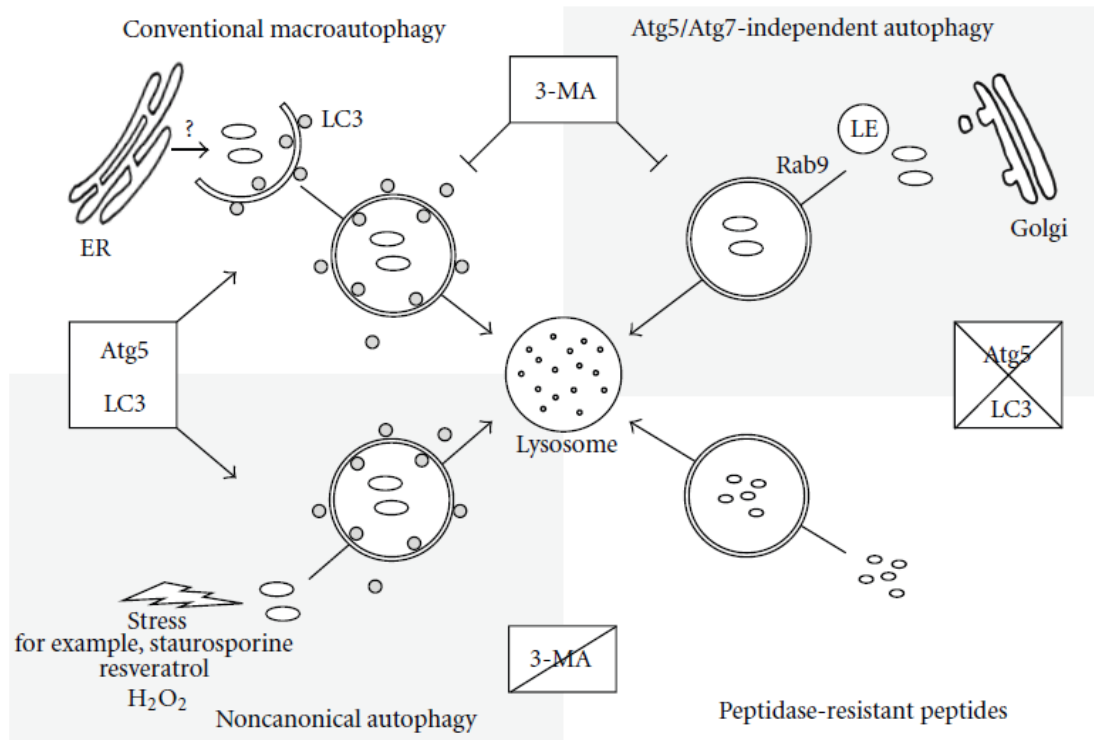
Appendix VII



Different types of autophagy.

(cited from Nature 451, 28, 2008)

Appendix VIII



Alternative macroautophagic pathways lead to lysosomal degradation.

(cited from International Journal of Cell Biology 2012, 8, 2012)



References

Armstrong, J.S., Whiteman, M., Yang, H., Jones, D.P., and Sternberg, P., Jr. (2004).

Cysteine starvation activates the redox-dependent mitochondrial permeability transition in retinal pigment epithelial cells. *Invest Ophthalmol Vis Sci* 45, 4183-4189.

Arsikin, K., Kravic-Stevovic, T., Jovanovic, M., Ristic, B., Tovilovic, G., Zogovic, N.,

Bumbasirevic, V., Trajkovic, V., and Harhaji-Trajkovic, L. (2012).

Autophagy-dependent and -independent involvement of AMP-activated protein kinase in 6-hydroxydopamine toxicity to SH-SY5Y neuroblastoma cells. *Biochim Biophys Acta* 1822, 1826-1836.

Averous, J., Gabillard, J.C., Seiliez, I., and Dardevet, D. (2012). Leucine limitation

regulates myf5 and myoD expression and inhibits myoblast differentiation. *Exp Cell Res* 318, 217-227.

Baird, S.D., Turcotte, M., Korneluk, R.G., and Holcik, M. (2006). Searching for IRES.

RNA 12, 1755-1785.

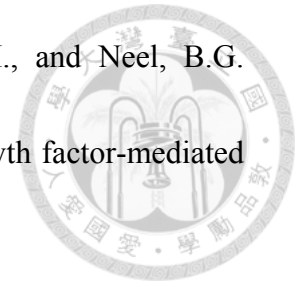
Baumann, F., Leukel, P., Doerfelt, A., Beier, C.P., Dettmer, K., Oefner, P.J.,

Kastenberger, M., Kreutz, M., Nickl-Jockschat, T., Bogdahn, U., *et al.* (2009).

Lactate promotes glioma migration by TGF-beta2-dependent regulation of matrix metalloproteinase-2. *Neuro Oncol* 11, 368-380.

Bennett, A.M., Hausdorff, S.F., O'Reilly, A.M., Freeman, R.M., and Neel, B.G.

(1996). Multiple requirements for SHPTP2 in epidermal growth factor-mediated cell cycle progression. *Mol Cell Biol* 16, 1189-1202.



Bor, Y.C., Swartz, J., Morrison, A., Rekosh, D., Lodomery, M., and Hammariskjold,

M.L. (2006). The Wilms' tumor 1 (WT1) gene (+KTS isoform) functions with a CTE to enhance translation from an unspliced RNA with a retained intron. *Genes Dev* 20, 1597-1608.

Brahimi-Horn, M.C., Chiche, J., and Pouyssegur, J. (2007). Hypoxia signalling

controls metabolic demand. *Curr Opin Cell Biol* 19, 223-229.

Braun, F., Bertin-Ciftci, J., Gallouet, A.S., Millour, J., and Juin, P. (2011).

Serum-nutrient starvation induces cell death mediated by Bax and Puma that is counteracted by p21 and unmasked by Bcl-x(L) inhibition. *PLoS One* 6, e23577.

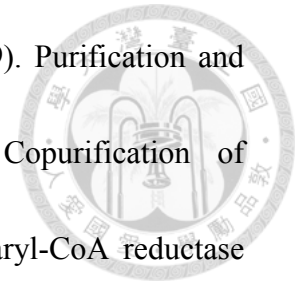
Bushell, M., Stoneley, M., Kong, Y.W., Hamilton, T.L., Spriggs, K.A., Dobbyn, H.C.,

Qin, X., Sarnow, P., and Willis, A.E. (2006). Polypyrimidine tract binding protein regulates IRES-mediated gene expression during apoptosis. *Mol Cell* 23, 401-412.

Carling, D. (2004). The AMP-activated protein kinase cascade--a unifying system for

energy control. *Trends Biochem Sci* 29, 18-24.

Carling, D., Clarke, P.R., Zammit, V.A., and Hardie, D.G. (1989). Purification and characterization of the AMP-activated protein kinase. Copurification of acetyl-CoA carboxylase kinase and 3-hydroxy-3-methylglutaryl-CoA reductase kinase activities. *Eur J Biochem* 186, 129-136.

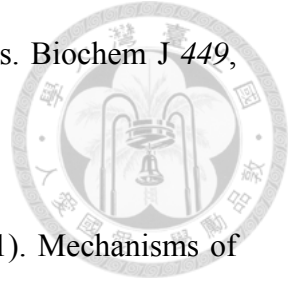


Chang, M.Y., Ho, F.M., Wang, J.S., Kang, H.C., Chang, Y., Ye, Z.X., and Lin, W.W. (2010). AICAR induces cyclooxygenase-2 expression through AMP-activated protein kinase-transforming growth factor-beta-activated kinase 1-p38 mitogen-activated protein kinase signaling pathway. *Biochem Pharmacol* 80, 1210-1220.

Christofk, H.R., Vander Heiden, M.G., Harris, M.H., Ramanathan, A., Gerszten, R.E., Wei, R., Fleming, M.D., Schreiber, S.L., and Cantley, L.C. (2008a). The M2 splice isoform of pyruvate kinase is important for cancer metabolism and tumour growth. *Nature* 452, 230-233.

Christofk, H.R., Vander Heiden, M.G., Wu, N., Asara, J.M., and Cantley, L.C. (2008b). Pyruvate kinase M2 is a phosphotyrosine-binding protein. *Nature* 452, 181-186.

Damiano, F., Rochira, A., Tocci, R., Alemanno, S., Gnoni, A., and Siculella, L. (2013). hnRNP A1 mediates the activation of the IRES-dependent SREBP-1a



mRNA translation in response to endoplasmic reticulum stress. *Biochem J* 449, 543-553.

De Flora, S., Izzotti, A., D'Agostini, F., and Balansky, R.M. (2001). Mechanisms of N-acetylcysteine in the prevention of DNA damage and cancer, with special reference to smoking-related end-points. *Carcinogenesis* 22, 999-1013.

Depre, C., Rider, M.H., and Hue, L. (1998). Mechanisms of control of heart glycolysis. *Eur J Biochem* 258, 277-290.

Dewhirst, M.W. (2007). Intermittent hypoxia furthers the rationale for hypoxia-inducible factor-1 targeting. *Cancer Res* 67, 854-855.

Diebold, I., Petry, A., Djordjevic, T., Belaiba, R.S., Fineman, J., Black, S., Schreiber, C., Fratz, S., Hess, J., Kietzmann, T., *et al.* (2010). Reciprocal regulation of Rac1 and PAK-1 by HIF-1alpha: a positive-feedback loop promoting pulmonary vascular remodeling. *Antioxid Redox Signal* 13, 399-412.

Drogat, B., Bouhecareilh, M., North, S., Petibois, C., Deleris, G., Chevet, E.,

Bikfalvi, A., and Moenner, M. (2007). Acute L-glutamine deprivation compromises

VEGF-a upregulation in A549/8 human carcinoma cells. *J Cell Physiol* 212, 463-472.

Droge, W. (2005). Oxidative stress and ageing: is ageing a cysteine deficiency syndrome? *Philos Trans R Soc Lond B Biol Sci* 360, 2355-2372.



Farfariello, V., Amantini, C., and Santoni, G. (2012). Transient receptor potential vanilloid 1 activation induces autophagy in thymocytes through ROS-regulated AMPK and Atg4C pathways. *J Leukoc Biol* 92, 421-431.

Ferreira, J.V., Fofó, H., Bejarano, E., Bento, C.F., Ramalho, J.S., Girao, H., and Pereira, P. (2013). STUB1/CHIP is required for HIF1A degradation by chaperone-mediated autophagy. *Autophagy* 9, 1349-1366.

Fischer, K., Hoffmann, P., Voelkl, S., Meidenbauer, N., Ammer, J., Edinger, M., Gottfried, E., Schwarz, S., Rothe, G., Hoves, S., *et al.* (2007). Inhibitory effect of tumor cell-derived lactic acid on human T cells. *Blood* 109, 3812-3819.

Frede, S., Freitag, P., Otto, T., Heilmaier, C., and Fandrey, J. (2005). The proinflammatory cytokine interleukin 1beta and hypoxia cooperatively induce the expression of adrenomedullin in ovarian carcinoma cells through hypoxia inducible factor 1 activation. *Cancer Res* 65, 4690-4697.

Galban, S., Kuwano, Y., Pullmann, R., Jr., Martindale, J.L., Kim, H.H., Lal, A., Abdelmohsen, K., Yang, X., Dang, Y., Liu, J.O., *et al.* (2008). RNA-binding proteins HuR and PTB promote the translation of hypoxia-inducible factor 1alpha. *Mol Cell Biol* 28, 93-107.



Garcia-Navas, R., Munder, M., and Mollinedo, F. (2012). Depletion of L-arginine induces autophagy as a cytoprotective response to endoplasmic reticulum stress in human T lymphocytes. *Autophagy* 8, 1557-1576.

Giaccia, A., Siim, B.G., and Johnson, R.S. (2003). HIF-1 as a target for drug development. *Nat Rev Drug Discov* 2, 803-811.

Goetze, K., Walenta, S., Ksiazkiewicz, M., Kunz-Schughart, L.A., and Mueller-Klieser, W. (2011). Lactate enhances motility of tumor cells and inhibits monocyte migration and cytokine release. *Int J Oncol* 39, 453-463.

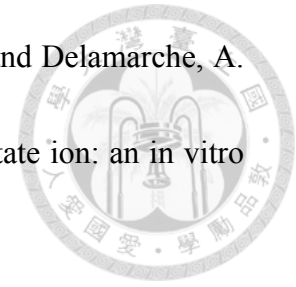
Gonzalez, C.D., Lee, M.S., Marchetti, P., Pietropaolo, M., Towns, R., Vaccaro, M.I., Watada, H., and Wiley, J.W. (2011). The emerging role of autophagy in the pathophysiology of diabetes mellitus. *Autophagy* 7, 2-11.

Gottfried, E., Kunz-Schughart, L.A., Ebner, S., Mueller-Klieser, W., Hoves, S., Andreesen, R., Mackensen, A., and Kreutz, M. (2006). Tumor-derived lactic acid modulates dendritic cell activation and antigen expression. *Blood* 107, 2013-2021.

Grishchuk, Y., Ginet, V., Truttmann, A.C., Clarke, P.G., and Puyal, J. (2011). Beclin 1-independent autophagy contributes to apoptosis in cortical neurons. *Autophagy* 7, 1115-1131.

Groussard, C., Morel, I., Chevanne, M., Monnier, M., Cillard, J., and Delamarche, A.

(2000). Free radical scavenging and antioxidant effects of lactate ion: an in vitro study. *J Appl Physiol* (1985) 89, 169-175.



Grover, R., Ray, P.S., and Das, S. (2008). Polypyrimidine tract binding protein regulates IRES-mediated translation of p53 isoforms. *Cell Cycle* 7, 2189-2198.

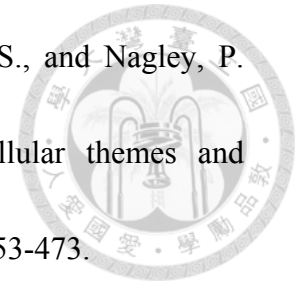
Hardie, D.G. (2003). Minireview: the AMP-activated protein kinase cascade: the key sensor of cellular energy status. *Endocrinology* 144, 5179-5183.

Hardie, D.G. (2004). The AMP-activated protein kinase pathway--new players upstream and downstream. *J Cell Sci* 117, 5479-5487.

Hawley, S.A., Boudeau, J., Reid, J.L., Mustard, K.J., Udd, L., Makela, T.P., Alessi, D.R., and Hardie, D.G. (2003). Complexes between the LKB1 tumor suppressor, STRAD alpha/beta and MO25 alpha/beta are upstream kinases in the AMP-activated protein kinase cascade. *J Biol* 2, 28.

Herrera, B., Alvarez, A.M., Sanchez, A., Fernandez, M., Roncero, C., Benito, M., and Fabregat, I. (2001). Reactive oxygen species (ROS) mediates the mitochondrial-dependent apoptosis induced by transforming growth factor (beta) in fetal hepatocytes. *FASEB J* 15, 741-751.

Higgins, G.C., Beart, P.M., Shin, Y.S., Chen, M.J., Cheung, N.S., and Nagley, P. (2010). Oxidative stress: emerging mitochondrial and cellular themes and variations in neuronal injury. *J Alzheimers Dis 20 Suppl 2*, S453-473.



Hubbi, M.E., Hu, H., Kshitiz, Ahmed, I., Levchenko, A., and Semenza, G.L. (2013). Chaperone-mediated autophagy targets hypoxia-inducible factor-1alpha (HIF-1alpha) for lysosomal degradation. *J Biol Chem 288*, 10703-10714.

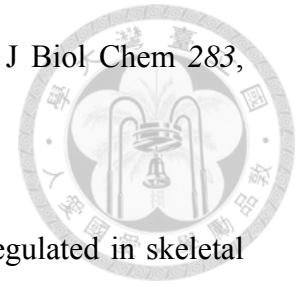
Ivan, M., Kondo, K., Yang, H., Kim, W., Valiando, J., Ohh, M., Salic, A., Asara, J.M., Lane, W.S., and Kaelin, W.G., Jr. (2001). HIFalpha targeted for VHL-mediated destruction by proline hydroxylation: implications for O2 sensing. *Science 292*, 464-468.

Jaakkola, P., Mole, D.R., Tian, Y.M., Wilson, M.I., Gielbert, J., Gaskell, S.J., von Kriegsheim, A., Hebestreit, H.F., Mukherji, M., Schofield, C.J., *et al.* (2001). Targeting of HIF-alpha to the von Hippel-Lindau ubiquitylation complex by O2-regulated prolyl hydroxylation. *Science 292*, 468-472.

Jin, S., and White, E. (2007). Role of autophagy in cancer: management of metabolic stress. *Autophagy 3*, 28-31.

Jo, O.D., Martin, J., Bernath, A., Masri, J., Lichtenstein, A., and Gera, J. (2008). Heterogeneous nuclear ribonucleoprotein A1 regulates cyclin D1 and c-myc

internal ribosome entry site function through Akt signaling. *J Biol Chem* 283, 23274-23287.



Jorgensen, S.B., and Rose, A.J. (2008). How is AMPK activity regulated in skeletal muscles during exercise? *Front Biosci* 13, 5589-5604.

Juenemann, K., and Reits, E.A. (2012). Alternative macroautophagic pathways. *Int J Cell Biol* 2012, 189794.

Jung, S.N., Yang, W.K., Kim, J., Kim, H.S., Kim, E.J., Yun, H., Park, H., Kim, S.S., Choe, W., Kang, I., *et al.* (2008). Reactive oxygen species stabilize hypoxia-inducible factor-1 alpha protein and stimulate transcriptional activity via AMP-activated protein kinase in DU145 human prostate cancer cells. *Carcinogenesis* 29, 713-721.

Kalaany, N.Y., and Sabatini, D.M. (2009). Tumours with PI3K activation are resistant to dietary restriction. *Nature* 458, 725-731.

Kim, J.W., and Dang, C.V. (2006). Cancer's molecular sweet tooth and the Warburg effect. *Cancer Res* 66, 8927-8930.

Kim, J.W., Tchernyshyov, I., Semenza, G.L., and Dang, C.V. (2006). HIF-1-mediated expression of pyruvate dehydrogenase kinase: a metabolic switch required for cellular adaptation to hypoxia. *Cell Metab* 3, 177-185.

Kim, S.H., Hwang, J.T., Park, H.S., Kwon, D.Y., and Kim, M.S. (2013). Capsaicin stimulates glucose uptake in C2C12 muscle cells via the reactive oxygen species (ROS)/AMPK/p38 MAPK pathway. *Biochem Biophys Res Commun* 439, 66-70.

Kim, Y.K., Hahm, B., and Jang, S.K. (2000). Polypyrimidine tract-binding protein inhibits translation of bip mRNA. *J Mol Biol* 304, 119-133.

Klionsky, D.J., Cregg, J.M., Dunn, W.A., Jr., Emr, S.D., Sakai, Y., Sandoval, I.V., Sibirny, A., Subramani, S., Thumm, M., Veenhuis, M., *et al.* (2003). A unified nomenclature for yeast autophagy-related genes. *Dev Cell* 5, 539-545.

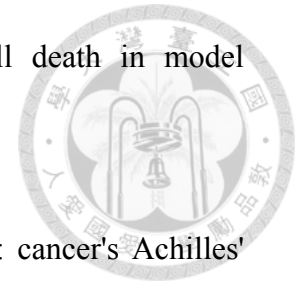
Klionsky, D.J., and Emr, S.D. (2000). Autophagy as a regulated pathway of cellular degradation. *Science* 290, 1717-1721.

Knoechel, T.R., Tucker, A.D., Robinson, C.M., Phillips, C., Taylor, W., Bungay, P.J., Kasten, S.A., Roche, T.E., and Brown, D.G. (2006). Regulatory roles of the N-terminal domain based on crystal structures of human pyruvate dehydrogenase kinase 2 containing physiological and synthetic ligands. *Biochemistry* 45, 402-415.

Komar, A.A., and Hatzoglou, M. (2011). Cellular IRES-mediated translation: the war of ITAFs in pathophysiological states. *Cell Cycle* 10, 229-240.

Komar, A.A., Mazumder, B., and Merrick, W.C. (2012). A new framework for understanding IRES-mediated translation. *Gene* 502, 75-86.

Kourtis, N., and Tavernarakis, N. (2009). Autophagy and cell death in model organisms. *Cell Death Differ* 16, 21-30.



Kroemer, G., and Pouyssegur, J. (2008). Tumor cell metabolism: cancer's Achilles' heel. *Cancer Cell* 13, 472-482.

Kullmann, M., Gopfert, U., Siewe, B., and Hengst, L. (2002). ELAV/Hu proteins inhibit p27 translation via an IRES element in the p27 5'UTR. *Genes Dev* 16, 3087-3099.

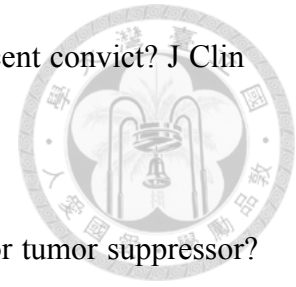
Kung, H.J. (2011). Targeting tyrosine kinases and autophagy in prostate cancer. *Horm Cancer* 2, 38-46.

Lang, K.J., Kappel, A., and Goodall, G.J. (2002). Hypoxia-inducible factor-1alpha mRNA contains an internal ribosome entry site that allows efficient translation during normoxia and hypoxia. *Mol Biol Cell* 13, 1792-1801.

Lee, M.F., Chan, C.Y., Hung, H.C., Chou, I.T., Yee, A.S., and Huang, C.Y. (2013). N-acetylcysteine (NAC) inhibits cell growth by mediating the EGFR/Akt/HMG box-containing protein 1 (HBP1) signaling pathway in invasive oral cancer. *Oral Oncol* 49, 129-135.

Levine, B., and Klionsky, D.J. (2004). Development by self-digestion: molecular mechanisms and biological functions of autophagy. *Dev Cell* 6, 463-477.

Levine, B., and Yuan, J. (2005). Autophagy in cell death: an innocent convict? *J Clin Invest* 115, 2679-2688.



Liang, J., and Mills, G.B. (2013). AMPK: a contextual oncogene or tumor suppressor? *Cancer Res* 73, 2929-2935.

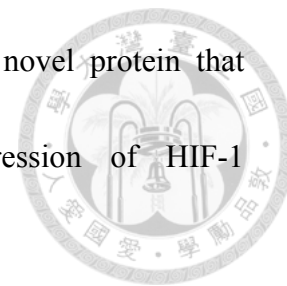
Liochev, S.I. (2013). Reactive oxygen species and the free radical theory of aging. *Free Radic Biol Med* 60, 1-4.

Liu, L.Z., Hu, X.W., Xia, C., He, J., Zhou, Q., Shi, X., Fang, J., and Jiang, B.H. (2006). Reactive oxygen species regulate epidermal growth factor-induced vascular endothelial growth factor and hypoxia-inducible factor-1alpha expression through activation of AKT and P70S6K1 in human ovarian cancer cells. *Free Radic Biol Med* 41, 1521-1533.

Liu, S.Y., Chen, C.L., Yang, T.T., Huang, W.C., Hsieh, C.Y., Shen, W.J., Tsai, T.T., Shieh, C.C., and Lin, C.F. (2012). Albumin prevents reactive oxygen species-induced mitochondrial damage, autophagy, and apoptosis during serum starvation. *Apoptosis* 17, 1156-1169.

Lum, J.J., DeBerardinis, R.J., and Thompson, C.B. (2005). Autophagy in metazoans: cell survival in the land of plenty. *Nat Rev Mol Cell Biol* 6, 439-448.

Mahon, P.C., Hirota, K., and Semenza, G.L. (2001). FIH-1: a novel protein that interacts with HIF-1alpha and VHL to mediate repression of HIF-1 transcriptional activity. *Genes Dev* 15, 2675-2686.



Majeski, A.E., and Dice, J.F. (2004). Mechanisms of chaperone-mediated autophagy. *Int J Biochem Cell Biol* 36, 2435-2444.

Mathew, R., and White, E. (2011). Autophagy in tumorigenesis and energy metabolism: friend by day, foe by night. *Curr Opin Genet Dev* 21, 113-119.

McFate, T., Mohyeldin, A., Lu, H., Thakar, J., Henriques, J., Halim, N.D., Wu, H., Schell, M.J., Tsang, T.M., Teahan, O., *et al.* (2008). Pyruvate dehydrogenase complex activity controls metabolic and malignant phenotype in cancer cells. *J Biol Chem* 283, 22700-22708.

Meley, D., Bauvy, C., Houben-Weerts, J.H., Dubbelhuis, P.F., Helmond, M.T., Codogno, P., and Meijer, A.J. (2006). AMP-activated protein kinase and the regulation of autophagic proteolysis. *J Biol Chem* 281, 34870-34879.

Meng, T.C., Buckley, D.A., Galic, S., Tiganis, T., and Tonks, N.K. (2004). Regulation of insulin signaling through reversible oxidation of the protein-tyrosine phosphatases TC45 and PTP1B. *J Biol Chem* 279, 37716-37725.

Meng, T.C., Fukada, T., and Tonks, N.K. (2002). Reversible oxidation and inactivation of protein tyrosine phosphatases in vivo. *Mol Cell* 9, 387-399.

Mitchell, S.A., Brown, E.C., Coldwell, M.J., Jackson, R.J., and Willis, A.E. (2001).

Protein factor requirements of the Apaf-1 internal ribosome entry segment: roles of polypyrimidine tract binding protein and upstream of N-ras. *Mol Cell Biol* *21*, 3364-3374.

Mitchell, S.A., Spriggs, K.A., Bushell, M., Evans, J.R., Stoneley, M., Le Quesne, J.P.,

Spriggs, R.V., and Willis, A.E. (2005). Identification of a motif that mediates polypyrimidine tract-binding protein-dependent internal ribosome entry. *Genes Dev* *19*, 1556-1571.

Mitchell, S.A., Spriggs, K.A., Coldwell, M.J., Jackson, R.J., and Willis, A.E. (2003).

The Apaf-1 internal ribosome entry segment attains the correct structural conformation for function via interactions with PTB and unr. *Mol Cell* *11*, 757-771.

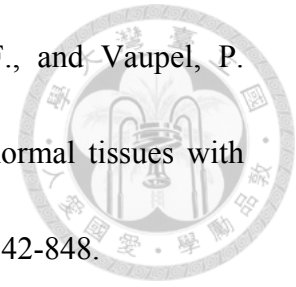
Mizushima, N., Yoshimori, T., and Levine, B. (2010). Methods in mammalian autophagy research. *Cell* *140*, 313-326.

Montcourrier, P., Silver, I., Farnoud, R., Bird, I., and Rochefort, H. (1997). Breast

cancer cells have a high capacity to acidify extracellular milieu by a dual mechanism. *Clin Exp Metastasis* *15*, 382-392.

Mueller-Klieser, W., Walenta, S., Paschen, W., Kallinowski, F., and Vaupel, P.

(1988). Metabolic imaging in microregions of tumors and normal tissues with bioluminescence and photon counting. *J Natl Cancer Inst* 80, 842-848.



Mukhopadhyay, P., Rajesh, M., Hasko, G., Hawkins, B.J., Madesh, M., and Pacher, P.

(2007). Simultaneous detection of apoptosis and mitochondrial superoxide production in live cells by flow cytometry and confocal microscopy. *Nat Protoc* 2, 2295-2301.

Mukhtar, M.H., Payne, V.A., Arden, C., Harbottle, A., Khan, S., Lange, A.J., and

Agius, L. (2008). Inhibition of glucokinase translocation by AMP-activated protein kinase is associated with phosphorylation of both GKR and 6-phosphofructo-2-kinase/fructose-2,6-bisphosphatase. *Am J Physiol Regul Integr Comp Physiol* 294, R766-774.

Muller, O., Sattler, T., Flotenmeyer, M., Schwarz, H., Plattner, H., and Mayer, A.

(2000). Autophagic tubes: vacuolar invaginations involved in lateral membrane sorting and inverse vesicle budding. *J Cell Biol* 151, 519-528.

Nishida, Y., Arakawa, S., Fujitani, K., Yamaguchi, H., Mizuta, T., Kanaseki, T.,

Komatsu, M., Otsu, K., Tsujimoto, Y., and Shimizu, S. (2009). Discovery of Atg5/Atg7-independent alternative macroautophagy. *Nature* 461, 654-658.



Nogueira, V., and Hay, N. (2013). Molecular pathways: reactive oxygen species homeostasis in cancer cells and implications for cancer therapy. *Clin Cancer Res* 19, 4309-4314.

Ohsumi, Y., and Mizushima, N. (2004). Two ubiquitin-like conjugation systems essential for autophagy. *Semin Cell Dev Biol* 15, 231-236.

Olmos, G., Arenas, M.I., Bienes, R., Calzada, M.J., Aragonés, J., Garcia-Bermejo, M.L., Landazuri, M.O., and Lucio-Cazana, J. (2009). 15-Deoxy-Delta(12,14)-prostaglandin-J(2) reveals a new pVHL-independent, lysosomal-dependent mechanism of HIF-1alpha degradation. *Cell Mol Life Sci* 66, 2167-2180.

Park, I.J., Hwang, J.T., Kim, Y.M., Ha, J., and Park, O.J. (2006). Differential modulation of AMPK signaling pathways by low or high levels of exogenous reactive oxygen species in colon cancer cells. *Ann N Y Acad Sci* 1091, 102-109.

Ponisoyskiy, M.R. (2011). Warburg effect mechanism as the target for theoretical substantiation of a new potential cancer treatment. *Crit Rev Eukaryot Gene Expr* 21, 13-28.

Porporato, P.E., Dhup, S., Dadhich, R.K., Copetti, T., and Sonveaux, P. (2011). Anticancer targets in the glycolytic metabolism of tumors: a comprehensive review. *Front Pharmacol* 2, 49.

Pouyssegur, J., Dayan, F., and Mazure, N.M. (2006). Hypoxia signalling in cancer and approaches to enforce tumour regression. *Nature* 441, 437-443.

Ray, P.D., Huang, B.W., and Tsuji, Y. (2012). Reactive oxygen species (ROS) homeostasis and redox regulation in cellular signaling. *Cell Signal* 24, 981-990.

Roche, T.E., and Hiromasa, Y. (2007). Pyruvate dehydrogenase kinase regulatory mechanisms and inhibition in treating diabetes, heart ischemia, and cancer. *Cell Mol Life Sci* 64, 830-849.

Rozhin, J., Sameni, M., Ziegler, G., and Sloane, B.F. (1994). Pericellular pH affects distribution and secretion of cathepsin B in malignant cells. *Cancer Res* 54, 6517-6525.

Rutter, G.A., Da Silva Xavier, G., and Leclerc, I. (2003). Roles of 5'-AMP-activated protein kinase (AMPK) in mammalian glucose homeostasis. *Biochem J* 375, 1-16.

Rygiel, T.P., Mertens, A.E., Strumane, K., van der Kammen, R., and Collard, J.G. (2008). The Rac activator Tiam1 prevents keratinocyte apoptosis by controlling ROS-mediated ERK phosphorylation. *J Cell Sci* 121, 1183-1192.

Sattler, T., and Mayer, A. (2000). Cell-free reconstitution of microautophagic vacuole invagination and vesicle formation. *J Cell Biol* 151, 529-538.

Sattler, U.G., Meyer, S.S., Quennet, V., Hoerner, C., Knoerzer, H., Fabian, C., Yaromina, A., Zips, D., Walenta, S., Baumann, M., *et al.* (2010). Glycolytic metabolism and tumour response to fractionated irradiation. *Radiother Oncol* 94, 102-109.

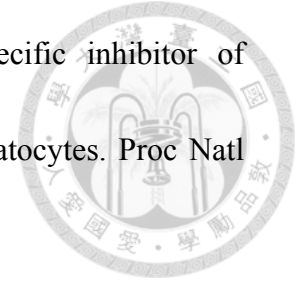
Sawicka, K., Bushell, M., Spriggs, K.A., and Willis, A.E. (2008). Polypyrimidine-tract-binding protein: a multifunctional RNA-binding protein. *Biochem Soc Trans* 36, 641-647.

Scarlatti, F., Maffei, R., Beau, I., Codogno, P., and Ghidoni, R. (2008a). Role of non-canonical Beclin 1-independent autophagy in cell death induced by resveratrol in human breast cancer cells. *Cell Death Differ* 15, 1318-1329.

Scarlatti, F., Maffei, R., Beau, I., Ghidoni, R., and Codogno, P. (2008b). Non-canonical autophagy: an exception or an underestimated form of autophagy? *Autophagy* 4, 1083-1085.

Schepens, B., Tinton, S.A., Bruynooghe, Y., Beyaert, R., and Cornelis, S. (2005). The polypyrimidine tract-binding protein stimulates HIF-1 α IRES-mediated translation during hypoxia. *Nucleic Acids Res* 33, 6884-6894.

Scherz-Shouval, R., Shvets, E., Fass, E., Shorer, H., Gil, L., and Elazar, Z. (2007). Reactive oxygen species are essential for autophagy and specifically regulate the activity of Atg4. *EMBO J* 26, 1749-1760.



Seglen, P.O., and Gordon, P.B. (1982). 3-Methyladenine: specific inhibitor of autophagic/lysosomal protein degradation in isolated rat hepatocytes. *Proc Natl Acad Sci U S A* 79, 1889-1892.

Semenza, G.L. (2003). Targeting HIF-1 for cancer therapy. *Nat Rev Cancer* 3, 721-732.

Semenza, G.L. (2011). Regulation of metabolism by hypoxia-inducible factor 1. *Cold Spring Harb Symp Quant Biol* 76, 347-353.

Sena, L.A., and Chandel, N.S. (2012). Physiological roles of mitochondrial reactive oxygen species. *Mol Cell* 48, 158-167.

Shaw, R.J., Bardeesy, N., Manning, B.D., Lopez, L., Kosmatka, M., DePinho, R.A., and Cantley, L.C. (2004). The LKB1 tumor suppressor negatively regulates mTOR signaling. *Cancer Cell* 6, 91-99.

Shi, Y., Frost, P., Hoang, B., Yang, Y., Fukunaga, R., Gera, J., and Lichtenstein, A. (2013). MNK kinases facilitate c-myc IRES activity in rapamycin-treated multiple myeloma cells. *Oncogene* 32, 190-197.

Shi, Y., Sharma, A., Wu, H., Lichtenstein, A., and Gera, J. (2005). Cyclin D1 and c-myc internal ribosome entry site (IRES)-dependent translation is regulated by AKT activity and enhanced by rapamycin through a p38 MAPK- and ERK-dependent pathway. *J Biol Chem* 280, 10964-10973.

Smith, D.M., Patel, S., Raffoul, F., Haller, E., Mills, G.B., and Nanjundan, M. (2010).

Arsenic trioxide induces a beclin-1-independent autophagic pathway via modulation of SnoN/SkiL expression in ovarian carcinoma cells. *Cell Death Differ* 17, 1867-1881.

Sugden, M.C., Kraus, A., Harris, R.A., and Holness, M.J. (2000). Fibre-type specific modification of the activity and regulation of skeletal muscle pyruvate dehydrogenase kinase (PDK) by prolonged starvation and refeeding is associated with targeted regulation of PDK isoenzyme 4 expression. *Biochem J* 346 Pt 3, 651-657.

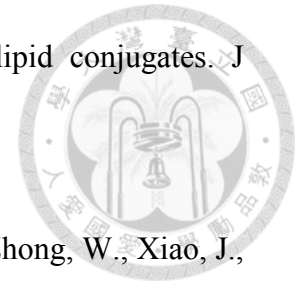
Swietach, P., Vaughan-Jones, R.D., and Harris, A.L. (2007). Regulation of tumor pH and the role of carbonic anhydrase 9. *Cancer Metastasis Rev* 26, 299-310.

Taloczy, Z., Jiang, W., Virgin, H.W.t., Leib, D.A., Scheuner, D., Kaufman, R.J., Eskelinen, E.L., and Levine, B. (2002). Regulation of starvation- and virus-induced autophagy by the eIF2alpha kinase signaling pathway. *Proc Natl Acad Sci U S A* 99, 190-195.

Tanida, I., Sou, Y.S., Ezaki, J., Minematsu-Ikeguchi, N., Ueno, T., and Kominami, E. (2004). HsAtg4B/HsApg4B/autophagin-1 cleaves the carboxyl termini of three human Atg8 homologues and delipidates microtubule-associated protein light

chain 3- and GABAA receptor-associated protein-phospholipid conjugates. *J*

Biol Chem 279, 36268-36276.



Tian, S., Lin, J., Jun Zhou, J., Wang, X., Li, Y., Ren, X., Yu, W., Zhong, W., Xiao, J.,

Sheng, F., *et al.* (2010). Beclin 1-independent autophagy induced by a

Bcl-XL/Bcl-2 targeting compound, Z18. *Autophagy* 6, 1032-1041.

Torii, S., Kurihara, A., Li, X.Y., Yasumoto, K., and Sogawa, K. (2011). Inhibitory

effect of extracellular histidine on cobalt-induced HIF-1 α expression. *J*

Biochem 149, 171-176.

Vander Heiden, M.G., Cantley, L.C., and Thompson, C.B. (2009). Understanding the

Warburg effect: the metabolic requirements of cell proliferation. *Science* 324,

1029-1033.

Vaupel, P., Kallinowski, F., and Okunieff, P. (1989). Blood flow, oxygen and nutrient

supply, and metabolic microenvironment of human tumors: a review. *Cancer Res*

49, 6449-6465.

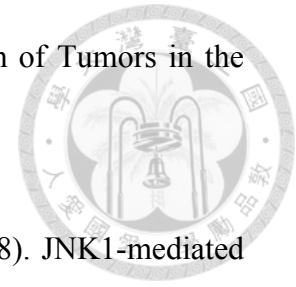
Wakisaka, N., Kondo, S., Yoshizaki, T., Murono, S., Furukawa, M., and Pagano, J.S.

(2004). Epstein-Barr virus latent membrane protein 1 induces synthesis of

hypoxia-inducible factor 1 α . *Mol Cell Biol* 24, 5223-5234.

Warburg, O. (1956). On the origin of cancer cells. *Science* 123, 309-314.

Warburg, O., Wind, F., and Negelein, E. (1927). The Metabolism of Tumors in the Body. *J Gen Physiol* 8, 519-530.



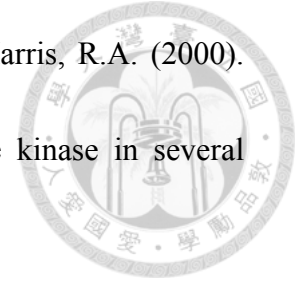
Wei, Y., Pattingre, S., Sinha, S., Bassik, M., and Levine, B. (2008). JNK1-mediated phosphorylation of Bcl-2 regulates starvation-induced autophagy. *Mol Cell* 30, 678-688.

Weljie, A.M., and Jirik, F.R. (2011). Hypoxia-induced metabolic shifts in cancer cells: moving beyond the Warburg effect. *Int J Biochem Cell Biol* 43, 981-989.

Whitehouse, S., Cooper, R.H., and Randle, P.J. (1974). Mechanism of activation of pyruvate dehydrogenase by dichloroacetate and other halogenated carboxylic acids. *Biochem J* 141, 761-774.

Woods, A., Johnstone, S.R., Dickerson, K., Leiper, F.C., Fryer, L.G., Neumann, D., Schlattner, U., Wallimann, T., Carlson, M., and Carling, D. (2003). LKB1 is the upstream kinase in the AMP-activated protein kinase cascade. *Curr Biol* 13, 2004-2008.

Wu, C.A., Chao, Y., Shiah, S.G., and Lin, W.W. (2013). Nutrient deprivation induces the Warburg effect through ROS/AMPK-dependent activation of pyruvate dehydrogenase kinase. *Biochim Biophys Acta* 1833, 1147-1156.



Wu, P., Blair, P.V., Sato, J., Jaskiewicz, J., Popov, K.M., and Harris, R.A. (2000).

Starvation increases the amount of pyruvate dehydrogenase kinase in several mammalian tissues. *Arch Biochem Biophys* 381, 1-7.

Wu, S.B., and Wei, Y.H. (2012). AMPK-mediated increase of glycolysis as an adaptive response to oxidative stress in human cells: implication of the cell survival in mitochondrial diseases. *Biochim Biophys Acta* 1822, 233-247.

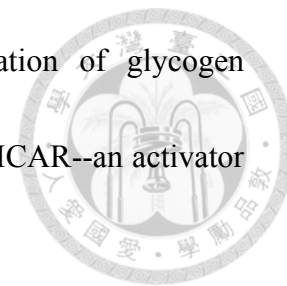
Wu, Y.T., Tan, H.L., Shui, G., Bauvy, C., Huang, Q., Wenk, M.R., Ong, C.N., Codogno, P., and Shen, H.M. (2010). Dual role of 3-methyladenine in modulation of autophagy via different temporal patterns of inhibition on class I and III phosphoinositide 3-kinase. *J Biol Chem* 285, 10850-10861.

Xing, Y., Musi, N., Fujii, N., Zou, L., Luptak, I., Hirshman, M.F., Goodyear, L.J., and Tian, R. (2003). Glucose metabolism and energy homeostasis in mouse hearts overexpressing dominant negative alpha2 subunit of AMP-activated protein kinase. *J Biol Chem* 278, 28372-28377.

Yang, L., Zhao, D., Ren, J., and Yang, J. (2014). Endoplasmic reticulum stress and protein quality control in diabetic cardiomyopathy. *Biochim Biophys Acta*.

Yoshida, H., Matsui, T., Yamamoto, A., Okada, T., and Mori, K. (2001). XBP1 mRNA is induced by ATF6 and spliced by IRE1 in response to ER stress to produce a highly active transcription factor. *Cell* 107, 881-891.

Young, M.E., Radda, G.K., and Leighton, B. (1996). Activation of glycogen phosphorylase and glycogenolysis in rat skeletal muscle by AICAR--an activator of AMP-activated protein kinase. *FEBS Lett* 382, 43-47.



Yu, J., Li, J., Zhang, S., Xu, X., Zheng, M., Jiang, G., and Li, F. (2012). IGF-1 induces hypoxia-inducible factor 1 α -mediated GLUT3 expression through PI3K/Akt/mTOR dependent pathways in PC12 cells. *Brain Res* 1430, 18-24.

Zahid, M., Saeed, M., Ali, M.F., Rogan, E.G., and Cavalieri, E.L. (2010). N-acetylcysteine blocks formation of cancer-initiating estrogen-DNA adducts in cells. *Free Radic Biol Med* 49, 392-400.

Zhou, C., Zhou, J., Sheng, F., Zhu, H., Deng, X., Xia, B., and Lin, J. (2012). The heme oxygenase-1 inhibitor ZnPPiX induces non-canonical, Beclin 1-independent, autophagy through p38 MAPK pathway. *Acta Biochim Biophys Sin (Shanghai)* 44, 815-822.

Zhou, J., Callapina, M., Goodall, G.J., and Brune, B. (2004). Functional integrity of nuclear factor kappaB, phosphatidylinositol 3'-kinase, and mitogen-activated protein kinase signaling allows tumor necrosis factor alpha-evoked Bcl-2 expression to provoke internal ribosome entry site-dependent translation of hypoxia-inducible factor 1 α . *Cancer Res* 64, 9041-9048.

Zhu, J.H., Horbinski, C., Guo, F., Watkins, S., Uchiyama, Y., and Chu, C.T. (2007).

Regulation of autophagy by extracellular signal-regulated protein kinases during

1-methyl-4-phenylpyridinium-induced cell death. *Am J Pathol* 170, 75-86.

Zwingmann, C., and Bilodeau, M. (2006). Metabolic insights into the

hepatoprotective role of N-acetylcysteine in mouse liver. *Hepatology* 43,

454-463.



Publications

Ching-An Wu, Duen-Yi Huang, and Wan-Wan Lin (2014) Beclin-1-independent autophagy positively regulates internal ribosomal entry site-dependent translation of hypoxia-inducible factor 1 α under nutrient deprivation. *Oncotarget*. Jul 26. [Epub ahead of print].

Ching-An Wu, Yee Chao, Shine-Gwo Shiah, and Wan-Wan Lin (2013) Nutrient deprivation induces the Warburg effect through ROS/AMPK-dependent activation of pyruvate dehydrogenase kinase. *Biochimica et Biophysica Acta-Molecular Cell Research* 1833(5):1147-1156